NOTE TO USERS

RADIATION- AND LAG-ERRORS IN THE MEASUREMENT OF TURBULENT TEMPERATURE FLUCTUATIONS

by

James E. Mc Donald

A Dissertation Submitted to the
Graduate Faculty in Partial Fulfillment of
The Requirements for the Degree of
DOCTOR OF PHILOSOPHY

Major Subject: Physics

Approved:

Signature was redacted for privacy.

In Charge of Major Work

Signature was redacted for privacy.

Head of Major Department

Signature was redacted for privacy.

Dean of Graduate College

Iowa State College
1951

TABLE OF CONTENTS

Page

I. INTRODUCTION

The record of a rapidly responding temperature-sensing element located at a fixed position near the ground on a clear day reveals that the natural wind is thermally heterogeneous to an extent that would remain wholly unsuspected if only inert instruments, such as the conventional mercurial thermometer, were used to study the temperature field. This heterogeneity is a consequence of turbulent exchange of air between strata characterized by mean temperatures which vary systematically with height above the ground. The meteorologist is fundamentally interested in the final results of such exchange processes, since these processes are responsible for the vertical transport of heat, momentum, water vapor, and other properties in the lower layers of the atmosphere.

In the past there has been very little attention given to the details of the fluctuations themselves, other than those of wind velocity; but growing interest in the structure of atmospheric turbulence has recently led to some preliminary theoretical analyses of the thermal fluctuation problem (Lettau, 1949; Sutton, 1948). Aware of the paucity of data suitable for testing the validity of the theoretical conclusions of these investigations, the Geophysical Research Directorate of the Air Force Cambridge Research Laboratories has sponsored a study of turbulent temperature fluctuations to be carried out by members of the Department of Physics of the Iowa State

College.[1] The work described herein has been done as a part of this contract research.

The development of instrumentation, organization of field observations, and planning of analysis techniques for this investigation of temperature fluctuations called for analyses of a number of problems which have received scarcely any previous attention due to prior lack of interest in the fluctuations as observable quantities. Those problems which will be examined here fall into two principal categories: radiation errors and lag effects.

When a thermal element is exposed to radiative heating its temperature rises above that of the ambient air until the rate of dissipation of heat from the element by conduction to the passing air reaches equality with the rate of addition by radiation. If the irradiation is constant while the ambient air speed fluctuates, then no steady-state radiation error can develop; rather the error fluctuates, with the undesirable consequence that spurious fluctuations of indicated temperature become superimposed on the fluctuations due to true air temperature fluctuations. A study of the magnitude of such spurious fluctuations is presented here for two particular sensing elements (bead-type thermistor and thermocouple).

When a thermal element is exposed to fluctuating ambient air temperatures its instantaneous indication is not, in gen-

---

[1]This work is being done under Contract No. AF19(122)-440.

eral, the true instantaneous temperature due to effects of lag. The lag problem has been explored both in terms of general relationships that must exist between true and apparent fluctuation statistics as determined from the record of a lagging sensor, and also in terms of the specific magnitudes of lag effects to be expected when either thermistors or thermocouples are employed.

Throughout the following discussions, "temperature fluctuations" are to be understood to be those implied in the Eulerian time derivatives and never the Lagrangian[1]. Since the Lagrangian "eddy diameter" is related, through the instantaneous wind velocity, to the Eulerian "period", all of the current ambiguity of the former term is passed on to the lat-

---

[1]The Lagrangian (or "individual") and Eulerian (or "local") time-differential operators of hydrodynamic theory are related according to

$$\frac{d}{dt} = \frac{\partial}{\partial t} + u \frac{\partial}{\partial x} + v \frac{\partial}{\partial y} + w \frac{\partial}{\partial z} ,$$

where $\frac{d}{dt}$ is the Lagrangian operator, $\frac{\partial}{\partial t}$ is the Eulerian operator, and u, v, w are the particle velocity components in the directions x, y, z, respectively. Experimentally, it is very much simpler to measure the Eulerian time derivative of a meteorological variable than it is to measure the Langrangian so most observational programs in dynamic meteorology are based on an Eulerian framework in spite of the fact that the Lagrangian point of view is conceptually more straightforward. The almost complete lack of progress towards Lagrangian observational techniques must be admitted to be one of the most serious defects in the present development of the subject of dynamic meteorology, and this same defect exists in the present study of turbulent temperature fluctuations to the extent that the study is regarded as an effort to elucidate the dynamical processes involved in turbulent heat transfer.

ter, aggravating a semantic problem of meteorology which will not be attacked here. Instead, the spectrum of periods (or frequencies) will here be tacitly regarded as that derived from a Fourier analysis of the fluctuations observed over a definite period of time. This point of view, it must be noted, neglects the serious difficulties inherent in the (essential) open-endedness of the time-series comprised by the temperature fluctuations occurring at any fixed point of observation.

A very rough criterion may be introduced at this point to indicate the approximate upper and lower limits on the periods of temperature fluctuations one might expect to encounter in the lower atmosphere. If the mean speed of a layer of air bounded below by the earth's surface is U, and if the depth of the layer is H, then on the crude but plausible assumption that thermally distinct masses of air ("eddies") whose horizontal diameters are of the order of H may be embedded in this flow, the Eulerian periods of the fluctuations caused by the passage of these eddies past a fixed sensor will be of the order of H/U. Considering the lowest layer of interest to be characterized by H of the order of 1 decimeter and U of the order of 1 meter per second, periods as low as 10^{-1} second may be anticipated. Considering, at the other extreme, the whole boundary layer with H of the order of 1 kilometer and U of the order of 10 meters per second, periods as large as 10^{2} seconds may be expected

to occur. Undoubtedly fluctuations of both smaller and larger periods than those lying between these approximate bounds do occur in the atmosphere, but it is unlikely that those of periods lower than 10^{-1} second can contribute appreciably to turbulent transport of heat, and those of periods greater than 10^{2} seconds are of too large a scale to warrant treatment as "turbulent" fluctuations. Hence the following analyses will deal with problems encountered in the measurement and analysis of fluctuations with periods of from 10^{-1} to 10^{2} seconds, approximately. It will become apparent that fluctuations near the lower limit of this range of periods pose serious problems of instrumentation and analysis.

II. REVIEW OF LITERATURE

There certainly does not exist in the literature a definitive study of turbulent temperature fluctuations. Such work as has been reported can frequently not be clearly interpreted due to omission of information concerning response characteristics of the sensing element employed, especially its lag-time. Hence no attempt will be made to cite all of the literature references wherein temperature fluctuation data have been mentioned.

Giblett (1932) and his associates made an early contribution to the study of longer period fluctuations, and called attention to the negative correlation that normally exists between wind speed and air temperature. Such a correlation arises because the surface wind speed increases when a mass of air descends from the faster-moving overlying layers which are usually also cooler than the surface layers at midday. Best (1931) analysed the instantaneous temperature differences observed at two points separated by a horizontal distance of fifty feet. His work drew well-founded criticism from Bilham (1935) on the grounds that the observations were seriously biased by instrument lag effects. Bilham's paper appears to represent the first (and also the last) serious effort undertaken to assay the statistical distortions which lag can impose upon data obtained from inert instruments. The analyses of lag problems presented below in Part IV may be regarded

as an extension of the point of view first taken by Bilham in this 1935 paper.

Haude (1934) has described surprisingly non-correlated temperature fluctuations at levels of 1 millimeter and 1 centimeter above a level desert surface. More recent observations of temperature profiles and fluctuations very near a desert surface (at heights of 0.01 to 1.0 inch) have been reported by Vehrencamp (1951); but the 0.003-inch diameter thermocouples used must have developed appreciable radiation errors which interacted with wind speed variations to add spurious fluctuations. Schilling and others (1946) mentioned briefly some measurements made with a 0.0005-inch diameter resistance wire thermometer from which they concluded that the air temperature at a fixed point may rise or fall by as much as 10 C^{o} in a second or two, notable here as the most extreme oscillation reported in the literature examined. Hoehndorf, quoted by Slater (1948), reported "average fluctuations" of 3.9 C^{o} at a height of 1 meter, 2.4 C^{o} at 10 meters, and 1.8 C^{o} at 20 meters above an airport surface near midday on a cloudless summer day.

Data such as those just cited, sparse as they are, help point out the nature of the measurement and analysis problems one must expect to face in the investigation of turbulent temperature fluctuations. They provide, however, practically no answer to questions concerning the intensity spectrum of the

fluctuations, dependence of fluctuation statistics on height, wind speed, stability of vertical temperature distribution, and degree of correlation between fluctuations occurring simultaneously at nearby points. The answers to these latter questions should, when they are found, shed considerable light on the problem of the ultimate details of the process of turbulent transport of heat. To fill some of these large remaining gaps is the objective of the fluctuation study of which the present work is a part.

III. RADIATION ERRORS IN FLUCTUATION MEASUREMENTS

The fundamental requirement for accurate measurement of the temperature of a fluid is that the thermal sensing element shall be in thermal equilibrium with the fluid which immediately surrounds it. If the element is in radiative communication with matter located at some position remote from that element, then the fundamental requirement will not, in general, be satisfied, and hence the temperature indicated by the element will not represent the temperature of the enveloping fluid. Instead, some positive or negative radiation error will exist.

Whereas such radiation errors can be avoided in many meteorological temperature measurements by enclosing the sensing element within some suitable shield, they are almost inescapable in fluctuation studies because the radiation shields would so interfere with the free flow of the wind past the element that something quite different from the true fluctuations would be indicated by the element.

If the rate of irradiation of an element were constant over the period of observation of a series of air temperature fluctuations, it might appear admissible to ignore the radiation error since it would seem to affect only the mean temperature, leaving unaltered the deviations from the mean which are of principal interest in fluctuation studies. However, if simultaneous fluctuations of wind speed are occurring, these latter imply fluctuations in the ventilation rate and hence

in the heat dissipation rate of the element, with the unfortunate consequence that the error level fluctuates. Hence spurious fluctuations of indicated temperature will be superimposed as background "noise" on the true fluctuations. By this action of wind speed fluctuations on a radiatively heated element, the true fluctuations become confounded with the spurious ventilational effects, so the associated errors may be referred to as "confounding errors".

Since no analyses of such confounding effects had been made in conjunction with any of the previous limited studies of temperature fluctuations, it was considered necessary to explore this problem quite carefully and quantitatively with particular reference to the element tentatively selected for use in the fluctuation measurements, the Western Electric bead thermistor No. D-176980. In addition, a comparison with the confounding effects to be expected with a representative type of thermocouple was desirable since this element probably provides the best alternative to the use of the bead thermistor in fluctuation studies.

A brief description of the general plan of attack used to study the confounding problem will help to clarify the steps actually taken and the results obtained. First, for each element (bead thermistor and thermocouple) the magnitudes of the several radiative fluxes involved were determined as a function of time of day and year. With these magnitudes

available, the total radiative power to be converted into heat in the element and dissipated by heat transfer to the ambient air was computed. Then the dissipation function of each element (rate of heat loss per degree excess temperature as a function of wind speed) was determined and used in conjunction with representative data on actual wind conditions prevailing near the earth's surface to evaluate the steady-state radiation errors and the confounding errors under various conditions likely to be encountered in the field. These analyses will be most conveniently described by considering the two sensing elements separately.

A. Thermistor Radiation Errors

The Western Electric D-176980 bead thermistor is a roughly spherical mass of semiconductor material (oxides of nickel and manganese) enclosed in a vitreous envelope through which a pair of lead wires pass to make contact with the semiconducting nucleus within. The entire bead is quite small, only 0.033 centimeters in diameter, so the absolute magnitude of the radiative power which it absorbs is not large. For analysis purposes its shape will be regarded as that of a sphere although it is perhaps most aptly described as lemon-shaped. The photographs of Figures 1 and 2 show the details of the bead structure and the method of mounting for field use.

Figure 1. Close-up view of mounted thermistor.

Background scale is a centimeter scale, the smallest divisions being millimeters. The thermistor bead is at the extreme right, supported on four fine wires. (Bead is below and slightly to the right of the "1" of the "14" on the scale in the background.)

Figure 2. Photomicrographs of a Western Electric D-176980 bead thermistor.

A - View perpendicular to plane of wires exhibiting symmetry but non-circular outline. (The four fine wires have here been arranged to lie in the plane containing the portions of those wires surrounded by the thermistor itself.)

B - View parallel to wires exhibiting nearly circular outline. Diameter of this section is approximately 0.033 centimeters.

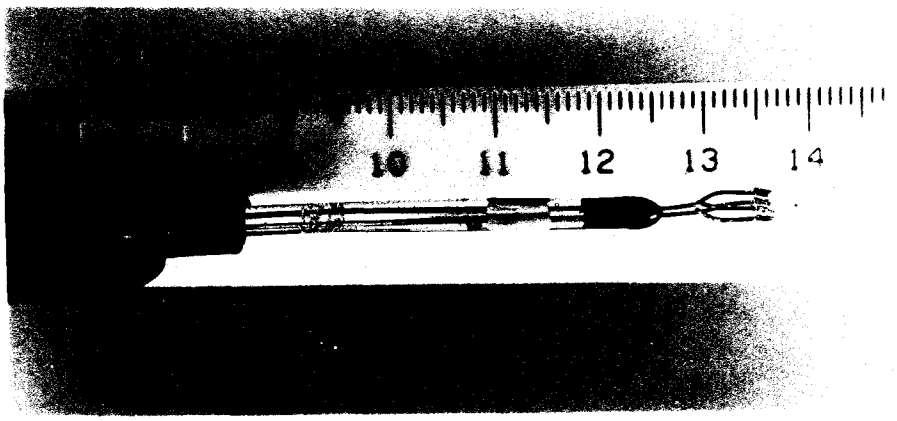
10
11
12
13
14

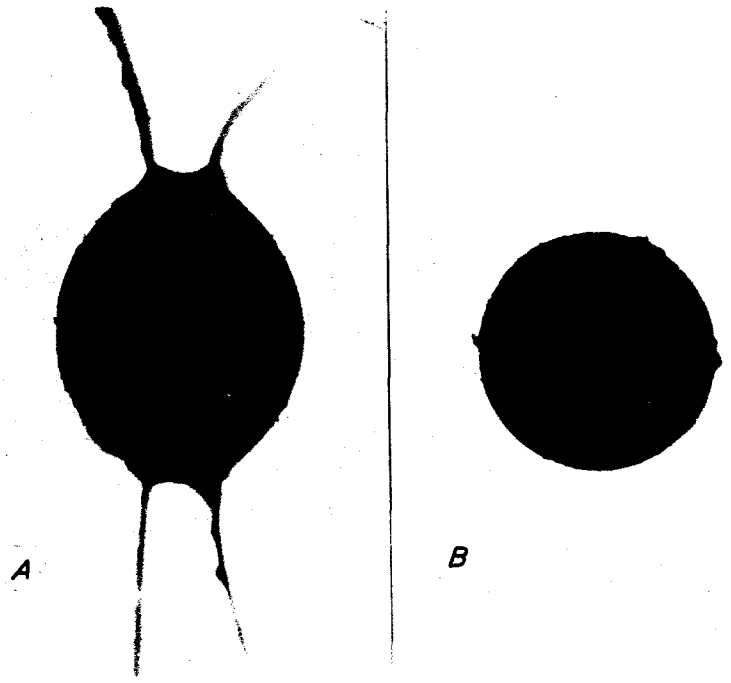
A
B

1. Calculations of the components of the total radiative exchange

A freely exposed thermal sensing element may fail to be in perfect thermal equilibrium with the immediately adjacent air because of the disturbing influences of the following remote energy sources: the sun, the scattering particles in the atmosphere, the ground acting as a reflector of direct solar and indirect scattered radiation, and the ground and atmosphere acting as infrared sources. Concurrently the ground and atmosphere act as infrared sinks. The role of each of these sources and sinks was evaluated quantitatively in order to draw a total radiation balance for the bead thermistor. These several flux calculations for the thermistor will be discussed in the following paragraphs.

a. Direct solar radiation. Since a thermistor bead is nearly spherical, its direct solar radiative heating will be dependent not upon the insolation rate per unit horizontal area (a rate which is of great climatological importance), but rather upon the insolation intensity measured normal to the solar beam, i.e., upon the "intensity" of photometric terminology. This intensity varies seasonally because of (1) variation of solar declination, and (2) variation of precipitable water vapor in the atmosphere (water vapor being the only seasonally variable absorbing constituent of any importance).

To secure the necessary data on seasonal and diurnal variations of intensity of the solar beam at the earth's surface, the Solar Radiation Data sections of the Monthly Weather Review were used. Lincoln, Nebraska was selected as the station whose observations could be expected to be most representative of conditions that will prevail during observations to be made in the course of the present study. The 1949 cumulative average intensities for Lincoln for each of the several tabulated solar altitudes were obtained for each of the four principal climatological months, January, April, July, and October (Monthly Weather Review, 1949, pp. 28, 131, 216, 300).

Since the objective of the present analysis was to determine the largest values of radiation error that might be attained, it is important to point out here that intensity measurements are never made at U. S. Weather Bureau stations on cloudy days, so the averages employed here have not been lowered by dilution with decreased intensities characteristic of cloudy days. In order to see how valid it would be to use mean intensities here, a statistical examination of the individual daily values was carried out on five years of observations at Lincoln and, as a check, on a similar group of observations at Madison, Wisconsin. This study revealed that the mean values which have been utilized here do not represent the means of a widely fluctuating variable; for near noon, when radiation errors are the greatest, the

extreme insolation intensities for very dry, clear days exceed the means by only about 10 per cent of the means themselves. In view of this result, the means, which were readily available from the Monthly Weather Review, have been employed here.

The details of the calculation of intensities for all the desired solar hour angles from the few values which are tabulated in the Monthly Weather Review need not be elaborated here, being quite straightforward. It will be sufficient to point out that the tabulated intensities were plotted against their respective air masses on log-log coordinates, a smooth curve drawn through them and values for other air masses obtained by interpolation and extrapolation. Figure 3 shows the resulting mean insolation intensities for each of the four months, plotted against solar hour angle on the abscissa. (Plotting the data against solar hour angle as if it were simply symmetric does obscure the frequently occurring excess of afternoon insolation values over morning values of the same hour angle, but these asymmetries are seldom greater than a few per cent of the means.) The scale of the ordinate shown at the left gives these intensities in langleys per minute (gram-calories per square centimeter per minute), while that at the right gives the corresponding radiant power, in milliwatts, intercepted by a spherical bead thermistor of cross-sectional area 8.5×10^{-4} square centimeters (D-176980). These values of power intercepted will be regarded as values of power absorbed because of the low reflectivity of the

Figure 3. Direct solar radiation intensities.

Monthly average intensities for each solar hour angle from noon to sunset (sunrise) are shown for four different months of the year. Ordinate scale at left gives beam intensities in langleys per minute; ordinate scale at right gives rates of power interception by the 0.033-centimeter diameter Western Electric D-176980 bead thermistor in milliwatts.

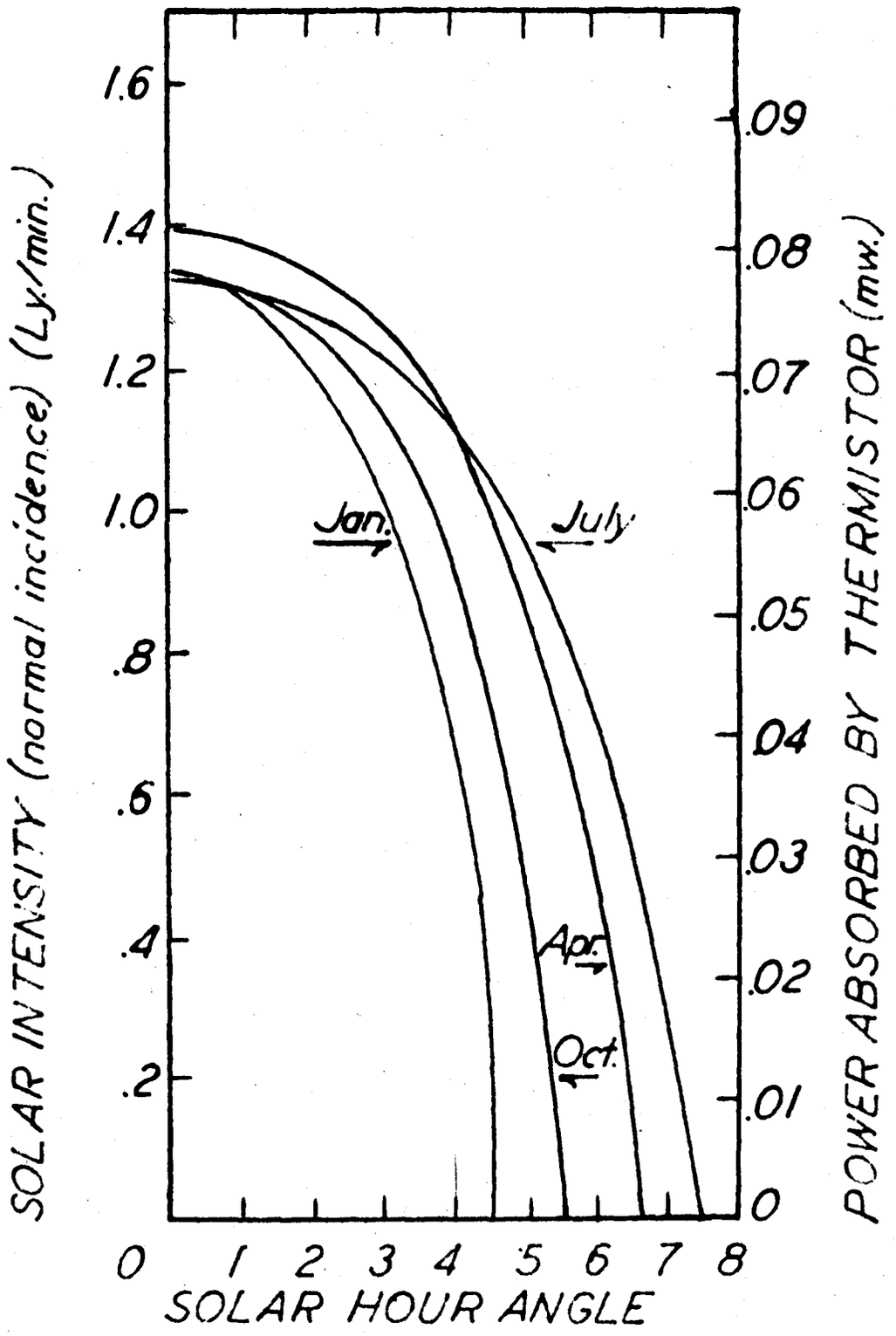
SOLAR INTENSITY (normal incidence) (Ly./min.)
POWER ABSORBED BY THERMISTOR (mw.)
SOLAR HOUR ANGLE
1.6
1.4
1.2
1.0
.8
.6
.4
.2
.09
.08
.07
.06
.05
.04
.03
.02
.01
0
0 1 2 3 4 5 6 7 8
Jan.
July
Apr.
Oct.

glass surface and high absorptivity of the dark nucleus.

That the extreme annual maximum value of intensity comes in Spring is apparently a consequence of the phase difference between the seasonal variations of noon solar altitude and of total precipitable water in the atmospheric column. The annual maximum of the latter is displaced from the summer solstice to about the middle of July in the central United States with the result that the struggle between decreasing optical path length and increasing absorption coefficient along that path length leads to an extremum around the first of April, in the mean. It is a curious result of the compromise between these same two factors that the noon intensities for January, July, and October are all the same to within a few per cent at Lincoln, equaling very nearly 1.32 langleys per minute.

The right-hand power scale of Figure 3 reveals that bead thermistors will be subjected to daily maximum values of intercepted radiation of around 0.08 milliwatts when only the direct solar beam is considered. Added to this component are the several other radiant fluxes of which the next one to be considered will be the diffuse sky radiation.

b. Diffuse sky radiation. The existing literature concerning the physics of radiation errors, sparse as it is, includes little mention of the role that may be played by scattered radiation reaching a thermal element from all parts of the sky. However, some figures given in one of the reports

of the Johns Hopkins University Laboratory of Climatology (Thornthwaite, 1949) suggested that even when an element is shaded from the direct rays of the sun an appreciable residual error due to diffuse sky radiation may exist, so this source of error has been examined quantitatively and was found to be too large to be neglected in a complete radiation error analysis.

The first question that arose in considering diffuse sky radiation was that of whether a series of separate calculations must be made, each for a different solar zenith angle, as was necessarily the case for the direct solar radiation intensities calculated above. To answer this, the problem of the dependence of diffuse sky irradiation of a sphere upon varying solar zenith angle was solved to a first approximation in which the density of scattering particles was assumed constant throughout the total scattering volume and in which primary but not secondary (or higher) order scattering was considered.

The intensity of scattered sunlight, dL, originating in an element of volume dV at distance r from the point of observation was taken as

$$dL = \frac{kn}{r^2}(1 + \cos^2\gamma)dV \ , \qquad (1)$$

where k is a constant for given wavelength and nature of scattering particles, n is the density of scattering particles, and γ is the angle between the direction of the primary radiation and the scattered ray from dV to the point of observation

(see, for example, Humphreys, 1940, p. 561). On putting γ in terms of the solar zenith angle and of the altitude and azimuth of the volume element dV, (solar azimuth taken as zero) expressing dV in terms of spherical coordinates, and integrating over a hemispherical space of radius R (of the order of several tens of kilometers), one finds the total diffuse sky radiation incident upon a sphere of unit cross-sectional area to be

$$L_s = \frac{8\pi knR}{3}, \qquad (2)$$

independent of the solar zenith angle, to the first approximation employed. That the diffuse sky radiation is independent of the position of the sun is a fortunate result as it implies that a calculation of the diffuse irradiation made for any one solar zenith angle will give at once the irradiation rate for all solar zenith angles, i.e., for all times of day and year. This lack of dependence of diffuse irradiation upon solar position is not true for bodies of arbitrary shape. A unit horizontal area, for example, receives appreciably less sky radiation with the sun near the horizon than with the sun near zenith (Humphreys, 1940, p. 564).

As the next step in the analysis, the actual calculations of the magnitude of the diffuse irradiation of the bead thermistor might appear to have been achievable on theoretical grounds, using (2) above. However, the appropriate values to assign

to k, n, and R were seriously in doubt, so experimentally observed diffuse irradiation rates for a plane horizontal surface were obtained and these converted into equivalent rates for a sphere by an indirect method which will be explained next.

Any portion of the sky contributes to the intensity of sky radiation at a point on the ground an amount that is proportional to (1) the solid angle which that portion of sky subtends at the surface point, and (2) the local brightness of that portion of the sky. If the contribution of each element's flux to the total sky irradiation of a unit horizontal area is to be computed, then the intensity contribution from each element of sky must be weighted by the sine of the angle of altitude of that element and then the sum of the weighted fluxes obtained for the whole sky. If on the other hand, the total sky irradiation of a sphere of unit cross-sectional area is to be computed, then since a sphere possesses the unique property of presenting the same projected area in all directions, the flux contributions are to be summed directly over all elements of the dome of the sky unweighted by any geometric factor.

As a means of removing from the final numerical results any slight dependence of diffuse irradiation on solar zenith angle that might have been obscured by the approximations employed above, the actual determinations were carried through for a middle value of solar zenith angle, 50°, rather than for

either a very low or a very high zenith angle. Observational data on the variation of sky brightness with altitude and azimuth were not available for any station in the central United States, but Kimball and Hand (1921) have given very extensive reports on sky brightness for Washington, D. C. so these were employed to determine the relative contributions of the various parts of the sky, while the final fixing of an absolute magnitude of total flux reaching the sphere was based upon a single observational datum for Lincoln, Nebraska, as will be explained below. Both the sky brightness values for Washington and the datum (total diffuse radiative flux on unit horizontal surface) for Lincoln corresponded to a solar zenith angle of 50°.

The actual computations began by reading off the local mean clear-sky brightness values at the centers of sky elements bounded by vertical circles 10° apart and almucantars 10° apart on the chart given by Kimball and Hand (ibid.), weighting each of these values by the cosine of the angle of altitude of the center of its respective element (to allow for decreasing solid angle subtended by 10°-square elements of increasing altitude), and then summing over azimuth and altitude. This summation represented a double numerical integration over the entire sky and, in view of what was said earlier, yielded a result that was proportional to the total sky radiation received by a sphere at the ground.

The unknown quantity that remained to be determined was

the proportionality constant, which was not dependent upon the spherical nature of the receiver, but only upon the particular numerical units employed in expressing relative sky brightnesses. (The numerical magnitudes actually used happened to represent ratios of local sky brightness to zenith sky brightness.) By using those same numerical units to carry through a similar double numerical integration for the case of a plane horizontal surface and then equating this latter result to actually observed diffuse sky radiation receipts on a unit horizontal area at Lincoln, Nebraska, (0.017 langleys per minute according to Kimball (1927)), the proportionality constant was determined.

By the above indirect method the rate of sky irradiation of a sphere of unit cross-sectional area was found to be appreciably larger than for the horizontal area, equaling 0.40 langleys per minute in contrast to the 0.17 langleys per minute for the horizontal plane surface. If a sphere of unit cross-sectional area receives 0.40 langleys per minute, a thermistor bead of 8.5×10^{-4} square centimeters cross-sectional area will receive diffuse sky radiation at a rate of about 0.025 milliwatts; and according to the first approximation analysis described above, this rate will remain constant throughout the day and year. The validity of this approximation undoubtedly deteriorates as the altitude of the sun approaches zero (due to increasing importance of higher-order scattering in the long oblique path through the atmosphere), but this value was

employed as a constant in the present analysis.

Hence, to each value of direct solar radiation intercepted by the bead as shown by Figure 3 there was to be added a constant value of 0.025 milliwatts due to diffuse sky radiation. Since the direct solar beam delivers only 0.080 milliwatts to the bead in the April noon extremal case, the diffuse radiation is seen to contribute an additional amount which is always over 30 per cent of the direct solar contribution itself. For large hour angles, when the direct solar beam intensity decreases due to increased depletion in the long oblique path through the atmosphere, the diffuse sky radiative contribution to thermistor heating will actually become larger than that of the sun itself. Clearly, sky radiation is not a negligible factor in the total radiative balance of this thermal element.

c. Ground-reflected radiation. An unshielded thermal element receives short wavelength radiation[1] not only directly from the sun and indirectly from scattering particles in the atmosphere, but also indirectly from ground reflection of both of these first two components. Of all three short

---

[1]"Short wavelength radiation" is used in meteorology to denote the portion of the electromagnetic spectrum in which the sun radiates appreciably, hence from about 0.2 to 4 microns. This range is to be distinguished from "long wavelength radiation" which refers to the spectral interval within which a blackbody at normal atmospheric temperature radiates, approximately 4 to 25 microns.

wavelength contributions to radiative heating of a thermal element, this one is least subject to precise evaluation because the albedo of the earth's surface depends considerably upon the nature and state of the surface. Geiger (1950, p. 129) summarizes most of the important past studies of surface reflectivity and from his compilation a value of 0.15 was selected as a representative working value for grass covered soil. The same albedo was found typical of bare sandy soil as measured recently by Thornthwaite (1950, p. 11).

Except for the special case of a water surface, where nearly specular reflection will occur, the ground and its vegetative cover will act as a diffuse reflector. The angular distribution of the intensity of reflected radiation will then follow, to fair approximation, the cosine law of diffuse reflection so that

$$B(\theta) = B_o \cos\theta \qquad (3)$$

where $B(\theta)$ is the brightness of the reflecting surface when viewed from an angle of θ from the normal to that surface, and B_o is the brightness when viewed from $\theta = 0$, i.e., normal to the surface. (See, for example, Moon, 1936, p. 256.) It is the defining characteristic of perfectly diffuse reflectors that they obey (3) independent of the angle of incidence of the primary radiation which is undergoing reflection. Sod (or soil) is undoubtedly not a perfectly diffuse reflector and, unfortunately, there appeared to be no observations

reported in the literature showing how closely various natural ground covers follow the cosine law. Nevertheless, it seemed permissible to use (3) in view of the extent to which sod must possess the essential requirement for diffuse reflection -- a large surface density of randomly oriented reflected surfaces. On this basis the ideal relation (3) was assumed to hold here.

Before (3) could be used computationally in the problem at hand it was found necessary to analyze the experimental process by which the albedo of a ground cover is measured, in order to learn how the quantity B_o is related to the albedo and the total incident flux; for this relation was, somewhat surprisingly, not discussed in any of the literature references consulted in examining the ground reflection problem. This analysis will be summarized next and the result then used to evaluate the ground-reflected component of the thermistor radiation balance.

The technique of determining the albedo of the ground surface consists in measuring the incident flux when the sensitive face of a pyrheliometer (type of thermopile) is turned directly downward towards the surface so that its horizontal face receives reflected radiation from the full terrestrial hemisphere, next measuring the incident flux when the face is turned directly upward towards the sky so that it receives direct solar and diffusely scattered sky radiation from the full celestial hemisphere, and then

dividing the first flux by the second. The quotient is defined to be the albedo of the surface in question.

When the pyrheliometer is turned downward, the contribution dE to its illumination made by an annular strip of ground of radius $r\sin\theta$ and radial width $rd\theta\sec\theta$ centered about the vertical through the pyrheliometer (see Figure 4) is

$$dE = B_o \frac{\cos\theta}{r^2} \cos\theta \; 2\pi \; r\sin\theta \; rd\theta\sec\theta$$

in view of (3), the inverse square law, and the geometry of the problem. Integration over the full terrestrial hemisphere gave as the total reflected radiation received by the face of the instrument

$$E = \pi B_o \qquad (4)$$

per unit area of the pyrheliometer face.

When the pyrheliometer is then turned upward to receive the direct solar and the diffuse sky radiation, the total incident flux, F_i, which strikes unit area of the face of the instrument is the same as that striking unit area of horizontal ground surface. By definition, then, the albedo of the ground surface is

$$\alpha = \frac{\pi B_o}{F_i}$$

so that

$$B_o = \frac{\alpha F_i}{\pi} \qquad (5)$$

which identified B_o, the normal brightness of the surface, with the albedo and the total incident flux on unit horizon-

tal area. This relation is needed in the evaluation of the ground-reflected radiation incident upon any given thermal element for a specified F_i.

For the bead thermistor of diametral cross-sectional area A, the contribution made by an annular strip of ground of radius $r\sin\theta$ and width $rd\theta\sec\theta$ is

$$dE = B_o \frac{\cos\theta}{r^2} 2\pi r\sin\theta rd\theta\sec\theta A, \qquad (6)$$

the projection factor, $\cos\theta$, not appearing now as it did for the case of reflective illumination of the plane horizontal pyrheliometer face. Integration of (6) over the whole terrestrial hemisphere gave as the total ground-reflected radiation incident on the sphere

$$E = 2\pi B_o A = 2 \alpha F_i A \qquad (7)$$

in view of (5). Comparison of (7) and (4) shows that a sphere of given cross-sectional area intercepts just twice as much ground-reflected radiation as does a horizontal disc of equal area, the difference being due to the dissimilarity in the variation of projected area of sphere and disc with variation of the angle θ.

To evaluate (7) for the bead thermistor the magnitudes of F_i, the total flux of short wavelength radiation reaching unit area of ground surface, were determined as a function of time of day for the four principal climatological months of January, April, July, and October. The procedure used consisted of weighting the direct solar intensities (found

Figure 4. Geometry of pyrheliometric measurement of ground albedo.

Figure 5. Ground-reflected radiation.

Solid curves give diurnal variation of ground-reflected flux (in milliwatts) intercepted by the bead thermistor for each of four months for a surface albedo of 0.15 (grass cover).

Dashed curve gives diurnal variation of reflected flux in January for an albedo of 0.85 (snow cover).

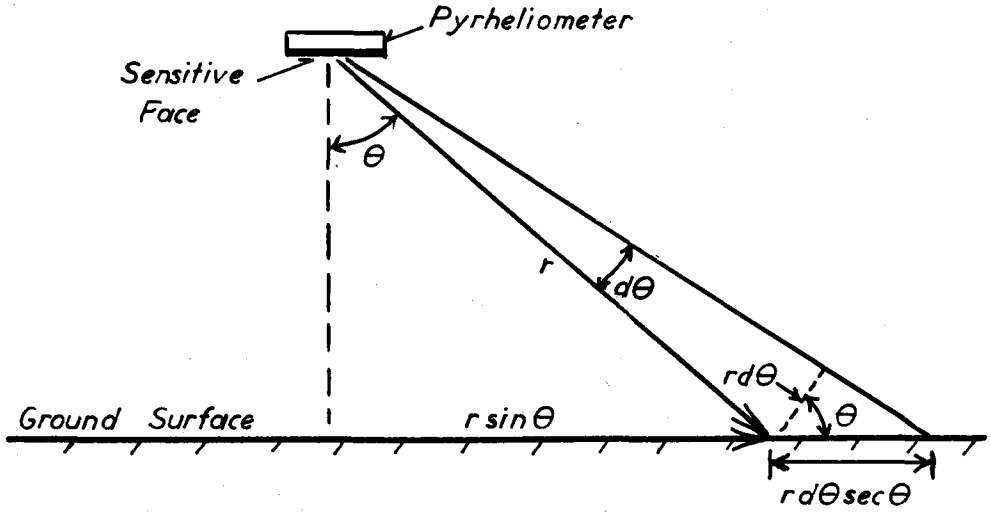
Pyrheliometer
Sensitive Face
θ
r
dθ
rdθ
θ
Ground Surface
r sin θ
rdθsecθ

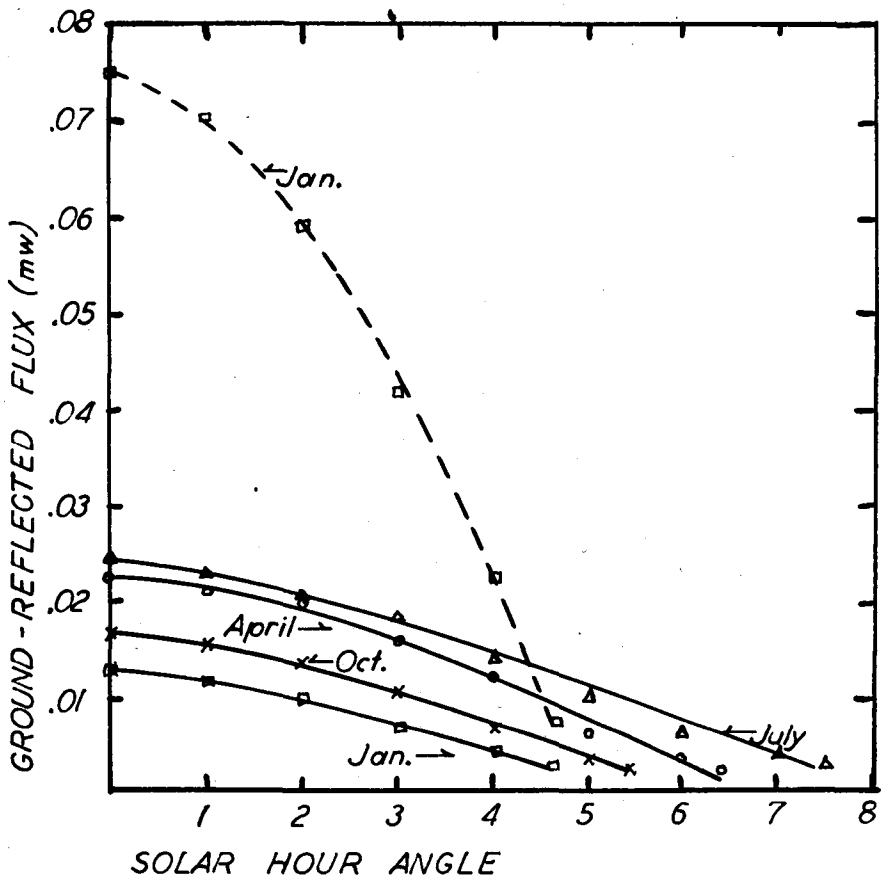
.08
.07
.06
.05
.04
.03
.02
.01
GROUND-REFLECTED FLUX (mw)
Jan.
April
Oct.
Jan.
July
1
2
3
4
5
6
7
8
SOLAR HOUR ANGLE

earlier in this Section) by the sines of the respective solar altitude angles and adding to this weighted value a flux of 0.170 langleys per minute representing the diffuse sky radiation flux on unit area of ground surface. (Although the diffuse irradiation of a plane horizontal surface, unlike the sphere, does vary somewhat with solar zenith angle, using the above value which corresponds to a 50° zenith angle yielded results which were found to have a maximum error of only about 4 per cent of the true value, so the assumption of a constant value of 0.170 langleys per minute was employed at this point.)

The resulting sums of F_i inserted into (7) gave the ground-reflection flux incident upon the bead when its area A was used and an appropriate value of the ground albedo was employed. The value selected above, $\alpha = 0.15$, was used to compute the reflective fluxes which are plotted in Figure 5 as representative of grass-covered soil or bare sandy soil. It may be seen from Figure 5 that the contribution of ground reflection to the radiative heating of the bead thermistor becomes largest at noon on clear July days but is only slightly smaller on April noons. For these extreme cases reflective heating is approximately equal to heating by diffuse sky radiation (0.025 milliwatts) but is only about one-third as important as direct solar heating at the same times (about 0.080 milliwatts).

In addition to the reflective fluxes for the case of an albedo of 0.15 for sod or soil, the flux for the special case of the very high albedo of a snow cover was also determined, since field observations on the present study are expected to be carried out throughout the year. Geiger (1950, p. 164) reports snow-cover albedo measurements which suggest a mean value of about 0.85. Using this value and January ground irradiation rates, the reflective flux on the thermistor was computed and the results shown as the dashed curve in Figure 5. Near noon on a clear January day with a fresh snow surface, the ground-reflection flux (0.075 milliwatts) is seen to be nearly equal to the direct solar flux (0.077 milliwatts). This implies the unexpected result that for the year as a whole the most serious total radiation error of the bead thermistor will appear in winter on clear days with snow cover, at which times the error may be expected to be almost twice as great as on clear summer noons.

The determination of the ground-reflected flux completes the treatment of the short wavelength contributions to the radiative heating of the bead thermistor. There remains only the long wavelength (infrared) contribution to be examined.

d. Infrared radiation. The absorption and emission of radiation in the wavelength range of from about 4 microns to about 20 microns must be examined for its role in the overall radiation balance of any thermal sensing element. Unlike the

previous three short wavelength components of the total radiative exchange, this last possesses the possibility of constituting a net cooling influence under certain conditions. Since the outer coating of the Western Electric bead thermistor is glass, which is almost completely opaque to the far infrared and to most of the near infrared, the bead will not only absorb but also, in view of Kirchoff's law, emit very nearly as a blackbody at atmospheric temperatures[1]. The slight departures from blackbody characteristics in a few bands peculiar to each variety of glass, have been ignored in the analysis of infrared exchanges at the bead surface.

The approximately spherical thermistor bead will radiate uniformly into the full hemisphere at a rate that will, for reasons just cited, be taken as full blackbody emission. This emission tends to cool the bead. On the other hand, the bead tends to heat up as a result of receiving infrared radiation from the full hemisphere; but this incoming radiation is not of uniform intensity from all directions. It is necessary to distinguish the terrestrial hemisphere from the celestial hemisphere in treating the incoming infrared. The horizon plane separates these two regions of space.

---

[1]The wavelength of maximum emission intensity for a blackbody at 300°K is about 9 microns, well beyond the redward cutoff of about 3 microns characteristic of most glasses.

If the absorption and reemission of infrared radiation within the slab of air lying between the soil surface and the level of the thermistor could be completely neglected, then assuming a soil surface of uniform temperature and possessing blackbody emitting characteristics (the latter being a very acceptable assumption in the wavelength range of importance here (Brunt, 1944, p. 138)), the infrared radiation incident upon the bead from the terrestrial hemisphere would be uniform in intensity and equal to blackbody radiation at the soil temperature. Actually, near the horizon the bead will see so much air between it and the distant soil surface that it will receive from these directions atmospheric radiation in those bands to which water vapor is opaque, plus soil radiation in the transparent band of the water vapor spectrum, near 10 microns. So long as one considers measurements made in about the first 10 meters above the surface, the fraction of total "terrestrial radiation" which originates in the air itself in these long oblique paths and which may thus differ in intensity from that of blackbody emission at the soil temperature will be small, since the path length must approach some 50 meters before the bead sees predominantly atmospheric rather than soil radiation in the opaque bands. Even for a point 10 meters off the ground, only 15 per cent of the terrestrial hemisphere lies close enough to the horizon (in the sense of solid angle subtended at the measuring point) that atmospheric rather than purely soil radiation

would have to be considered in a thorough analysis. For lower points of observation a smaller fraction of the hemisphere is involved. In the present study, where most of the observations will be made below about 6 meters elevation, this effect may be ignored with little error. Only if it appears that the net infrared radiative contributions are so large that very careful allowance must be made for all factors will this refinement have to be made. It must be noted that the effect in question makes a difference in the calculations only when the mean air temperature along the oblique path length differs markedly from soil temperatures, and even then the coincidence of the gap in the water vapor absorption spectrum with the wavelength of maximum emission at atmospheric temperatures renders the discrepancy less noticeable.

In view of the working assumption of negligible contribution of atmospheric radiation from the terrestrial hemisphere, the bead was regarded as seeing itself surrounded in this lower hemisphere by a blackbody at soil temperature so that the net power gain, G_t, via infrared exchange with the terrestrial hemisphere was just

$$G_t = 2\pi r^2 \sigma (T_s^4 - T^4) \qquad (8)$$

where r is the bead radius, σ is the Stefan-Boltzmann constant, T_s is the soil temperature, and T is the bead temperature. That the geometric factor $2\pi r^2$ is the appropriate one for this expression may be seen intuitively from symmetry conditions by imagining the spherical bead completely enveloped

by a sphere at T_s emitting as a blackbody and then taking just half of the accompanying net gain. (The relation (8) can also be obtained directly by integration of an expression of the same form as (6) above.)

In turning to the celestial hemisphere, one sees that the bead emits uniformly towards all zenith angles but receives back-radiation whose intensity increases from a minimum from the zenith to a maximum from near the horizon due to the lower effective radiating temperature of the elevated sources overhead (assuming the normal daytime decrease of air temperature with height in the surface layers of air). The calculational problem for the celestial hemisphere is thus that of estimating the magnitude of the net power gain, G_c, due to the exchange between the celestial hemisphere and the bead integrated over all zenith angles, taking account of varying back-radiation.

A closely related problem has been treated by Linke (1931) who found that Dubois' measurements of nocturnal radiation[1] from surfaces oriented at various zenith angles could be described by

$$N_z = N_0(\cos z)^k \qquad (9)$$

where N_z is the nocturnal radiation per unit area from a plane

---

[1]In physical meteorology the term, "nocturnal radiation", is defined to represent the net infrared radiative loss of energy from a surface. Paradoxically, it is largest at about noon.

surface whose normal is directed towards zenith angle z, N_o is the value of N_z for z = 0, and k is a function of atmospheric humidity tabulated by Linke on an empirical basis. Linke integrated this exchange function over zenith angle for several different cases including that of the horizontal surface, the sphere, and the vertical cylinder. The quantity N_o enters into each result so it was necessary to evaluate N_o in some way before Linke's integrals could be applied to the problem at hand. It was possible to effect this evaluation through consideration of the problem of the nocturnal radiation from a plane horizontal surface, a case for which numerous observations exist.

Linke's integral for the case of the horizontal surface represents the same net power loss found by Brunt (1944, p. 136) to be described with good accuracy over the range of meteorological interest by the expression

$$\sigma T^4 \left[1 - (0.44 + 0.080 \sqrt{e}) \right]$$

where T is the bead temperature and e is the vapor pressure in millibars at the level of the bead. By taking an e-value of 13 millibars (largest value for which Linke tabulated his exponent k), the nocturnal radiation from unit horizontal area into the full celestial hemisphere was computed from Brunt's formula, equated to Linke's integral for the same quantity, and the parameter N_o obtained therefrom. For the particular numerical magnitudes selected here as representa-

tive, N_o was found to equal $0.10\sigma T^4$.

With this value of N_o inserted into Linke's integral for the total nocturnal radiation from a sphere of radius r into the celestial hemisphere, a (negative) net power gain from this hemisphere amounting to

$$G_c = -0.43\pi r^2\sigma T^4 \qquad (10)$$

was obtained. The above procedure which takes account of the particular geometry of the sphere becomes necessary even in deriving only an approximate value for the celestial exchange because the sphere may lose energy at a rate almost twice that of a horizontal surface of equivalent vertically projected area.

The values of net power gain from the terrestrial and celestial hemispheres as given by (8) and (10) were added to get the total net gain via infrared exchange

$$G = 2\pi r^2\sigma\left(T_s^4 - T^4 - \frac{0.43T^4}{2}\right)$$

$$= 2\pi r^2\sigma T^4\left[\left(\frac{T_s^4}{T^4}\right) - 1.22\right] . \qquad (11)$$

The exchange expression (11) was used to investigate two particular cases of interest:

Case 1. $T \doteq T_s$. If the soil temperature is approximately equal to the air (and bead) temperature, the net power gain at the bead due just to infrared flux becomes

$$-0.43\pi r^2\sigma T^4.$$

This, of course, represents just the total nocturnal radiation to the celestial hemisphere, since complete cancella-

tion of emission and absorption occurs for the terrestrial hemisphere for this case. For a temperature of bead and soil of 300°K, and for the radius of the bead thermistor, the net exchange represents a loss at a rate of very nearly 0.020 milliwatts. Since this first case of nearly equal soil and air temperatures is likely to prevail near low-sun periods, a comparison with the incident insolational power at, say, an hour angle of 6 on a July day will be pertinent in forming some notion of how significant a factor infrared exchange may then be. Reference to Figure 3 reveals that for this time of day in July the direct insolational receipts themselves amount to only about 0.02 milliwatts. To this must be added about 0.025 milliwatts of sky radiation plus a small amount of ground-reflection (0.006 milliwatts according to Figure 5) giving a short wavelength absorption of about 0.05 milliwatts. For this case, then, a net loss via infrared amounting to 0.02 milliwatts would decrease the radiation error to about three-fifths of the value it would have in the absence of infrared exchange. If net infrared exchange were this significant a factor under all meteorologically important conditions it would have been in order to redo the above exploratory analysis under more refined assumptions. However, the conditions prevailing near midday remain to be examined as the other case of importance.

Case 2. $T_S > T$. When during midday conditions, in summer especially, the absorption of insolation at the soil

surface raises its temperature appreciably above the air temperature at instrument shelter level, the typical net loss by nocturnal radiation into the celestial hemisphere will tend to be canceled by net gain via exchange between bead and hot soil surface. Rather than consider a series of different T_S-values, sufficient orientation in the matter was thought to be attainable by determining only that soil surface temperature for which the bead just gains as much from the terrestrial exchange as it loses in the celestial exchange. Setting G equal to zero in (11) gave for this critical soil temperature value 45°C. This condition for zero net infrared exchange is, surprisingly, very close to the maximum soil surface temperatures observed under normal summer conditions with moderately dry soil (excepting deserts and artificial surfaces such as pavements which often reach 60 - 70°C).

Since soil-and air-temperature conditions more closely approximate Case 2 than Case 1 during that part of the day when turbulent temperature fluctuations are of interest as indicators of the process of vertical heat transport, it was decided to omit the infrared contributions entirely in all calculations, because for these conditions the net exchange by infrared is quite small. The remaining contributions would then yield a heating rate estimate which, if anything, would tend to be slightly too large, thus precluding any underestimate of the seriousness of radiation errors.

Hence, adding the contributions of direct solar radiation,

diffuse sky radiation, and reflected radiation, the total (short wavelength) radiative heating of the bead thermistor was found to vary as shown in Figure 6 for which the ground albedo has been taken as $\alpha = 0.15$ throughout the whole year for the solid curves, while $\alpha = 0.85$ for the dashed curve for January days with snow cover. These curves provided the information necessary to the prediction of thermistor radiation errors and hence of thermistor confounding errors. Before treating the other factor which must be known in making the error predictions, the dissipation function of the thermistor, an analysis of the role played by bead surface properties in controlling the level of radiation absorption will be summarized briefly and consideration given to the possibility of modifying the radiation errors by altering the surface properties.

2. Analysis of thermistor absorption cross-section

In all of the previous discussions the thermistor has been treated as if it were effectively black to incident short wavelength radiation. The basis for this point of view, as mentioned earlier, is that the glass coating possesses very low reflectivity, transmitting almost all of the incident radiation to the dark semiconductor nucleus inside. This viewpoint has neglected the effects of increasing reflectivity of the glass surface at those peripheral zones of the bead where the angle of incidence approaches 90°. To deter-

Figure 6. Sum of all short wavelength radiation intercepted by the bead thermistor.

Solid curves represent case for surface albedo of 0.15 (grass-cover); dashed curve represents case of surface albedo of 0.85 (snow-cover) for January only.

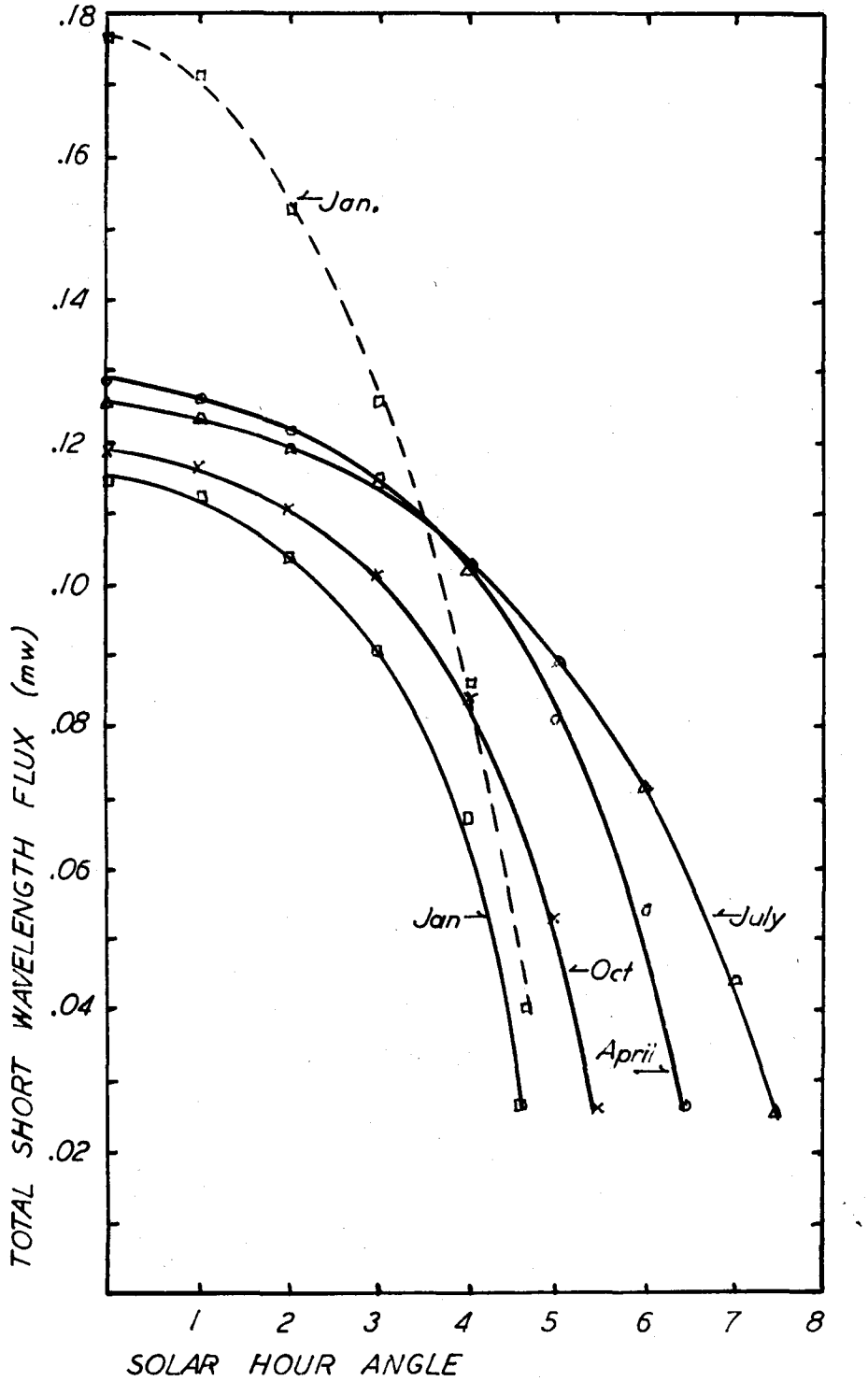
.18
.16
.14
.12
.10
.08
.06
.04
.02
TOTAL SHORT WAVELENGTH FLUX (mw)
1
2
3
4
5
6
7
8
SOLAR HOUR ANGLE
Jan.
Jan
Oct
Aprii
July

mine whether this latter effect is appreciable, the variation of the reflectivity with angle of incidence was taken into account in a calculation of what may be called the "absorption cross-section" of the bead.

After dividing the surface of the bead into 10^{o}-zones of latitude about a polar axis taken parallel to the incident radiation and computing the projected area of each zone as seen from the source of radiation each projected area was weighted by the reflection coefficient characteristic of the angle of incidence of the rays striking the central parallel of latitude of that zone. The reflectivities as a function of angle of incidence were taken from Jenkins and White (1937, p. 390). Summing these weighted projected areas gave an effective absorption cross-section, as distinguished from the geometric cross-section of the bead. The result for the effective absorption cross-section was 0.91A, where A is the geometric cross-section; so the previous treatment of the bead as fully black has involved an overestimate of radiation absorption which amounts to an error of about 10 per cent. To correct for this difference between geometric and effective cross-sections, all radiation totals have been reduced by multiplication by 0.9 before being used elsewhere. (The correction is certainly not significant to more than one digit in view of the fact that the beads are not perfect spheres.)

Having determined the correction factor needed to allow

for reflective losses at the glass surface of the beads there remained the question of the extent of transmission losses. Those incident rays which strike the bead near its equator (defined with reference to the spherical coordinate system used in the preceding paragraph) may, upon undergoing refraction, fail to be deviated far enough to strike the dark absorbing nucleus of semiconductor material, with the consequence that all such rays will again reach the glass-air interface and (except for slight internal reflection losses) escape.

The extent of such transmission losses of rays incident on the low-latitude zones depends on the refractive index of the glass and on the ratio of nucleus radius to overall radius. On assuming an index of refraction of 1.5 for the glass and considering the case of the rays which just strike the equator of the bead at grazing angle of incidence (case most favorable for transmission losses), one finds, from geometrical optical considerations that these particular refracted rays would fail to reach the absorbing nucleus only if the latter's radius were less than two-thirds as large as the radius of the glass-air interface. For all cases wherein the nucleus radius exceeded this critical value, and hence for which no transmission losses could occur, the very refractive effects responsible for the deviation of the rays towards the nucleus would serve to make the nucleus appear, on visual inspection, to fill completely the spherical space lying

within the actual glass-air interface. And, in general, to determine the extent of transmission losses, one need only compare the visually apparent projected area of the dark nucleus with the total projected area of the bead to determine the ratio of effective absorbing cross-section to geometric cross-section.[1]

Ten specimen beads were examined under a microscope to determine the ratio of the apparent projected area of the nucleus to the total projected bead area. The results of this examination were distrubing to the above analysis in that the nuclear masses of semiconductor were found to be neither spherical nor concentric with the outer surface in most beads, as had been assumed in the above analysis. Furthermore, the diameters of the beads were uniformly higher than the value of 0.033 centimeters given in the manufacturer's specifications and used in numerical calculations above. (The overall diameters as measured with a traveling microscope averaged 0.040 centimeters for the ten beads, the standard deviation being 0.002 centimeters.) But most significant of all, the ratio of the apparent diameter of the nucleus to the overall diameter averaged only 0.52, with a standard deviation of 0.07 for this ratio, the relative variability of nuclear size being somewhat greater than that of total size. Since the ratio of apparent areas must vary

---

[1]Drs. D. W. Stebbins and L. T. Earls called this point to the author's attention.

as the square of the linear dimensions, the effective absorption cross-section is only about $(0.52)^2 \approx 0.27$ times as large as the geometric cross-section. In view of the variability of the measured nuclear dimensions, this computed ratio is best rounded off to 0.3.

Since the measured overall diameters averaged 0.040 centimeters while 0.033 centimeters had been used earlier in the radiation calculations, the correction factor to take account both of transmission losses and of departures from manufacturer's specifications became $0.3(0.040/0.033)^2 = 0.44$, better taken simply as 0.4 here.

It should be noted that since the reflective losses discussed earlier occur predominately in the same peripheral zones of the projected area of the bead wherein the transmission losses occur, only the transmission loss factor of 0.4, and not 0.4 times 0.9 (reflection loss factor), is to be used to correct previous radiation absorption rates. That is, one would be discounting the loss of the peripheral rays twice if both factors were employed, so only the transmission loss factor of 0.4 is to be used.

There remained one other factor which had to be considered -- radiative absorption by the wires and supporting members

which are in thermal communication with the bead.[1] Figure 1 shows that the tiny bead is supported by four small copper wires (0.0025 centimeters in diameter and 0.4 centimeters long) which are, in turn, secured to four larger copper wires (0.040 centimeters in diameter). It is the question of possible thermal influences exerted on the bead by these wires that is to be considered.

If each of these wires were thermally isolated, they would be absorbing radiation at some rate which would cause them to heat up to such an excess over ambient temperature that, in the steady state, they would dissipate heat at exactly the rate of absorption. But because they are not thermally isolated, the possibility exists that they may be either losing part of their radiatively absorbed energy via intra-wire conduction to neighboring parts of the device or else gaining additional energy via conduction from neighboring parts. In general, those parts of the system which are poor absorbers but good dissipators will be gaining heat via conduction from those parts which are good absorbers but poor dissipators.

---

[1]The author is indebted to Dr. D. W. Stebbins for having suggested this study of the role played by the wires. The investigation, which was carried out after completion of the major part of this work, revealed that the very fine wire leads to the thermistor bead are of considerable importance both in the absorption of radiation and in the dissipation of heat to the ambient air. Unfortunately, the dissipation rates of small wires could not be determined precisely enough to carry out this analysis with satisfactory accuracy, but certain useful conclusions were attainable and are described in the following discussion.

The first question to be considered is whether it is at all possible that the wire parts might absorb radiation at a rate that would become appreciable compared with that absorbed by the bead itself. Assuming that each of the four 0.0025-centimeter diameter copper wires has an albedo of 0.5 and is 0.4 centimeters long, each will absorb 0.045 milliwatts if irradiated with just a direct solar intensity of 1.3 langleys per minute. (This maximum direct solar intensity (Figure 3) will be used here in lieu of a rate based upon all of the effective fluxes.) Hence all four wires will be absorbing a total of about 0.18 milliwatts, which is some three times more power than the bead itself will absorb under extreme conditions (taking transmission losses into account). Furthermore, the larger (0.040-centimeter diameter) copper wires composing the support for the fine wires may be expected to be absorbing still larger amounts of radiation, so it appears necessary to examine the whole problem fairly carefully.

Since the four fine wires that are in contact with the bead itself must be expected to influence the bead the most, their thermal contributions will be studied first. If each one of these wires receives radiative flux R per unit length, then the steady-state heat equation describing the fine wires alone becomes

$$R + K\pi r^2 \frac{d^2T}{dx^2} = 2\pi rh(T - T_a) , \qquad (11a)$$

where K is the thermal conductivity of the copper wire, r is

its radius, T is the temperature of the wire at a distance x from the bead, T_a is the ambient air temperature, and h is the dissipation rate in calories per square centimeter per second per degree excess of T over T_a. The solution to this equation is

$$T(x) = c_1 e^{bx} + c_2 e^{-bx} + T_a + \frac{R}{K\pi r^2 b^2}, \qquad (11b)$$

where c_1 and c_2 are integration constants, and

$$b^2 = \frac{2h}{Kr}. \qquad (11c)$$

The application of (11b) to the determination of actual magnitudes of conductional flow of heat from the wires to the bead requires that the dissipation rate, h, be known for the fine wires. As will become clearer from the discussion of thermocouple errors given below, there exists at present no sure basis for assigning a numerical value to this quantity. It will be sufficient here to point out that the calculations using (11b) were initially based on an equation given by King (1914) for the heat loss rates of small wires (see Equation (19) below). For a wire of 0.0025-centimeter diameter with an ambient wind speed of 0.25 meters per second (chosen low in order to place an upper limit on the errors), h is found from King's equation to be 4.0×10^{-2} calories per square centimeter per second per degree excess of wire temperature over ambient temperature. Using this value of h and imposing the boundary conditions that $T(0) = T_t$, the thermistor temperature,

and $T(0.4) = T_s$, the temperature of the heavy wire supports located at the end of the fine wires, one finds the temperature distribution within the wires to be given by

$$T(x) = (0.036T_s - 0.002T_t - 0.003)e^{8.3x} + (-0.036T_s + 1.002T_t - 0.086)e^{-8.3x} + 0.088, \quad (11d)$$

when the ambient temperature, T_a, is set equal to zero as a convenient reference value.

A plot of (11d) for almost any reasonable values of T_t and T_s revealed that the temperature within the fine wires would pass through a minimum value such that heat would be flowing by conduction from the bead thermistor and also from the heavier support wires. That is, the fine wires would appear, on the above assumptions, to be such good dissipators that they would be able to protect the bead from conductional heat-flow originating in the larger and hence hotter support wires, and would even assist the bead in dissipating some of its own radiatively absorbed power.

This promising conclusion was, however, subject to the same uncertainty as to the validity of the King equation that will be shown to exist in the later discussions of the radiation errors of thermocouples. There it will be pointed out that some grounds exist for suspecting that the actual dissipation rates of wires which are heated to only a few degrees above ambient temperature may be only about one-tenth as large as those predicted by King (and actually found by him to occur

for wires heated to several hundred degrees above room temperature).

To see what changes would be imposed on the problem if the fine wires were only one-tenth as good dissipators as was assumed above, (11b) was next evaluated for $h = 4.0 \times 10^{-3}$ calories per square centimeters per second per degree excess. It was found that if the bead were 0.4 C° above ambient temperature, then it would lose heat via conduction to the fine wires only as long as the heavy wire supports were no hotter than a mere 0.1 C° above ambient temperature. (It turned out that for this low value of the dissipation rate of the fine wires, the latter were predicted by (11b) to be even hotter than 0.4 C° unless the support wires were cool enough -- less than 0.1 C° above ambient temperature -- to withdraw heat from the fine wires themselves. This is clearly impossible, since the heavy support wires will always be still poorer dissipators than the fine wires.) As this requirement on the support wire temperatures cannot be met, the bead must surely suffer additional heating via inflow from the fine wires, which will be passing it along from the still hotter supports, if it is indeed true that the actual dissipation rate is as low as one-tenth the King value.

The question of the appropriate values to assign to the dissipation rates of small wires is so significant here and in the evaluation of thermocouple errors that it was felt worthwhile to extend the above analysis somewhat further in

the hope that some more reliable indication of the validity, or lack of validity, of the King equation might be found. The approach employed consisted of an analysis of the conditions existing during the experimental determination of the dissipation rates of the bead thermistor. (This experimental determination will be discussed below in enough detail that it need not be elaborated here. See pp. 44 ff.) It is necessary to point out that during this determination the wires were not irradiated; but rather, all of the heat which they were dissipating reached them by conduction from the bead which was Joule heated. In the analysis the assumption was made that the heavy wires were infinitely long, and the heat equations for the fine wire and the heavy wire were solved as a simultaneous system subject to continuity of temperature and of heat flux at the junction of the two wires. It was found that when the King value of the dissipation rate was used in a numerical evaluation of the solution, the predicted conductional heat flux out of the bead and into the fine wires was impossibly large, some six times greater (total for all four wires) than the experimentally measured Joule heating rate within the bead. This result appreciably strengthened the author's suspicions, to be elaborated later here, that the King equation overestimates the dissipation rates of wires operated at low excess temperatures. As a rough check, the same calculations were next performed using a dissipation rate only one-tenth as large as the

King value. It was found that even for this reduced dissipation rate the combined conductional flow via the fine wires was about 2.5 times greater than the total dissipation rate measured during the laboratory determinations of the thermistor dissipation rates, which suggests that the dissipation of heat from fine wires must be even less efficient than one-tenth the King rate.

With this result in mind, the problem of the irradiated bead-and-wire system was reexamined, using a trial dissipation rate one-tenth that given by King and it was found that for almost any plausible values of bead temperature and support-wire temperature, heat would be flowing into, not out of, the bead via conduction in the fine wires. For the case of a bead temperature of 0.5 C° (approximate value of radiation error actually measured under some preliminary field tests) and for a support temperature of 2 C° (approximate radiation error found by Thornthwaite (1949) for copper-constantan thermocouples made from wire of the same size as that comprising the heavy supports), the combined flux into the bead through all four fine wires was computed to be 0.27 milliwatts. This is about two times larger than the maximum radiative power absorption rate of 0.13 milliwatts computed for the bead and shown in Figure 6. This flux of 0.13 milliwatts was found prior to introduction of the correction factor of 0.4 for transmission losses. If the correction for transmission losses and also for influx of conductional heat are made on the basis of just the above rough

figures the total power load becomes about 0.4x0.13 + 0.27 = 0.32 milliwatts as an extreme value for high radiation intensity and low wind speed. (Recall that a wind speed of only 0.25 meters per second has been assumed throughout here.) This estimated total is about 2.5 times larger than the previously computed total radiation flux itself and about 80% of this newly estimated total is due to conductional flux.

This result may only be regarded as indicative of the general order of magnitude of the heat flux from the heavy support wires because it was based on a dissipation rate of one-tenth the King value, a rate which is still too large if the analyses discussed above are essentially correct. Lacking suitable experimental data on wire dissipation rates, it does not appear possible to make any more precise estimates of the overall heat balance of the bead thermistor than the above very rough one. In view of the uncertainties involved in assigning numerical values to the rates of heat loss from the wire components of the thermistor, the thermistor radiation error estimates given below will be based upon the numerical power values previously calculated just from radiative heating of the bead alone. Needless to say, the efforts made earlier to obtain fairly accurate values of these radiative contributions to input power are now rendered somewhat superfluous by the suspected large conductional heating effects due to the wires.

The results found above which indicate that the King

equation yields dissipation rates too high by a factor of at least ten do represent one useful outcome of this analysis of wire effects. Taken together with several isolated bits of confirming evidence to be cited in the discussion of thermocouple dissipation rates below, they focus suspicion on the validity of King's hot-wire anemometer equation for the analysis of wire-type thermal sensing elements. An experimental investigation of heat loss from only slightly heated wires is strongly recommended in order to provide precise information as to the dissipation rates, for which no accurate values can be obtained from the existing literature on this general subject.

As an additional comment on the importance of the fine wires in exchanging heat between the semiconductor nucleus and the ambient air, it may be pointed out that a calculation of the heat flux from semiconductor to air via the glass coating and a similar calculation for the copper wires indicated that at least three-fourths of the heat exchange is effected via the wires. The thermal conductivity of copper is about 500 times greater than that of glass and so, despite the fact that the conducting cross-section of the wires is very much smaller than that of the glass (of the order of one-hundredth as large), the copper wires must carry heat in or out about three times as well as does the glass coating. This result was found on the assumption that the inner surface of the glass shell and also the inner ends of the copper wires were at the nucleus temperature; but since the wires are actually embedded

in the nucleus while the inner surface of the glass is not in contact with the central section of the nucleus where the current density must be highest, the above results probably tend to be an underestimate of the relative contribution of the wires. This helps to understand why the thermistor exhibits directionality in its dissipation rate, a point to be discussed later here.

The seriousness of the radiation errors that develop as a result of radiative heating of the bead and wires may be reduced if it becomes possible to apply to them a high-albedo coating that will cut down the effective absorption cross-section. Thus, in the case of just the bead itself, a calculation of the ratio of effective absorption cross-section of a silvered bead to geometric cross-section revealed that this ratio might be lowered to 0.1 if the fullest reflecting possibilities were realizable. Attempts to realize this reduction of radiation error have not been carried out in complete enough fashion to state whether it is a practicable solution to the problem.

3. Determination of thermistor dissipation function

The next step towards the evaluation of radiation errors consisted in determining the rate at which heat is dissipated by convection[1] from the bead to the ambient air for given airspeed and excess of bead temperature over air temperature.

The steady-state error of temperature indication of the

---

[1]Since the bead temperature never exceeded the air temperature by more than about 0.5 C° in the process of measuring the dissipation rates, and since it was almost completely surrounded by a chamber whose walls were at air temperature, net radiative cooling was quite negligible.

element for given power input and given air speed must be the same whether that input power arrives as radiation or is supplied in any other fashion not altering the exterior heat transfer boundary conditions. A particularly convenient way of producing that heating effect was to employ internal Joule heating in the bead by operating the bead at so high a current level that the power dissipation was at some known value in the general neighborhood of the radiative power values to be encountered under field conditions. By measuring the electrical power dissipation at each of a series of wind speeds covering the meteorological range of interest, noting for each the steady-state excess of bead temperature over ambient air temperature, and then dividing the power dissipated by the observed temperature excess, a set of heat-loss rates was obtained. This set of values was regarded as defining the "dissipation function" of the element.

This electrical method of determining the dissipation function was used for a number of thermistor beads.[1] In Figure 7 the curve through the experimental points shows, for one particular specimen thermistor, a sample plot of the variation of excess of bead temperature over air temperature as the wind speed past the bead was varied (by

---

[1]The experimental work on the dissipation function was done by Dr. A. R. Kassander and Mr. R. W. Green of the Department of Physics, Iowa State College.

means of a rotating-arm technique at the low speeds and in a wind tunnel at higher speeds). This particular plot is for a Joule heating of 0.075 milliwatts. By dividing this power dissipation by the excess temperature measured at each wind speed, the dissipation function plotted as the solid curve in the same figure, with its ordinate scale at the right, was obtained. In this manner all of the dissipation function curves of Figure 8 were derived. The heavier curve in Figure 8 is identical with that of Figure 7 and is seen to represent a fairly typical dissipation function. As such it was used for all of the numerical computations to be discussed later.

As is to be expected, the dissipation function is smallest in still air, about 0.1 milliwatts per Centigrade degree for the heavy curve of Figure 8, and increases rather rapidly with wind speed at low speeds, less rapidly at higher speeds, and attains a value about four times the still-air value at speeds of around 20 meters per second. Half of the increase of the dissipation observed in going from 0 to 20 meters per second is already realized at speeds of only about 4 meters per second.

Unfortunately, the less than perfectly spherical shape of the beads and the asymmetrically affixed lead wires impose certain asymmetries of response of the beads to air currents arriving from different directions. However, it

Figure 7. Example of variation of excess bead temperature with varying wind speeds, and derived dissipation function.

The experimental points represent excess of bead temperature over ambient temperature and refer to the left-hand scale of ordinates. The dissipation function derived from the smoothed curve of excess temperatures refers to the right-hand scale of ordinates.

Figure 8. Dissipation functions of eight bead thermistors.

The curve drawn heavier than the rest is the dissipation function of the same bead as that represented by the curves of Figure 7 above.

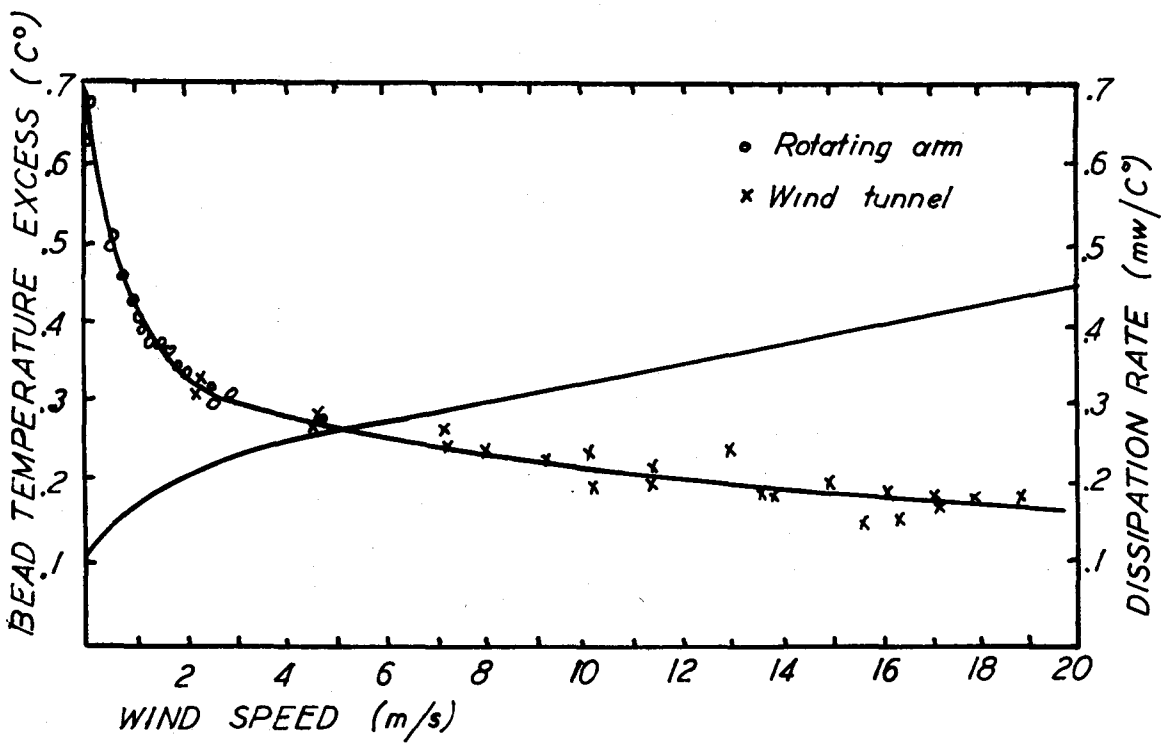
BEAD TEMPERATURE EXCESS (C°)
DISSIPATION RATE (mw/C°)
• Rotating arm
× Wind tunnel
.1
.2
.3
.4
.5
.6
.7
2
4
6
8
10
12
14
16
18
20
WIND SPEED (m/s)

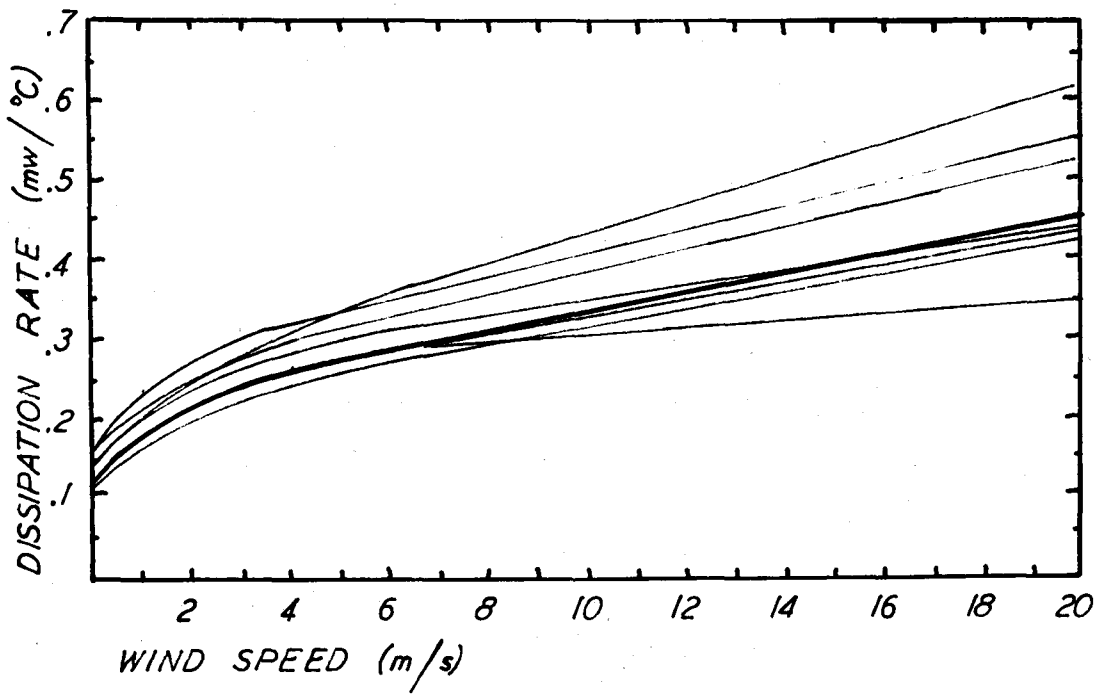
DISSIPATION RATE (mw/°C)
.1
.2
.3
.4
.5
.6
.7
2
4
6
8
10
12
14
16
18
20
WIND SPEED (m/s)

was found experimentally that the lead wires could be so deformed as to permit mounting of the beads in a manner that reduced the variations of dissipation function to a minimum for azimuthal variations of the wind vector. For this specially prepared condition, the azimuthal variations of the dissipation function were found to be less than 10% of the mean. Variations of the vertical component of the wind with this manner of mounting will lead to additional fluctuations of dissipation function, but these will not be taken into account here and are quite small anyway.

A description of the experimental techniques employed in the determination of the dissipation functions has been given by Kassander (1951). The wind tunnel employed in the work has been discussed by Sanford (1951) in a paper on thermistor anemometry.

4. Evaluation of radiation errors and confounding effects

As was pointed out at the end of the discussion of the effects of the wire leads and supports, the exact values to be assigned to the total radiative absorption are quite uncertain and will be until experimental information is available concerning wire dissipation rates. Lacking this information, one can only make very rough estimates of the field performance of the bead thermistor. However, in order to get some idea as to how serious the radiation errors might possibly be, these will be analysed in this section on the basis that the absorbed radiative flux is that given by just the flux absorbed by the bead,

treated as a black absorber. That is, no allowance will be made for transmission losses. Neglect of these losses will tend to cancel the similarly neglected effects of the wires in heating the bead. The results can, of course, be regarded as only very rough approximations to the real errors.

a. Steady-wind radiation errors. The first application of the available radiation and dissipation data will be to a determination of the radiation error level associated with each of a number of steady wind speeds over the full daytime range of hour angles from noon to sunset (or sunrise to noon) for a clear July day.

Using the total short wavelength radiation receipts as given in Figure 6, reducing them by a factor of 0.9 to allow for the difference between effective and geometric cross-sections, and multiplying the several results by the dissipation rates (Figure 7) characteristic of each of a series of wind speeds ranging from complete calm up to 20 meters per second, the radiation error curves of Figure 9 were obtained. Since the actual wind speed almost never remains constant over a period of a whole day, it should be emphasized that these curves do not depict directly the diurnal variation of thermistor radiation errors on any one day. They are presented to indicate the general magnitudes of mean errors associated with various possible combinations of time of day and of wind speed.

The case most conducive to large thermistor radiation

Figure 9. Dependence of steady-wind radiation error of a bead thermistor upon wind speed and hour angle for a clear July day.

Each curve is labeled with the steady wind speed to which that curve applies.

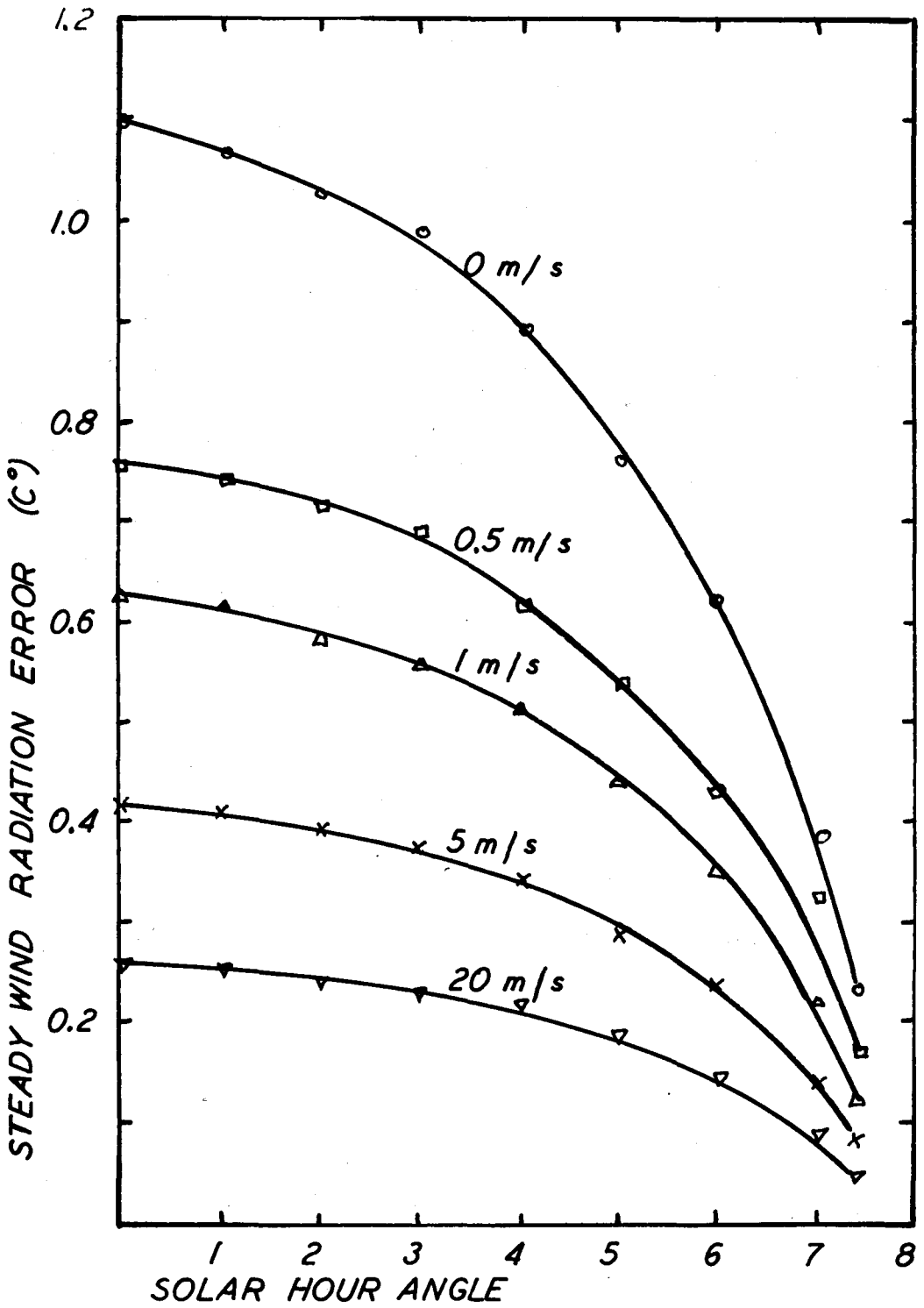
1.2
1.0
0.8
0.6
0.4
0.2
STEADY WIND RADIATION ERROR (C°)
0 m/s
0.5 m/s
1 m/s
5 m/s
20 m/s
1
2
3
4
5
6
7
8
SOLAR HOUR ANGLE

error, complete calm, is seen from Figure 9 to lead to a predicted error which becomes as great as 1.1 C° at noon, and is still about 0.2 C° at sunset (sunrise), due to twilight sky radiation and to ground-reflected sky radiation. As the wind speed increases from zero the errors at any given solar hour angle fall off fairly rapidly at first and less rapidly later due to the nature of the dissipation function. Even for very strong winds of 20 meters per second the July noon error is more than 0.2 C°. The average surface wind speed in Iowa (at anemometer level) in the summer months is about 3 meters per second, so the radiation errors near the ground (at a height of perhaps 2 meters) might be expected to average about 0.5 C° near midday at that time of year. Very close to the ground surface (first millimeter), where the mean air speed is held to very low values by surface friction, the errors must approach those indicated by the uppermost curve of Figure 9.

A somewhat more revealing mode of representing essentially the same data is presented in the solid curves of Figure 10. Here the radiation errors to be expected on a clear July day at each of three different heights above level ground have been computed using actually observed wind speeds corresponding to each of the three heights. No suitable wind data for any central U. S. station were available for use here, so mean wind speeds observed throughout

Figure 10. Dependence of radiation error of a bead thermistor upon elevation and hour angle for a clear July day (solid curves) and dependence of mean wind speed upon elevation and hour angle for summer months at Potsdam (Hellmann).

Radiation error scale is at left, wind speed scale at right. Each curve is labeled with the height to which it applies.

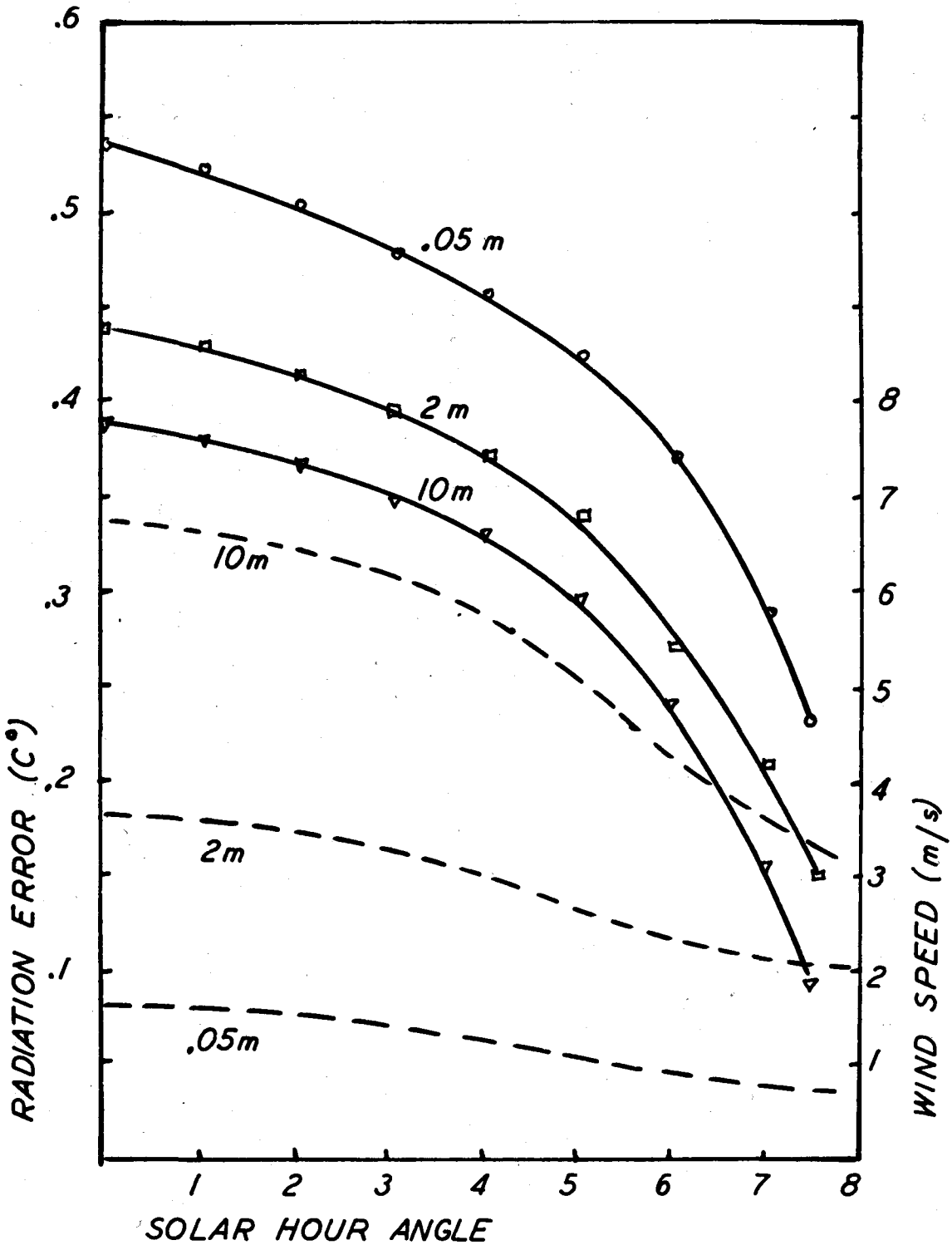
.6
.5
.4
.3
.2
.1
.05 m
2 m
10m
10m
2m
.05m
RADIATION ERROR (C°)
WIND SPEED (m/s)
8
7
6
5
4
3
2
1
1
2
3
4
5
6
7
8
SOLAR HOUR ANGLE

the summer months at Potsdam by Hellmann (reproduced in Geiger, 1950, p. 108) were employed for the levels at 0.05 meters and 2 meters above the ground. The values at the 10 meter level were obtained by extrapolation from Hellmann's data using a power law wind profile,

$$U_z = U_1 z^p,$$

where U_z is the mean speed at height z, U_1 is the mean speed at a height of 1 meter, and the exponent p was taken as 0.3 on the basis of the form of Hellmann's profiles in the first two meters. The wind speeds themselves are shown as the dashed curves in Figure 10, the wind speed scale being plotted at the right of the figure.

The chief implication of Figure 10 lies in the information it conveys concerning the variation of radiation errors with height under representative wind-profile conditions. Since the wind speed normally increases with height (in a manner indicated by the power law employed above) there will exist systematic bias in the temperature measurements made at a series of levels above the ground, due to systematic variations in the mean value of the dissipation function. The solid curves of Figure 10 reveal, however, that for the bead thermistor such bias is not extreme. Thus the mean indicated temperature at the 0.05 meter level will be only about 0.15 C^o higher than that at the 10 meter level as a result of the decrease of wind speed near the ground. Since a typical summer midday temperature

distribution may involve an air-temperature difference of 3 to 4 C° between these levels, an error difference of some 0.15 C° will not distort the measurement of lapse rates by more than a few per cent.

One may conclude from these results that the bead thermistor will yield lapse rate measurements which are not, by current micrometeorological standards of accuracy, seriously affected by radiation error. This conclusion is pertinent to the present study inasmuch as thermistors will be used to determine the lapse rates of temperature prevailing in the layers of air in which fluctuation measurements are made. The lapse rate of temperature is a measure of the stability of mass stratification of the air which in turn is of dominant importance in controlling the intensity of turbulence of the wind.

b. Confounding effects. By referring to Figure 9 and considering any one time of day, one sees that if the wind speed is fluctuating, then, as the speed changes from one value to another at the fixed point of temperature observation, the indicated temperature must oscillate concurrently even though no true air temperature fluctuations are occurring. It was the determination of the intensity which could be expected to characterize this sort of "confounding effect" that constituted the ultimate objective of the present radiation error study.

On examining the problem, one immediately recognizes that the degree of fluctuation of the wind speed must play as important a role as does the extent of the radiation error in controlling the amplitude of the spurious fluctuations due to confounding effects. Hence a careful search of the literature was undertaken to gather all available information concerning the degree of wind speed variability to be expected under field conditions.

In some excellent studies made by Sherlock and Stout (1936) using rapidly responding pressure-plate anemometers (lag-times of the order of 0.01 second), a standard deviation of 6.5 miles per hour was found for the fluctuations of wind speed about a mean of 31 miles per hour. This represents a 0.21 coefficient of variation (ratio of standard deviation to mean). It is pertinent to note here that Sherlock and Stout found the distribution of fluctuations to be skewed in the sense that there were only a few very large positive deviations from the mean but many small negative deviations. Inasmuch as the curvature of the dissipation function is such as to imply smaller confounding errors for positive deviations of given magnitude than for negative deviations of the same magnitude, one would tend to be erring on the side of overestimation of confounding effects to use their figure of a 0.21 coefficient of variation, as a simple analysis will show.

Giblett (1932, p. 49) studied the ratio of "mean eddy

speed" to mean speed and found an average value of 0.16 using pressure-tube anemometers at 50 feet above the ground. He defined his "mean eddy speed" as the mean of the absolute magnitude of the vector difference between the hourly mean wind vector and the individual 5-second mean wind vectors with which he dealt. It was possible to extract additional information from Giblett's work by making a statistical study of the wind speed fluctuations indicated in the numerous anemograph records produced in his paper. It was found that though occasional gusts involved temporary changes by as much as half the mean itself, the standard deviation of the fluctuations was only 0.3 times the mean.

Huss and Portman (1949) reported a coefficient of variation of 0.10 for a mean wind of 10 miles per hour, increasing to 0.15 for a mean of 30 miles per hour. Heywood (1931) defined a "gustiness factor" as the mean width of the anemograph trace divided by the mean wind itself, a quotient roughly comparable to the coefficient of variation. He found values of this factor ranging from 0.1 to 0.2 at 95 meters elevation, with values as large as 0.48 at 13 meters elevation.

Using a rapidly responding hot-wire anemometer, Richardson (1950) measured wind fluctuations within a few meters of level ground and his results imply coefficients of variation lying below 0.20 in the majority of cases, with the greatest value only 0.32. Richardson's results are in

good agreement with those of Cramer (1951) who found coefficients of variation of from 0.10 to 0.32 with a hot-wire anemometer of 0.1 second lag-time, the largest values of which were observed in the late afternoon or early evening, to his surprise. Schilling and others (1946) reported a limited series of hot-wire anemometer measurements from which they derived a coefficient of variation of 0.25. Since the coefficient of variation derived from analysis of the wind speed record of a very inert instrument would inevitably be lower than the true value, these last three references were of particular value here in that they involved studies made with the hot-wire anemometer, an instrument whose lag time is quite low.

On the basis of all of the above information on gustiness it was decided that a working value of 0.25 for the coefficient of variation ought to provide a realistic basis for estimating the seriousness of the confounding effects of a thermal element. Although individual excursions of the wind speed do produce departures from the mean of more than one-fourth of the mean speed, the average effect of confounding errors on the fluctuation statistics seemed fairly well represented by the 0.25 value of the coefficient of variation employed for the computations.

Since the case most conducive to large confounding action is that of noon, the July noon radiation total of

0.126 milliwatts (Figure 6) was used to determine the upper limit of error. Also, to err on the side of overestimation, the amplitudes of the confounding fluctuations were computed for lulls (rather than gusts) of 0.25 times the current means. Mean wind speeds of from 0.2 to 10 meters per second were used to compute the confounding error amplitudes shown in Figure 11 as the lower curve marked "0.25 $\bar{U}$". The curve reveals that the confounding error, under the assumptions employed to determine it here, varies between 0.04 C° and about 0.075 C° in the wind speed range represented. For comparison, and as an indication of extreme values that might be expected on very gusty days, the confounding errors for lulls of 0.5$\bar{U}$ have also been determined and are shown as the upper curve of Figure 11. These latter values are almost, but not exactly, twice those of the lower curve, the non-linearity of the dissipation function preventing an exact twofold relation.

To show the extent to which the background of confounding fluctuations might vary with height above the ground at different times of day, Figure 12 was prepared. Here the diurnal variations are those due to the joint action of varying radiation absorption (July curve, Figure 6) and of varying mean wind speeds at the three levels represented (dashed curves, Figure 10). These two factors were used to obtain from Figure 11 the values of confounding errors

Figure 11. Confounding error amplitudes of a bead thermistor at noon on a clear July day.

The lower curve has been computed for the case of wind speed lulls of $0.25\bar{U}$ where $\bar{U}$ is the mean wind speed represented on the abscissa. The upper curve has been computed for lulls of $0.5\bar{U}$.

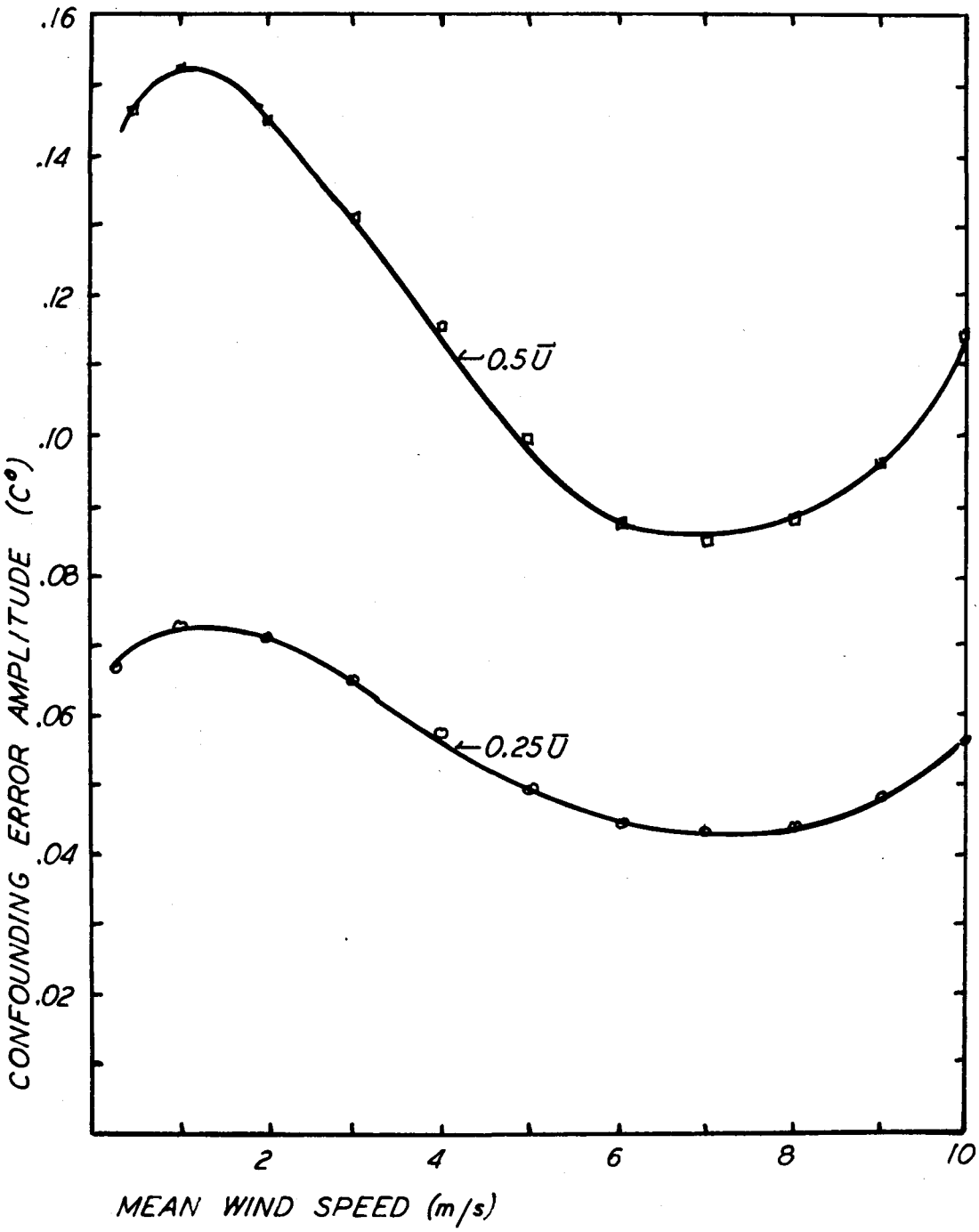
.16
.14
.12
.10
.08
.06
.04
.02
CONFOUNDING ERROR AMPLITUDE (C°)
←0.5 Ū
←0.25 Ū
2
4
6
8
10
MEAN WIND SPEED (m/s)

plotted in Figure 12. As is to be expected, the largest amplitudes of confounding effect (for the assumed 0.25$\bar{U}$ lulls) appear at the level closest to the ground where the ventilational fluctuations have the largest mean radiation error upon which to act, yielding an amplitude exceeding 0.07 C^{o} at midday. Thermistors located at greater heights will, however, enjoy only a slightly greater advantage, for even at 10 meters above the ground the midday amplitude of the confounding fluctuations is only 0.03 C^{o} smaller than that at 5 centimeters above the ground. Since the July irradiation rates are, with the exception of the anomalous January snow-cover case and the slight midday excess of the April rates, extremal for the year as a whole, it was concluded that the fluctuation statistics derived from the records of thermistors mounted at a series of levels from about 10 centimeters above the surface (lowest planned) to about 6 meters above the surface (highest planned) would not suffer serious differential distortion tending to obscure real height variations of the fluctuations within the turbulent flow.

Having found that the height-variations of the confounding error are negligible, there remained the problem of finding a criterion by which to decide whether the actual error itself at any given level was tolerably low. Since the problem under consideration here is essentially

Figure 12. Dependence of confounding errors of a bead thermistor upon height and hour angle on a clear July day.

The height above the ground to which each curve applies has been entered above each curve.

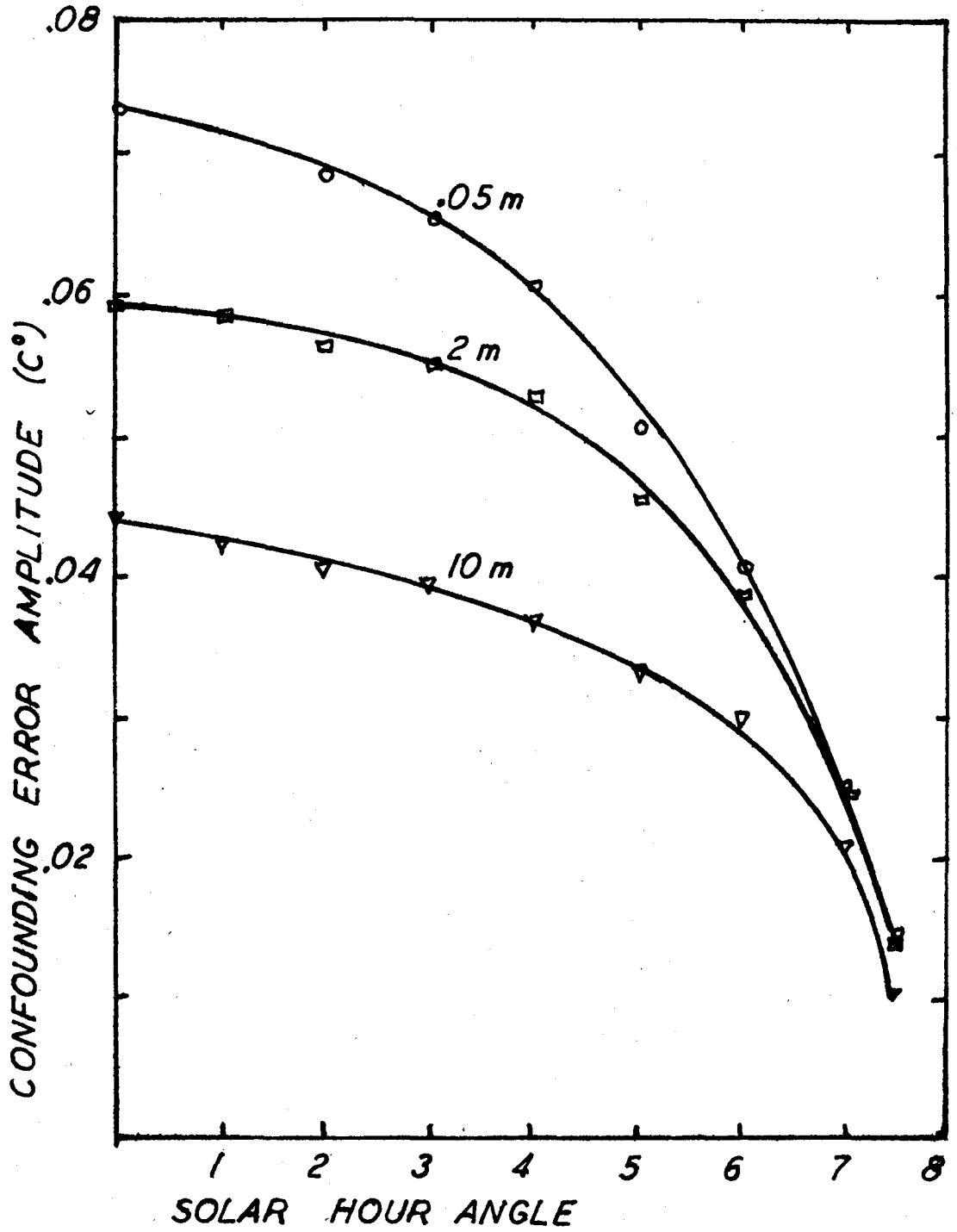
.08
.06
.04
.02
.05 m
2 m
10 m
CONFOUNDING ERROR AMPLITUDE (C°)
1
2
3
4
5
6
7
8
SOLAR HOUR ANGLE

a "signal-to-noise ratio" problem, with the true air temperature fluctuations constituting the signal and the confounding errors constituting the noise, the critical question hinged upon the magnitude of the true fluctuations themselves. No extensive series of measurements of temperature fluctuations has ever been made (this, in fact, being just the reason for the initiation of the present study), but some of the work cited in Part II above may be recalled as an aid in answering the present question. Hoehndorf's reports of average fluctuations of 3.9 C° at a height of 1 meter suggest that the signal-to-noise ratio may be of the order of 4.0/0.05 or about 80, if by "fluctuations" Hoehndorf meant "amplitudes" and not peak-to-trough changes. In unpublished studies previously made by members of the Department of Physics of the Iowa State College, fluctuation amplitudes of about 2 C° were often observed, though the average fluctuation amplitude was more nearly 1 C°, suggesting that Hoehndorf's values may have been peak-to-trough changes. If, conservatively, a signal amplitude of 1 C° and a noise amplitude of 0.07 C° be taken, the predicted signal-to-noise ratio for the thermistor becomes about 14, as a minimum estimate. Rounding this off still more conservatively to 10, one may conclude that the recorded response of a radiatively heated bead thermistor will contain spurious fluctuations whose amplitudes will never average more than about 10% of those of the true

air temperature fluctuations. Hence, despite the fact that this noise component will exhibit frequency characteristics peculiar to the turbulently fluctuating wind velocity and not to the air temperature, its low predicted amplitude precludes really serious distortion of the observed fluctuation statistics. In view of these results it was decided to proceed with the use of the bead thermistor in the present investigations of turbulent temperature fluctuations.

Several attempts have been made to check the validity of the thermistor radiation error analysis described above. Although the prediction of the confounding effect was the principal objective of the entire analysis, that effect does not in itself provide a basis for a simple experimental check due to its rather small magnitude and the obvious difficulty of independently measuring the true fluctuations. Instead an effort has been made to check just the mean error values by comparing the mean temperature indication of a shielded thermistor against that of an unshielded thermistor. Although work is still under way at this time on this problem, it may be said that such checks as have been possible indicate that the analysis is in agreement with experiment. A major difficulty has been that of accurately measuring the effective air speed at the element. For near-calm conditions very slight air motions produce appreciable reductions in error. If future checks, made under

known ventilation conditions, confirm the theoretical predictions of steady-wind radiation errors, then it will seem safe to conclude that the analysis of the confounding effect is also substantially correct.

B. Thermocouple Radiation Errors

Prior to the development of thermistors as thermal sensing elements, the thermocouple was almost universally the instrument of choice in micrometeorological studies. Its property of providing an electrical signal which is an accurately determinable function of air temperature, its comparative ease of manufacture, and its stability of calibration still recommend its use; so in perhaps half of the current programs of investigations of micrometeorological thermal problems thermocouples are being employed. Their greatest weakness is that they deliver a very weak direct current voltage (in the microvolt range) which is not, in the case of rapidly varying air temperatures, easily and accurately handled by existing electrical or electronic techniques. In contrast to this latter weakness, the bead thermistor's room-temperature resistance of the order of 75,000 ohms constitutes a very attractive property of this newer thermal element since it insures easily measurable voltage drops at current levels which are low enough that lead losses become negligible.

An examination of the literature, made for the purpose

of learning whether the electrical disadvantages of thermocouples might be outweighed by possible advantages of lower radiation error and lower lag-time, revealed an almost complete lack of investigation of either of these two properties which become of such critical importance in fluctuation studies. Previous meteorological applications of the thermocouple have almost always involved study of the mean temperatures as distinguished from the instantaneous temperatures; so it had typically been feasible to employ shields to eliminate the radiation difficulty. (Lag considerations are never of consequence when mean values of temperature are being sought.) This surprising lack of existing information on radiation and lag errors of the thermocouple plus a suggestion (from the organization sponsoring the present studies) that thermocouples might be less subject to radiation difficulties than thermistors seemed to call for an attempt at analysis of the response characteristics of this older instrument. Such an analysis was carried out, though with less final assurance of validity than was attainable in the thermistor analysis, because of uncertainties in the determination of the dissipation function.

Whereas no question of orientation entered into the analysis of the bead thermistor due to its nearly spherical symmetry, the thermocouple, even when idealized as being a circular cylindrical object, will vary in its response characteristics as it is rotated with respect to the sun

and with respect to the wind vector. It is, then, rather fortunate for the simplicity of the analysis that one particular orientation, axis vertical, is a preferred orientation that would almost certainly be used under field conditions in fluctuation researches. When the axes of the wires composing the couple are vertical, the ever-present fluctuations of horizontal direction of the wind do not lead to fluctuations in the dissipation rate of the element, for symmetry reasons. Were the couple mounted horizontally, then the very marked dependence of dissipation rate upon angle of attack of the relative wind (angle between axis and wind vector) for small angles of attack would lead to very serious "directional confounding" effects. To be sure, vertical mounting does not entirely eliminate this type of error, for the natural wind has a turbulently fluctuating vertical component; but the vertical component is seldom greater than the concurrent horizontal component of the wind vector, so the angle of attack almost always fluctuates within $\pm 45^{\circ}$ of a 90° (horizontal) value. As shown by Simmons and Bailey (1926) and also by King (1914), the variation of the dissipation rate of a heated cylinder for varying angle of attack is not appreciable until the angle of attack falls below about 50°, so in practice vertical mounting of a thermocouple serves to suppress directional confounding to a quite tolerable level. That this circumstance is, indeed, fortunate for the simplicity

of the analysis is obvious upon considering the geometry of any of the radiation calculations.

1. Calculations of the total radiative exchange

An assumption, experimentally attainable with proper fabrication techniques, was made throughout all of the following calculations. That was that the thermocouple was of the butt-welded type. A lap-welded couple would not possess the axial symmetry of response characteristics that has already been tacitly assumed although the degree of azimuthal variation in absorption cross-section and dissipation function of a well-honed lap-welded couple probably need not be great.

A second assumption that was made was that the albedo of the wire in the couple was 0.5. The most common pair of materials used to form thermocouples for meteorological use is copper and constantan. Since constantan is an alloy composed of 60% copper and 40% nickel, and since the (integrated) radiative characteristics of copper and nickel are very similar (Moon, 1936, p. 289; Barrows, 1912, p. 9), it seemed permissible to regard the couple as a copper wire. Barrows (ibid.) gives 0.65 for the albedo of highly polished copper and 0.40 to 0.50 for burnished copper. Although it is common practice to buff the wires of thermocouples prior to use, tarnishing under field conditions must lower the surface reflectivity rather rapidly, so it was decided to use an albedo of 0.50 in all calculations as a reasonably good approximation to the albedoes likely to prevail. With as

much uncertainty as exists in such an assumption it would have been unwarranted to have carried out any such analysis of effective absorption cross-section here as was done for the bead thermistor. Hence the final radiation error estimates were based on the assumption that the couple absorbed just one-half of the radiation it intercepts in the short wavelength interval. The infrared radiative properties will be considered separately.

In addition to the above two working assumptions it was necessary to establish the size (or sizes) of wire to be investigated. Because 0.0025-centimeter (0.001-inch) diameter thermocouples have been used so frequently recently, all radiation calculations have been made for just this one diameter. Corresponding radiation absorption rates can be obtained readily from the figures obtained here since the rates (per unit length of wire) vary directly as the wire diameter.

a. Direct solar radiation. Using the direct solar beam intensities obtained for the calculations of solar flux intercepted by the bead thermistor (see Figure 3, left-hand scale of ordinates) and a table of solar altitudes (Hand, 1946) for the determination of the geometric weight factors, the direct solar radiation incident upon the vertical thermocouple was calculated as a function of time of day for the four months January, April, July, and October, multiplied by the assumed wire albedo of 0.5, and converted into milli-

Figure 14. Ground-reflected radiation absorbed per centimeter of a vertical 0.0025-centimeter diameter copper wire (albedo 0.5).

Solid curves are for grass-cover albedo of 0.15; dashed curve is for snow-cover albedo of 0.85.

Figure 13. Direct solar radiation absorbed per centimeter of a vertical 0.0025-centimeter diameter copper wire (albedo 0.5).

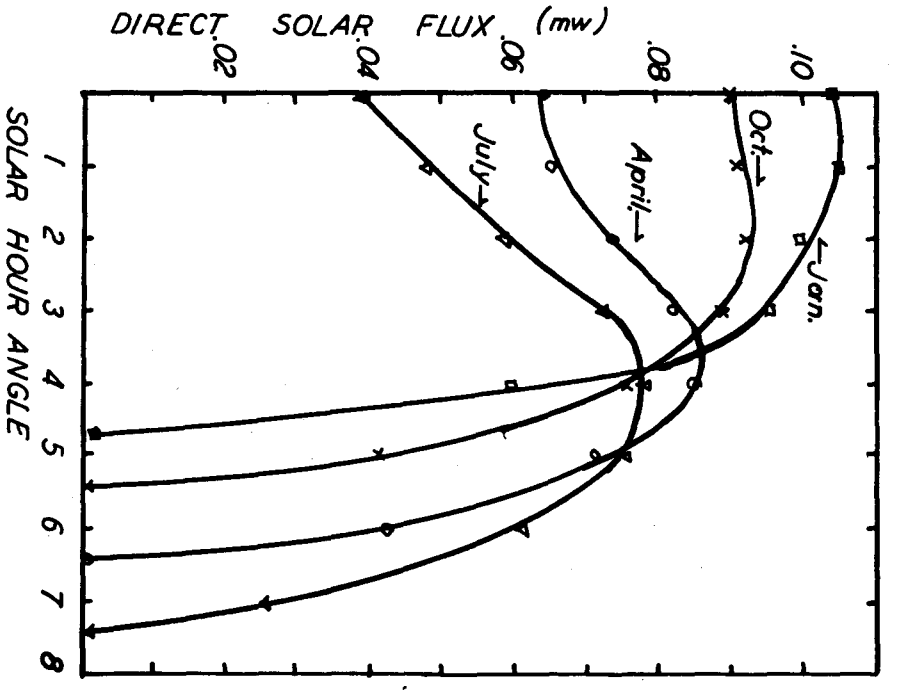
DIRECT SOLAR FLUX (mw)
.02
.04
.06
.08
.10
SOLAR HOUR ANGLE
1
2
3
4
5
6
7
8
July
April
Oct.
Jan.

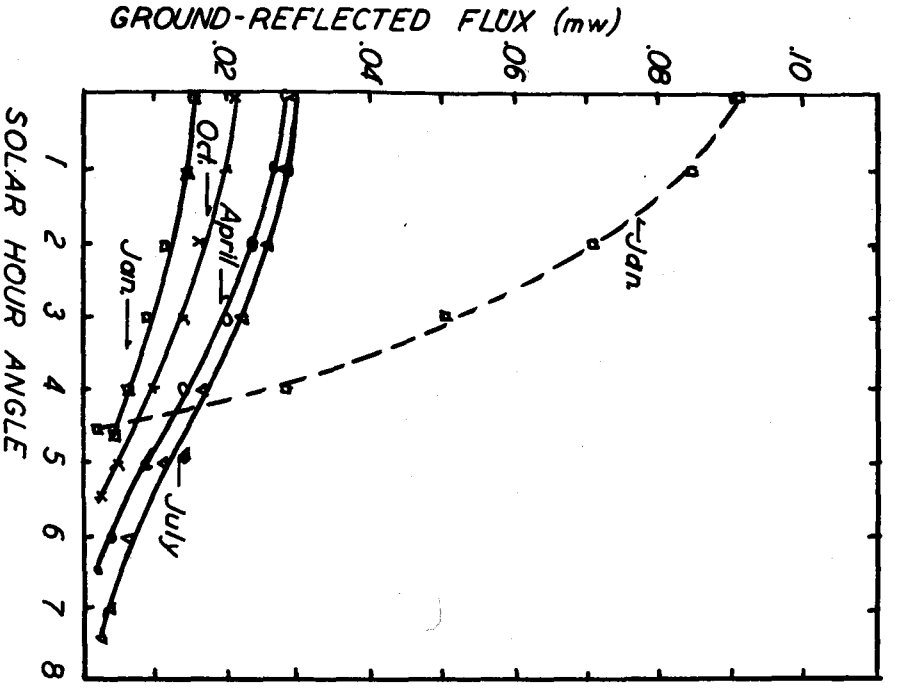
GROUND-REFLECTED FLUX (mw)
.02
.04
.06
.08
.10
SOLAR HOUR ANGLE
1
2
3
4
5
6
7
8
Oct.
April
Jan.
July
Jan.

watts per centimeter of wire length. The results are shown in Figure 13.

Unlike the corresponding curves for the sphere, which fell off monotonically from a noon maximum throughout the year, the curves of Figure 13 are neither monotonic nor maximal at noon. Each curve exhibits the counteracting influence of (1) the increase of absorbing cross-section (projected area as seen from the sun) with decrease of angle of incidence (angle between the normal to the wire axis and solar rays), and (2) decrease of beam intensity with decrease of angle of incidence due to greater depletion in the oblique path through the atmosphere for low solar altitudes. In January when the sun never does attain a high altitude (averaging 27° at noon in central Iowa) the optimum condition is attained for a very small hour angle because then the sun may move only a little distance from the celestial meridian before the rapid increase of path length and exponential depletion laws take hold. For July, however, the optimum combination of angle of incidence and path length occurs about four hours from noon, for the noon sun in summer is so high in the sky (70° for mean July noon in central Iowa) that more can be gained from increased absorbing cross-section than lost by path length increases when the hour angle increases from zero. It was noted that, for every one of the four months, maximum interception occurs when the solar

altitude is within a few degrees of 30°. The irradiation rate attains its maximum for the year as a whole near noon in January, for then the low atmospheric water vapor content permits high transmission even for the low angles of incidence (on a vertical cylinder) which favor large irradiation rates.

b. Diffuse sky radiation. The first point that was to be examined here, as also before in the case of the thermistor, was that of the degree of dependence of sky irradiation on solar zenith angle. Because a vertical cylinder does not present the same projected area to all parts of the sky, an extra geometric factor, the cosine of β, the altitude of the scattering volume element dV, appeared in the integrand formulated as (1) above. This geometric factor is a function of the volume element's altitude and not also of its azimuth because of the axial symmetry of the vertical thermocouple. Again putting the scattering angle γ in terms of the solar zenith angle and of the altitude (β) and azimuth of the volume element dV, expressing dV in terms of spherical coordinates centered on the thermocouple, and integrating as before over a very large hemisphere of radius R, one finds the total diffuse sky radiation incident upon a vertical cylinder of projected area A as seen from the horizon to be

$$L_c = A\,\pi\,knR\left(\frac{\pi}{2} + \frac{\pi}{8}\cos^2 z + \frac{3\,\pi}{16}\sin^2 z\right), \quad (12)$$

where z is the solar zenith angle. Thus the vertical cylinder,

in contrast to the sphere, intercepts sky radiation in amounts that do vary with solar zenith angle, even in the first approximation. On simplifying (12), one obtains

$$L_c = \frac{A\pi^2 knR}{16}(11 - \cos^2 z), \qquad (13)$$

which reveals that L_c is largest for a rising or setting sun and smallest for a zenith sun, but then only about 9% smaller. It was felt that the present purposes would be served well enough by evaluating the diffuse radiation rate for a middle value of solar zenith angle such that the maximum absolute value of the deviations of the irradiation rate on either side of that rate would be only about 5% of the rate itself. Accordingly the slight zenith angle dependence was ignored and the numerical evaluation of diffuse irradiation carried out for a zenith angle of 50°.

With the intermediate computational data available from the calculations of the sky irradiation of the sphere it was possible to perform the analogous integration for the vertical cylinder very quickly. Each zonal sum (the summation being over azimuth with each given 10°-zone bounded by two almucantars) had only to be weighted by the cosine of its mean angle of altitude to take account of the cylinder's projection geometry and the resulting weighted sums then summed over all altitudes. Using the proportionality factor already evaluated in the indirect manner elaborated earlier here, the final sums could be immediately converted into

the equivalent total flux of sky radiation on the cylinder. For unit length of the thermocouple under consideration here, and for the assumed albedo of 0.5, the (approximately constant) sky radiation flux absorbed by the couple was thereby found to be 0.030 milliwatts.

Hence to each value of direct solar flux represented in the curves of Figure 13 there was to be added 0.030 milliwatts of diffuse sky radiation. In addition to these two short wavelength components there was the variable ground-reflected flux, the analysis of which will be discussed next.

c. Ground-reflected radiation. For the case of the vertical cylinder the element of integration for the flux reflected from the annular strip of ground of radius $r\sin\theta$ and radial width $rd\theta\sec\theta$ is no longer simply (6) but rather

$$dE_c = B_o \frac{\cos\theta}{r^2} \sin\theta \; 2\pi r\sin\theta \; rd\theta\sec\theta A, \qquad (14)$$

where the new factor $\sin\theta$ is the projection factor appropriate to the cylinder and A is the projected area per unit length of the cylinder as seen from the horizon. Integration of (14) over the whole terrestrial hemisphere gave as the total ground-reflected radiation incident upon the cylinder

$$E_c = \frac{\pi^2 B_o A}{2} = \frac{\pi \alpha F_1 A}{2} \qquad (15)$$

in view of (5). Since the thermocouple is assumed to have an albedo of 0.5, only half of the incident radiation is

effective in heating the element so the above value of E_c is to be halved for absorption calculation purposes. The values of F_i, the total flux of short wavelength radiation reaching unit area of the ground surface, were the same values as those determined for the thermistor calculations, since F_i is no function of the element in question. The absorbed reflection flux was computed for the four months of January, April, July, and October for the case of a ground albedo of 0.15 and also for January alone for the snow-cover case of an albedo of 0.85. The results are plotted in Figure 14 as power absorption per unit length of thermocouple. These results need no particular comment at this point in view of their general similarity to those for the thermistor.

d. Infrared radiation. The calculations of the net infrared exchange for the vertical thermocouple were carried out on the same plan as were those for the sphere. For the exchange with the celestial hemisphere use was again made of the work of Linke (1931). Linke's integral for the case of a vertical cylinder, upon introduction of the numerical value of the proportionality constant N_o (see discussion of thermistor), gave for a blackbody cylinder of the dimensions of the thermocouple under consideration a net (negative) rate of gain from celestial exchanges amounting to

$$G_c = -4.4 \times 10^{-12} T^4 \text{ (milliwatts per centimeter).}$$

This exchange rate is not, however, that of a copper cylinder, since the infrared emissivity of copper is very much lower than unity. Mc Adams (1942, p. 393) gives values of the total emissivity of copper (integrated over both wavelength and hemisphere of emission) for a number of different surface conditions. Carefully polished electrolytic copper is quoted by Mc Adams as having a total emissivity of 0.018, polished copper is reported as 0.023, while commercial copper, scraped but not mirrorlike is listed as 0.072. (The first value is for a surface temperature of 176°F, the last two for room temperatures.) Under field conditions where a high initial polish must be expected to deteriorate rather quickly, the last valued cited would probably be most appropriate; so an emissivity of 0.07 was employed. After multiplication of the celestial blackbody infrared gain G_c, found above, by 0.07 the final estimate of gain per unit length by infrared exchanges between thermocouple and celestial hemisphere became

$$G_c = -3.1 \times 10^{-13} T^4. \qquad (16)$$

Next the net rate of gain of radiant energy by the cylinder from infrared exchanges with the terrestrial hemisphere was considered. Taking account of the symmetry conditions and using the Stefan-Boltzmann law and the second law of thermodynamics the net rate of gain per unit length was found to be

$$G_t = \tfrac{1}{2}\ 0.07\ 2\pi r \sigma (T_s^4 - T^4)$$

$$= 1.6\text{x}10^{-12}(T_s^4 - T^4), \qquad (17)$$

where r is the wire radius, σ is the Stefan-Boltzmann constant, T_s is the soil temperature, T is the bead temperature, and the initial factor of $\frac{1}{2}$ is to allow for the fact that only the exchanges with one hemisphere of exterior space are here involved. Combining the power gains from terrestrial and celestial hemispheres then gave

$$G = G_t + G_c = 1.6\text{x}10^{-12}(T_s^4 - 1.2T^4). \qquad (18)$$

For the dawn or sunset case where $T_s \doteq T = 300^\circ K$, say, (18) reveals that the net gain is negative and amounts to only 0.002 milliwatts per centimeter, a negligible rate of cooling compared with the other fluxes involved, e.g., the diffuse irradiation of 0.03 milliwatts. The smallness of this cooling rate is directly attributable to the very low infrared emissivity of copper.

The critical soil temperature for which the net cooling just vanishes due to compensating heating from soil exchanges was found from (18) by putting $G = 0$. The result was, for $T = 300^\circ K$, a soil temperature of about $315^\circ K$ ($108^\circ F$). Hence it is improbable that the thermocouple is appreciably heated even under summer midday conditions, since soil surface temperatures seldom exceed this value by very much as long as the soil moisture content is not extremely low. Furthermore, the coefficient in (18) is quite small, suppressing the magnitudes of any heating effects that may

develop when the soil surface temperature exceeds the critical value. Thus, even if T_s rose to 330°K with a T of 300°K, G would become only 0.001 milliwatt. By way of comparison, the other heating effects total about 0.100 milliwatts at noon on clear summer days. It seemed quite justifiable to neglect the infrared radiative exchanges completely in discussing the thermocouple errors.

The total radiative heating rates for the thermocouple could now be computed by summing, for each time of day and year investigated, the contributions of direct solar radiation, diffuse sky radiation, and ground-reflected radiation. The results are plotted in Figure 15. The dashed curve for January is based on a snow-cover albedo of 0.85; all the other curves are based on a grass-cover albedo of 0.15. With the exception of winter snow-cover days and of October with its flat midday maximum, all of the seasons are characterized by absorption maxima at times other than noon, a consequence of the irradiation geometry of a vertically oriented cylinder. Quite different forms would, of course, be assumed by the corresponding curves for a north-south horizontal thermocouple, and still other forms for an east-west orientation.

The particular numerical values of the radiative heating rates displayed in Figure 15 carry no meaning in terms of radiation errors until the dissipation function is determined. This problem will be examined next.

Figure 15. Total short wavelength radiation absorbed by a vertical 0.0025-centimeter diameter copper wire (albedo 0.5).

Solid curves are for grass-cover albedo of 0.15; dashed curve is for snow-cover albedo of 0.85.

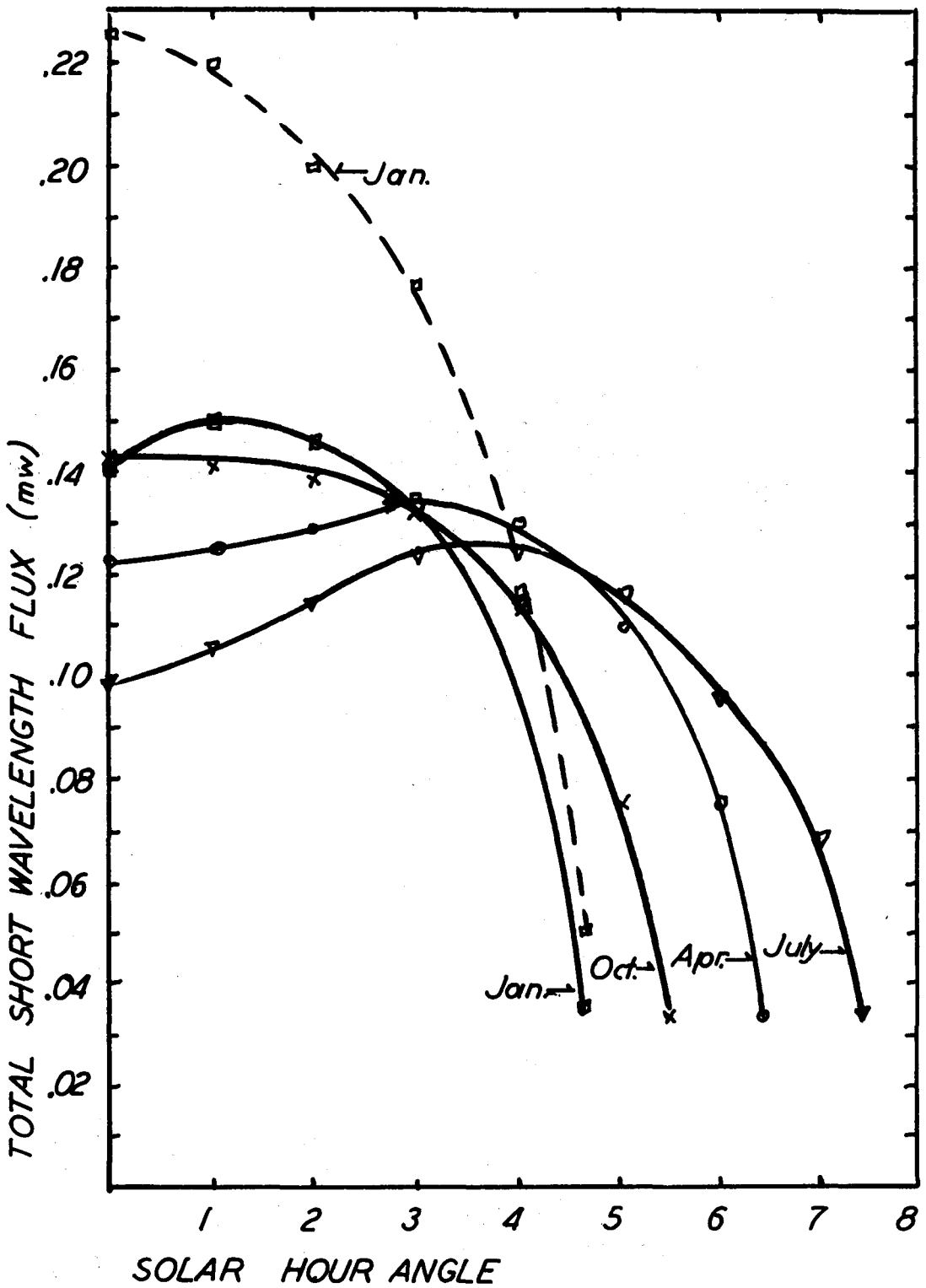
.22
.20
.18
.16
.14
.12
.10
.08
.06
.04
.02
TOTAL SHORT WAVELENGTH FLUX (mw)
Jan.
Jan.
Oct.
Apr.
July
1
2
3
4
5
6
7
8
SOLAR HOUR ANGLE

2. Determination of dissipation function.

The rate of loss of heat from small wires under conditions of natural and of forced convection has been studied by a large enough number of investigators that it seemed possible, in the absence of more specific experimental data, to deduce the dissipation function of a thermocouple of given dimensions from the results of these previous studies. A critical comparison of the past studies, however, revealed some serious discrepancies in their collective results, so the conclusions of this thermocouple error analysis must be regarded as tentative. Additional careful study of the heat dissipation characteristics of small wires operated at temperatures only a few degrees higher than ambient temperature appears indispensable to any further progress in thermocouple error analysis.

A question that arose immediately upon reviewing the literature was that concerning the effect of wire temperature upon the dissipation rate. Most of the existing information on heat loss from wires pertains to very hot wires, since the two principal applications of such information have been to incandescent filaments and hot-wire anemometers. The heat transfer processes occurring in the boundary layer surrounding a very hot filament were described theoretically by Langmuir (1912). He suggested that a gas-sheath whose viscosity was so high as to preclude appreciable convective transport would be present

just next to a glowing wire. Nevertheless, he concluded, the suppression of convective exchange would not leave the overall dissipation rate with a low value because the coefficient of thermal conductivity would also be very large at the temperatures prevailing in the gas-sheath, augmented molecular conduction thus compensating for decreased convection. Since the temperature dependence of molecular conductivity is almost the same as that of the viscosity (both varying nearly as $T^{\frac{1}{2}}$), Langmuir predicted and experimentally verified that there does exist some temperature dependence in the dissipation function of wires, but he found it to be quite small. The slight temperature dependence predicted by King (1914) from a somewhat different theoretical approach is in good agreement with Langmuir's results. In disconcerting contrast, Ayrton and Kilgour (1892), in what appears to have been a meticulously careful investigation, found dissipation rates whose temperature dependence for wire temperatures in excess of about 100°C was nearly identical with that deduced later by King and Langmuir, but their measured dissipation rates fell to very low values at room temperatures. (It may be well to note here that these are dissipation rates per degree excess of wire temperature over air temperature and not simply the absolute magnitudes of the power losses.) Langmuir appears not to have been aware of Ayrton and Kilgour's work. King made passing reference to their work, but did not discuss their low temperature

results, perhaps because King's experimental values did not apply to wire temperatures below about 150°C. Nothing in the methods employed by Ayrton and Kilgour suggests an explanation for the low dissipation rates shown by their plotted curves at low wire temperatures, but a closer examination of their tabulated data revealed that they had not plotted in their figures all of their experimental points in the low temperature range. In several cases, had they plotted all of their points, their curves could not have been drawn with the pronounced knee near 40 - 50°C which differs so from the other investigators' predictions. When it was noted further that a linear extrapolation of the higher-temperature portions of their curves down to low temperatures passed very close to values found from still another source (Albrecht, 1927) it was decided to ignore the anomalous behavior of the Ayrton and Kilgour data in favor of the other available information. This being somewhat arbitrary, it should be repeated that the results described below must be treated as tentative until better experimental data are obtained on wire dissipation rates.

King (loc. cit.), using some theoretical developments of Boussinesq, showed that the rate of heat loss H per unit length of cylinder of diameter d maintained at a temperature excess of t degrees above the ambient fluid which flows across it normally with speed V is given by

$$H = Kt + (2\pi Ks\rho d)^{\frac{1}{2}} V^{\frac{1}{2}} t, \qquad (19)$$

where K is the thermal conductivity of the fluid, s its specific heat at constant volume, and ρ its density. King showed this relationship should apply down to a velocity of about 20 centimeters per second when the fluid is air. Below that velocity a second relation which he obtained was expected to hold. Evaluating all of the physical constants in (19) for an air temperature of 300°K and computing the heat loss rates for each of a series of wind speeds over the range of interest, a working form of the dissipation function was obtained. For the still-air value, King's second relation was employed, using his suggestion that natural convection currents produce an effect equivalent to a velocity of about 10 centimeters per second. The resulting dissipation function, plotted in Figure 16 is similar in general form to that of the bead thermistor (Figures 7 and 8). It is the uncertainty in the subsequent use of this curve that needs to be removed by future experimental work.

3. Evaluation of radiation errors and confounding effects

The radiative heating rate for an hour angle of four on a clear July day (Figure 15) was taken as a measure of the worst conditions for summer (though not quite for the year) and the steady-wind errors computed with the aid of Figure 16 for speeds of from 0 to 10 meters per second. The estimated errors shown in Figure 17 are, except for

Figure 16. Dissipation function of a 0.0025-centimeter diameter wire computed from King's equation.

Figure 17. Steady-wind radiation errors of a vertical 0.0025-centimeter diameter copper thermocouple at hour angle 4 on a clear July day.

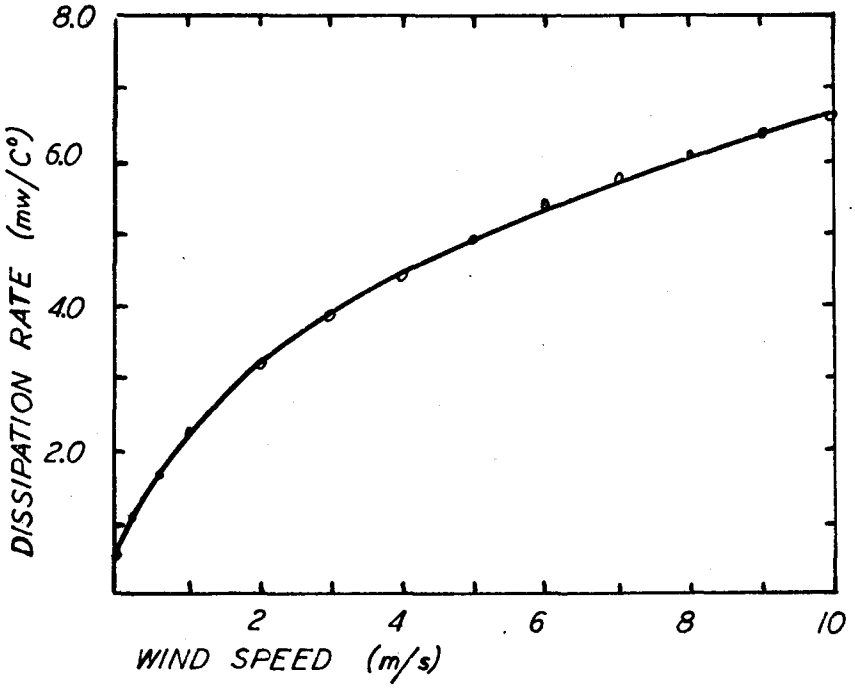
8.0
6.0
4.0
2.0
DISSIPATION RATE (mw/C°)
2
4
6
8
10
WIND SPEED (m/s)

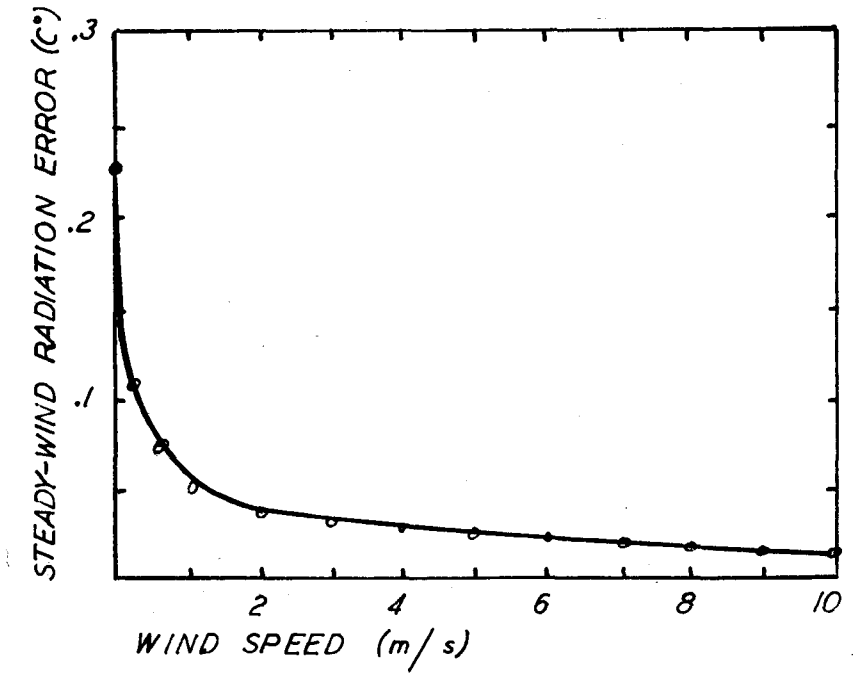
.3
.2
.1
STEADY-WIND RADIATION ERROR (C°)
2
4
6
8
10
WIND SPEED (m/s)

still-air conditions, very much lower than those of the bead thermistor under adverse summer conditions, as may be seen by comparing Figure 17 with Figure 9. For all wind speeds above 1 meter per second, the 0.0025-centimeter diameter thermocouple appears to suffer an error of less than 0.05 C°. Even for the very slight air motion of 0.2 meters per second the error becomes only a little more than 0.1 C°, and the still-air error itself is only 0.23 C°.

With such low steady-wind errors, the confounding errors must be expected to be wholly negligible. These were computed for the same assumption of a $0.25\overline{U}$ lull that was used in the case of the thermistor, but are not presented in graphic form here because they are so small as to make their variations with mean wind speed or time of day of little practical concern. At a mean speed of 1 meter per second the confounding error was computed to be 0.007 C°, and at 10 meters per second it had fallen to 0.002 C°. These are to be contrasted with the roughly 0.05 C° confounding error amplitudes predicted for the thermistor. The thermistor confounding amplitudes were estimated to be about 10% as large as the true temperature fluctuation amplitudes, so the thermocouple confounding amplitudes computed here must be only about 1% as great as the true fluctuation amplitudes. Unless (as is unfortunately possi-

ble) the thermocouple dissipation rates employed here are appreciably too large, a 0.0025-centimeter thermocouple would seem to be distinctly superior to the bead thermistor as regards radiation errors. But since the thermistor errors, though tenfold greater by the present estimates, are not intolerably large by existing standards of accuracy in micrometeorology, the electrical advantages of the thermistor may be permitted to decide the issue in the favor of the latter sensing element. It is interesting to note here that if the theoretical reduction of effective thermistor absorption cross-section by silvering could be realized in full, the thermistor radiation errors would be suppressed to almost exactly the level predicted here for a 0.0025 centimeter thermocouple.

Estimates of the radiation errors for thermocouples for diameters other than 0.0025 centimeter are readily made with the aid of the King equation (19) and the irradiation rates of Figure 15 corrected for differences in absorption cross-section. A No. 30 copper wire (size often used when rapid response is not essential) with a diameter of 0.025 centimeter (0.01 inch) was computed to have a still-air error of slightly greater than 0.4 C°, decreasing to about 0.1 C° at a wind speed of 1 meter per second, and 0.06 C° at 5 meters per second.

To document the need for caution in accepting the above

error estimates, two recently reported values of radiation errors of wire elements might be noted. Geiss (1949) compared the mean indicated temperatures of shaded and unshaded 0.002-centimeter diameter platinum wire resistance thermometers mounted with wires horizontal at a height of 1.75 meters above the ground on a clear July day with average winds of about 1 meter per second, and found the mean difference to be as large as 0.5 C°. Since platinum has an albedo of about 0.65 (in contrast to 0.5 for burnished copper) and since these wires were very nearly equal in diameter to that assumed in the main part of the thermocouple calculations above, Geiss' value is clearly contradictory to the value predicted here, even after allowance is made for differences in irradiation rates of horizontal and vertical wires. Because there seems little chance that the radiation calculations made in the first portion of this analysis can be off by one full order of magnitude (order of discrepancy with Geiss' observations) Geiss' study casts suspicion on the dissipation function here employed.

Using No. 30 copper-constantan thermocouples, Thornthwaite (1949) observed radiation errors as large as 2 C° in March under unspecified wind conditions and thermocouple orientation. This error is about five times larger than the still-air value predicted above for couples of this size, and would be still larger relative to the values pre-

dicted for even slight air motions. Thornthwaite's couples were of the lap-welded type and may have been in thermal communication, via the leads themselves, with components of the mounting which developed still larger radiative heating effects and warmed the thermojunction by conduction; so his result is no clear-cut check here. Nevertheless, the discrepancy which it implies is in the same sense as that implied in Geiss' figures.

Only one other paper was found in the literature to include any information on radiation errors of wire elements. Albrecht (1927) gave a formula for the radiation error of a platinum wire resistance thermometer. His equation yields error values in fairly good agreement with those obtained from the King equation when proper allowance is made for the higher albedo of platinum. It is not possible to conclude, from Albrecht's paper, whether his formula was empirical or theoretical. His only pertinent reference was to a paper dealing with heat losses from very hot wires; so if dissipation rates of very hot wires should in fact be incomparable with those of wires only slightly hotter than air temperatures, Albrecht may have given no really independent information from the point of view of the present question of the applicability of King's work.

As a last comment on the generally confused state in which this subject exists, it might be pointed out that Albrecht (loc. cit.) gave a table of values of errors of

indication of his resistance thermometer due to Joule heating under excessive current loads. Since this set of values constituted exactly the sort of data expressly obtained for the evaluation of the thermistor dissipation function, it was used to compute the still-air dissipation rate for Albrecht's platinum wire (diameter 0.0025 centimeter). The values so obtained were only about one-third as large as that implied in the equation given by Albrecht himself in the same paper.

In conclusion, it can only be said once more that experimental work specifically devoted to the study of the dissipation function of wires of various sizes operated at small excess temperatures must be undertaken before the serious disagreements revealed here can be resolved. If the very tentative results obtained here are confirmed, a 0.0025-centimeter thermocouple offers the advantage of appreciably lower confounding errors than the bead thermistor. If, on the other hand, the Ayrton and Kilgour work should be substantially correct, and the error reports of Geiss and of Thornthwaite well-founded, then even this small thermocouple is only about as good as the bead thermistor with respect to radiation errors. Because the thermistor enjoys indisputable electrical advantage over the thermocouple, and because its confounding errors seemed acceptably low, the current study of turbulent temperature fluctuations has been planned about the bead thermistor as the principal

sensing element.

IV. LAG EFFECTS IN FLUCTUATION MEASUREMENTS

When a thermal sensing element is immersed in a fluid whose temperature varies with time, the temperature indicated by the sensing element will not, in general, be the true temperature of the medium because the finite rate of response of the element to changes in ambient temperature prevents it from following those changes in an ideally instantaneous fashion. Under these conditions the element is said to "lag", or to exhibit "lag". A knowledge of the extent to which a given sensing element lags behind the variations of the true temperature is essential to an understanding of the meaning of measurements made with that element.

Among the measurement problems in which lag considerations arise, none is more critically concerned with the effects of lag than is the problem of measuring turbulent temperature fluctuations. The thermal inertia of most sensing elements (e.g., the mercury-in-glass thermometer) causes them to smooth out all of the shorter-period turbulent temperature fluctuations, yielding an apparently constant temperature indication, or at least one exhibiting only very slow undulations. Consequently, a first consideration in evaluating an instrument intended for use in fluctuation studies is that of determining the degree to which its lag will distort the fluctuation statistics that are to be derived from the record of its response.

It has been mentioned earlier that there have, in the past, been no thorough studies made of turbulent temperature fluctuations. Because of this neglect of the fluctuation problem in general, there have been almost no analyses of the effects of lag on fluctuation measurements. The only past contribution is a paper by Bilham (1935), in which he examined the response of a lagging thermal element to sinusoidal variations of temperature. Bilham used his results to show that Best (1931) had seriously erred in interpreting some micrometeorological temperature measurements made with a resistance thermometer whose lag was quite large.

As part of the present attempt to explore the fluctuation problem, analyses of a number of general lag effects have been carried out and several specific effects arising from the use of the bead thermistor in particular have been determined. The results of this work will be summarized after a brief discussion of the differential equation of response of a lagging element and some comments on methods of measuring the lag-times of sensing elements.

A. The Equation of Response of a Thermal Sensing Element

1. Formulation of the lag equation

Let $T(t)$ represent the instantaneous temperature of a sensing element exposed to an ambient air temperature of $T_a(t)$ which is not, in general, equal to $T(t)$. Due to the (generally existing) difference between T and T_a, heat

transfer will be occurring between element and air, with the result that T will be changing with time. (Concurrent changes in T_a are negligible under field conditions.) If dQ units of heat are transferred from the air to the element in a time dt, then

$$\frac{dT}{dt} \equiv \frac{dT}{dQ}\frac{dQ}{dt} \triangleq \frac{1}{C} P$$

where C is the heat capacity of the sensing element and P is the power gain.[1] According to Newton's law of cooling, P is proportional to the difference between T_a and T; so introducing a proportionality constant D (units of milliwatts/C°), the response equation becomes

$$\frac{dT}{dt} = \frac{D}{C}(T_a - T) = \frac{1}{\lambda}(T_a - T) \qquad (20)$$

if the definition

$$\lambda \triangleq \frac{C}{D} \qquad (21)$$

is introduced. Equation (20) is called the lag equation, and λ (characterized by dimensions of time) is known as the lag-time of the sensing element.

Whereas C, the heat capacity of the element, is a physical property of the element itself, D is dependent not only upon the geometrical and physical nature of the element, but also upon the speed and nature of the ambient fluid. In

---

[1]The symbol $\triangleq$ will be used here to mean "is defined to be".

meteorological measurements the fluid is always understood to be air, so D becomes a function only of the nature of the element and of the ambient air speed and is, in fact, just the dissipation function that has entered repeatedly into the discussions of radiation errors above.

Since the lag equation is essentially Newton's law of cooling, (20) is accurate only for small values of $|T_a - T|$, but this restriction is never violated in meteorological measurements where $|T_a - T|$ is, at most, of the order of degrees Centigrade. Experimental verification of the validity of (20) for several types of thermal elements has been discussed by Harper (1913), who also examined the dependence of D on the fluid speed for a number of fluids and sensing elements.

2. The inverted lag equation

Despite the simplicity of the lag differential equation (20) only a few of its properties have been discussed in the literature. In view of this, it may be permissible to note a very simple modification of (20) which proved quite useful in some of the work to be described later.

The conventional treatment of (20) involves solution of the differential equation for a specified $T_a(t)$, as for example, for a step-function change in T_a, linear change of T_a with time, etc. (Middleton, 1947, pp. 62-64). In practice exactly the inverse problem arises: one knows T(t) from the record of a lagging instrument and knows the

lag-time of the instrument, but seeks to determine what forcing function $T_a(t)$ must have led to the observed response. With this practical problem in mind, (20) may be rewritten with the sought-for T_a expressed in terms of the observationally known properties of T, yielding

$$T_a = T + \lambda \dot{T} \tag{22}$$

where the dot above a symbol has been used to indicate time differentiation. (22) may be referred to as the inverted lag equation. Although the difference between (20) and (22) is mathematically trivial, the latter form suggests certain useful properties of the differential relation in a much more obvious way than does the former. Some illustrations will serve to demonstrate this minor point.

For any $T_a(t)$, (22) states that the true ambient temperature at any instant is algebraically greater than the simultaneously indicated temperature T(t) by the amount $\lambda \dot{T}$. Thus, knowing the lag-time λ of the sensing element used to obtain the recorded T(t), and estimating or measuring the indicated time rate of change $\dot{T}$, one can determine what the true air temperature T_a must have been at any desired time. Dryden and Kuethe (1929) described essentially the same method for estimating errors due to lag, but because of having deduced it from the properties of the solution to the lag equation for a linearly varying forcing function, they incorrectly concluded that it is only valid for seg-

ments of the record which are very nearly linear. The inverted lag equation shows clearly, however, that such a relation is true at every instant regardless of the sinuosity of the record.

The relation just cited provides a handy means of quickly estimating from a record how much greater than the observed fluctuations the true air temperature fluctuations must have been. For example, an examination of a record of thermal fluctuations made under conditions of well-developed turbulence frequently reveals numerous small spurs of very short duration rather densely superimposed upon the longer-period undulations of much greater apparent amplitude. That this fine "embroidery" must be evidence of true air temperature excursions whose amplitudes often approach those of the longer-period components is apparent when one applies the $\lambda \dot{T}$ correction; for though these spurs on the indicated record never grow very large, they have slopes which are often many times greater than those of the slower oscillations. The same conclusion is, of course, reached by regarding the actual excursions of air temperature as being made up of a large number of Fourier components which suffer attenuation that tends to filter out the higher frequencies (as will be explained below), with the result that the response function contains only the little spurs as relics of the large pulses in the forcing function. The inverted

lag equation tells the same story here in a less elegant but more direct manner.

As corollaries to the preceding rule for estimating the instantaneous error of indication of a lagging element, it is to be noted first that the element is yielding an exact indication of air temperature at each instant for which $T(t)$ attains an extremum through which $\dot{T}(t)$ is continuous; and second that, at any point in the record where $\dot{T}(t)$ appears (to within the limits imposed by the time-scale of the record) to exhibit a discontinuity, there must have occurred a discontinuity in the true air temperature itself (to within the same time-scale approximation). If the discontinuity in $\dot{T}(t)$ involves a change in sign of $\dot{T}$, (22) implies that the sign of the error, $T-T_a$, must also change. The few published $T(t)$ records in the literature as well as the unpublished records obtained in earlier turbulence studies made by members of the Department of Physics, when examined with this last rule in mind, suggest that the temperature changes occurring at a fixed point may be considerably more abrupt than has been suspected in the past. A check on this point, using the above-mentioned method for determining the true fluctuations, should be made when field observations are obtained.

The error term, $\lambda \dot{T}$, in (22) also suggested the basis of a possible method of compensating the output of a lagging

element in such a way as to correct for lag effects prior to recording. The method, which becomes feasible only for elements yielding an electrical signal, consists of splitting the signal, differentiating one part with respect to time, multiplying this by λ, and then adding the product to the other part into which the signal was originally split, all operations being performed electrically. (22) shows that when these operations are correctly performed, the final output of the compensation circuit is the true air temperature, $T_a(t)$, free from lag distortion. To take account of variations of λ accompanying varying wind speeds, one might use the output of an anemometer to control the value of the λ-factor used in the multiplication stage; or this stage could be adjusted manually to correspond to the mean wind speed prevailing during a given run. Such an approach to the lag compensation problem was considered for the present study, but a quite different method suggested by Hall (1949) was found to be simpler and is being investigated currently by others.

B. Determination of the Lag-time of a Thermal Sensing Element

1. Past methods

The standard method of determining the lag-time of fairly inert sensing elements is based upon the solution to the lag equation (20) for the case of a step-function change in T_a. For this case the lag-time is found to be the time

required for the response to undergo e^{-1} of its full change (height of the step). (See, for example, Middleton (loc. cit).) In practice, the step-function change in the ambient temperature is brought about by rapidly transferring the element from a medium at one temperature to one at another temperature. Such a method fails when the lag-time is small (of the order of the attainable transfer times). In particular, the bead thermistor, with a still-air lag-time of the order of 0.5 second, could not be so studied.

Anderson and Heibeck (1951) devised a method of determining the lag-times of rapidly responding elements that yield an electrical signal. Imposing an almost square waveform of $T_a(t)$ on the sensing element by mechanically shifting it back and forth between two air jets of different temperatures and then comparing the observed ratio of amplitude of response to amplitude of square wave with the corresponding theoretical ratio deduced from the lag equation, Anderson and Heibeck showed how one can determine lag-times down to about 0.05 seconds.

Still another method that has been used (e.g., Swinbank, 1951) is that of computing the lag-time. When the heat capacity of the element is known accurately and the dissipation rate is determined for a range of ambient wind speeds, the lag-time can be computed for each wind speed with the aid of (21). Since, however, it is often very difficult

to distinguish the portions of the instrument which are thermally active in the measurement process from those which play no part in the process, this last method is not very satisfactory. Thus, in the case of the bead thermistor, the copper wire lead system can be shown to comprise a thermally active component of the sensing element, so in attempts to compute the thermistor's lag-time one would have to allow for lead contributions to C since lead effects are inescapably admitted into the picture in the actual measurements of D. It is definitely safer, when possible, to determine the lag characteristics by some experimental approach.

2. Measurement of thermistor lag-times

As part of the preliminary evaluation of bead thermistors for the study of which the present analyses are a part, a quite different method of determining the speed of response of the beads under varying ventilation rates (modified from that used by Becker, Green, and Pearson, 1946) was employed by Kassander (1951). The method consisted in applying a step-function change of voltage across a thermistor and a fixed resistor connected in series, and then presenting on the face of an oscilloscope a trace of the transient response of the thermistor as its temperature changed due to the accompanying step-function of Joule heating. The persistence-time of the fluorescent coating of the cathode-ray tube permitted determination of the lag-time by

actual measurement (on the curve traced out on the tube face) of the time for the response to undergo e^{-1} of its full change. The voltage step-function was as readily applied with the bead in calm air as in the wind tunnel or on the rotating arm, so the method proved quite flexible.

The results of the measurements of the lag-time of the same specimen thermistor whose dissipation function was presented in Figure 7 are plotted in Figure 18. From a still-air value of about 0.7 seconds, this element's lag-time fell rapidly with increasing wind speed, becoming almost constant at a value of about 0.1 second for winds in excess of about 10 meters per second. (This general behavior could, of course, have been predicted from (21) and the previously discussed form of the thermistor dissipation function.)

Certain questions as to the comparability of the thermal lag-time and the actually measured electrical lag-time plotted in Figure 18 arise here, but since experimental work is currently being carried out on this and related lag questions by another member of the group investigating temperature fluctuations, these questions will not be considered here. It may be pointed out, however, that a calculation of the still-air lag-time with the aid of the relation (21) yields a value of about 0.4 seconds when only the bead itself is considered as contributing to C, whereby, as pointed out above, one must expect to underestimate the lag-time because of lead effects.

Figure 18. Lag function of the Western Electric D-176980 bead thermistor.

Figure 19. Phase-lag and amplitude-suppression ratio in the response of a sensing element to sinusoidal variations of air temperature.

The scale of ordinates for the phase-lag is given in degrees at the left. The scale of ordinates for the amplitude-suppression ratio A'/A is at the right. On each of the two curves, numerical values of the ordinate are entered for four values (0.1, 1, 10, and 100) of the dimensionless ratio P/λ .

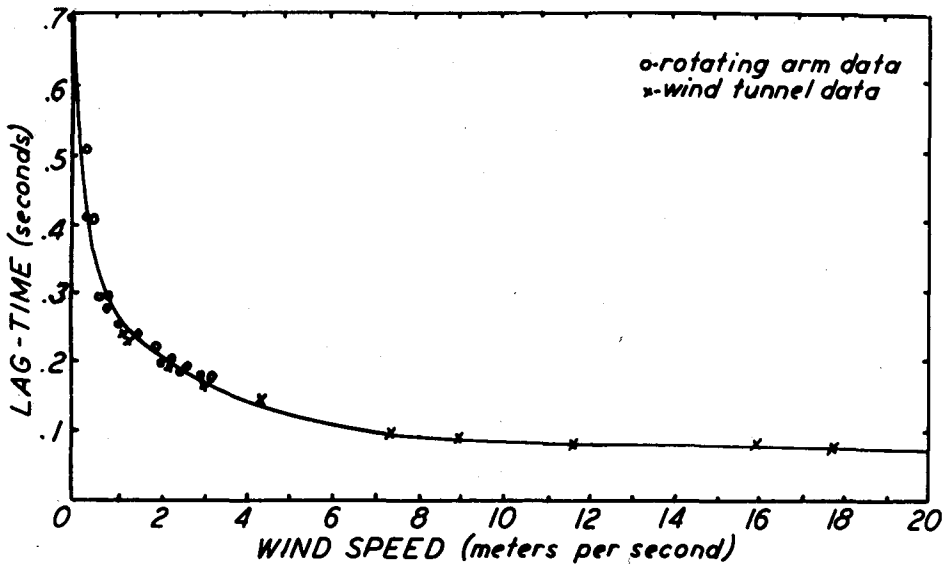
o-rotating arm data
x-wind tunnel data
LAG-TIME (seconds)
.7
.6
.5
.4
.3
.2
.1
0
2
4
6
8
10
12
14
16
18
20
WIND SPEED (meters per second)

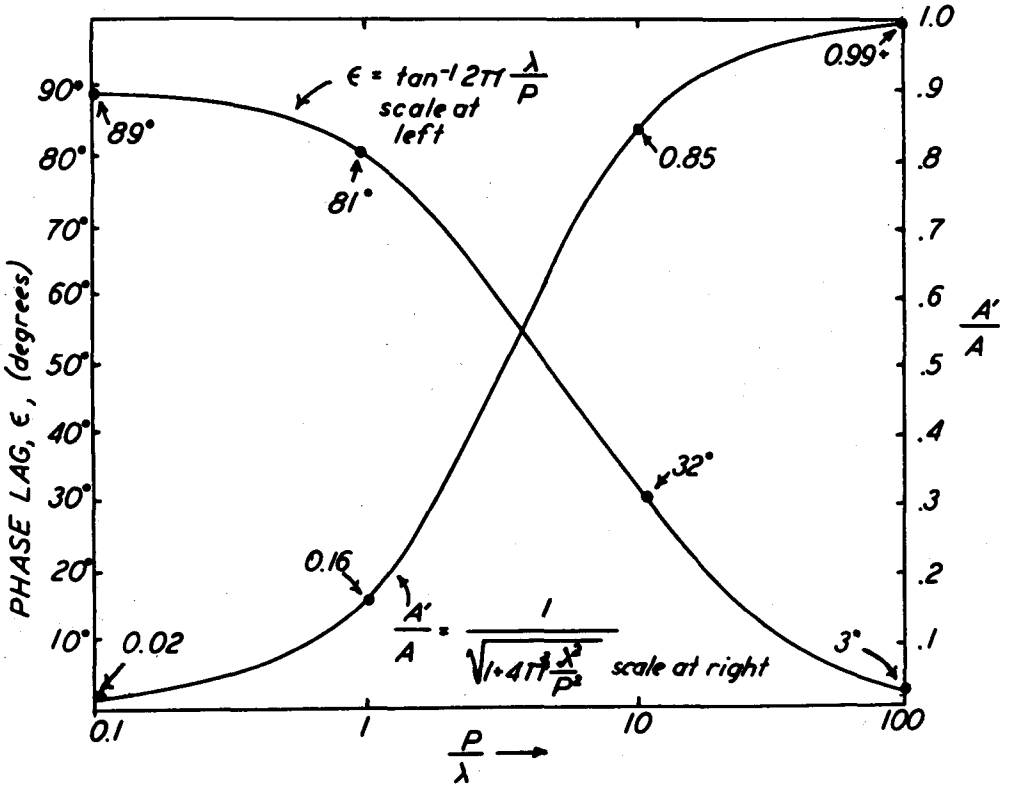
$\epsilon = \tan^{-1} 2\pi \frac{\lambda}{P}$
scale at left
89°
81°
32°
3°
0.02
0.16
0.85
0.99
$\frac{A'}{A} = \frac{1}{\sqrt{1+4\pi^2 \frac{\lambda^2}{P^2}}}$
scale at right
PHASE LAG, ε, (degrees)
90°
80°
70°
60°
50°
40°
30°
20°
10°
1.0
.9
.8
.7
.6
.5
.4
.3
.2
.1
$\frac{A'}{A}$
0.1
1
10
100
$\frac{P}{\lambda}$ →

Middleton (1947, p. 62) suggests that most sensing elements exhibit a u^{-n} dependence of lag-time upon wind speed u, so this hypothesis was checked by means of a semilogarithmic plot of the experimental data and the relation

$$\lambda(u) = \frac{2.8}{u^{\frac{1}{2}}} \quad (\lambda \text{ in seconds, u in meters per second}) \qquad (23)$$

was found to represent the experimental data with an error of less than 0.05 second (14%) for all speeds in excess of 0.5 meters per second, the poorest agreement occurring at the lower limit of wind speeds. Clearly (23) must fail to describe the curve of Figure 18 at very low wind speeds.

Just as the determination of the dissipation function of the bead thermistor made possible the analysis of a number of questions concerning the role played by radiation error in distorting fluctuation statistics, so also does the determination of the lag function, $\lambda(u)$, make possible the analysis of a number of questions concerning the effects of lag.

3. Calculation of thermocouple lag-times

Using the tentative thermocouple dissipation rates plotted in Figure 16, computing the heat capacity (per unit length) of a 0.0025-centimeter diameter copper wire, and using (21), a series of thermocouple lag-times were computed for comparison with those of the bead thermistor. The computed values were only about one-tenth as large as those

measured for the bead thermistor. For still air the computed value was 0.06 second. From this value it fell rapidly, becoming 0.01 second for an ambient air speed of 0.5 meter per second, 0.005 second for a speed of 2 meters per second, and 0.002 second for an air speed of 10 meters per second.

The previously expressed lack of assurance in the applicability of the King equation (19) to the problem of computing the dissipation rate of only slightly heated wires carries over directly to the calculations of thermocouple lag-times. Hence the computed thermocouple lag-times given just above may be only about one-tenth as large as the true values, in view of the roughly tenfold uncertainty in the dissipation rates employed in their calculation. However, even if the true values were ten times greater, the lag of the thermocouple would be everywhere lower than the values of the bead thermistor plotted in Figure 18.

4. Precision requirements in the determination of lag-times

Since the most satisfactory way in which to solve the analysis and interpretation problems created by lag effects is to use an element having zero lag-time, there will always be a tendency to try to devise elements with lower thermal inertia. As the lag-time is forced down, however, the experimental difficulties of carrying out an accurate determination of that lag-time go up rapidly. It is pertinent to ask how sensitive the lag bias effects are to variations in lag-time so that one may know how closely he must deter-

mine λ in order to carry out adequate corrections of observed data for lag effects.

A quantity which was found to give a very useful measure of lag bias in fluctuation studies was the amplitude-suppression ratio, A'/A, for the solution to the lag equation (20) for sinusoidally varying $T_a(t)$. (See equations (24) and (25) below for definitions of A'/A.) Logarithmic differentiation of A'/A with respect to λ yielded

$$\frac{d(A'/A)}{(A'/A)} = - \frac{d\,\lambda/\lambda}{1 + \frac{P^2}{4\,\pi^2\,\lambda^2}} \qquad (24)$$

as the relation between the relative error of the determination of lag-time and the associated relative error of estimate of A'/A. (P is here the period of $T_a(t)$.)

In the limit of very small P/λ (24) indicates that there will be the same relative error in A'/A as in λ itself; but that in the limit of very large P/λ the relative error in A'/A associated with a given relative error in the value ascribed to λ goes to zero (wide tolerance on λ-determinations at this limit). As three indicative magnitudes, it may be noted that (24) yields $d(\ln A'/A)/d(\ln \lambda)$ equal to -0.99 for a P/λ of 0.1, -0.97 for a P/λ of 1, and -0.28 for a P/λ of 10. Here, as elsewhere, the most serious difficulty attends the study of the highest-frequency components in $T_a(t)$; for one can apparently

not assess the importance of these components with much more accuracy than he can measure λ in the laboratory. It is most unfortunate that the reverse relationship does not obtain.

C. Lag Distortion of Fluctuation Statistics

The immediate objective of the present study of turbulent temperature fluctuations is that of statistical analysis of the fluctuations. It was therefore important to determine the extent to which lag effects may distort the apparent statistical characteristics of the recorded fluctuations. In the following discussions, a number of such effects are examined.

1. Some relations between true and apparent fluctuation statistics for constant lag-time

As long as the ambient wind speed is steady, λ is a constant and the lag equation falls within the particularly simple class of linear differential equations with constant coefficients. In this section some of the properties of the solutions of the lag equation for this special case are considered.

a. Response functions for periodic $T_a(t)$.

(1) Sinusoidal case. For later reference, the solution to (20) for a sinusoidally varying ambient temperature will be needed. Bilham (1935) pointed out that if

$$T_a(t) = \bar{T}_a + A \sin \frac{2\pi t}{P} , \qquad (25)$$

in which the bar over a symbol denotes a time average of that quantity and A is the amplitude of the ambient temperature fluctuations (assumed to occur purely sinusoidally with period P), then the response of an element of lag-time λ (assumed constant here) is found from (20) to be

$$T(t) = ce^{-t/\lambda} + \bar{T}_a + A' \sin\left(\frac{2\pi t}{P} - \epsilon\right), \qquad (26)$$

where the first term on the right is the transient term with integration constant c, A' is the response amplitude given by

$$A' \triangleq \frac{A}{\sqrt{1 + \frac{4\pi^2 \lambda^2}{P^2}}} \qquad (27)$$

and ϵ is the phase-lag angle given by

$$\epsilon \triangleq \tan^{-1} \frac{2\pi\lambda}{P} . \qquad (28)$$

(26) shows that after disappearance of the transient term, the response will represent suppressed and phase-shifted sinusoidal variations about the same mean temperature that is associated with the true fluctuations of (25).

The definitions (27) and (28) of Bilham's solution were used to plot the curves shown in Figure 19. It is important to note that the amplitude-suppression ratio A'/A and the phase-lag angle ϵ are both relatively flat functions of the

dimensionless ratio P/λ for either very large or very small values of P/λ, but that in the P/λ range from about 1 to 10 they are quite sensitive to the ratio of period to lag-time. Since the lag-time of the (uncompensated) bead thermistor appears to lie between 0.1 and 0.7 seconds in the range of wind speeds likely to be encountered near the ground (Figure 18), and since the periods expected to appear in the fluctuations have been shown to fall in a range of from about 0.1 to about 100 seconds, the principal region of operation will be very nearly coincident with the central segment of rapid variation on the characteristic curves plotted in Figure 19. This has the unfortunate implication that there will be appreciable spectral bias tending to suppress the periods at the 0.1 second end of the range while admitting the long periods almost without attenuation.

Thus, for sinusoidal fluctuations of 0.1 second period recorded with the bead thermistor at wind speeds where lag-time approaches 0.1 second (true for speeds in excess of 10 meters per second, roughly) the recorded amplitude of the fluctuations is seen, from Figure 19, to be only 16% of the true value; while even 10 second fluctuations are recorded with better than 99% of their true amplitudes for this same lower limiting value of the lag-time. Such strong spectral bias would not occur for a sensing element of ten times greater lag-time, nor would it occur for one of ten times smaller lag-time. In the former case, however, the elimina-

tion of spectral bias would be achieved at the expense of obtaining uniformly bad reproduction of all of the periods of interest, so it is no practical solution to turn to more inert elements. Rather, the desirable way to eliminate the sort of spectral bias to which the thermistor seems subject would be to resort to a still faster sensor.

The tentative values of lag-time assigned above to the thermocouple were all under one-tenth of the corresponding values for the bead thermistor, so the 0.0025-centimeter thermocouple would appear superior, with respect to lag effects too, to the bead thermistor if the dissipation rates ascribed to it are substantially correct. However, work is currently under way to devise electrical compensation techniques that may reduce the thermistor's effective lag-times to much lower values than those given in Figure 18, so a final comparison is not possible because of incomplete data on both instruments' optimum performance. The need for an accurate series of measurements of dissipation rates of thermocouples can be seen to be as pressing for use here in lag estimates as it was in the radiation error analyses above.

(2) Other cases of periodic $T_a(t)$. Since the lag equation (20) is linear, and since any meteorologically plausible $T_a(t)$, defined on a closed time interval, is expressible as a Fourier series, the corresponding response function is also expressible as a Fourier series. The

Fourier coefficients in the series representing the solution will depend not only upon the amplitudes of the corresponding components in the Fourier representation of $T_a(t)$ but also on the degree of attenuation imposed upon that component by the lag of the element. Such a method of expressing the response functions would be particularly convenient for periodic functions. There are, however, two simple types of periodic $T_a(t)$ which are of special interest for which the corresponding $T(t)$ function may be found by more direct means.

The first of these is the square wave, which enters into the experimental technique of Anderson and Heibeck (1951) for lag determinations. Regarding the square wave as a series of alternating step-functions and using the exponential solution to (20) for this case along with the requirement of periodicity of the response function, gave as the ratio of the response amplitude B' to the square wave amplitude B,

$$\frac{B'}{B} = \frac{1 - e^{-P/2\lambda}}{1 + e^{-P/2\lambda}}, \qquad (29)$$

where P is the period of the square wave.

The second special case of interest is the periodic saw-tooth wave. Actual records of turbulent temperature fluctuations frequently suggest a waveform of this type, although a condition of nice periodicity is almost never

found. The temperature is observed to rise slowly and rather steadily only to fall very sharply to a low value from which it again climbs to the next peak. Idealizing this behavior by considering $T_a(t)$ to be composed of linear segments of period P rising from -C to +C within each period and falling abruptly from +C to -C at the end of each period, one finds, by direct solution of (20) and imposition of requirements of periodicity of T(t), that the ratio of response amplitude C' to the true amplitude C is

$$\frac{C'}{C} = \frac{2}{1 - e^{-P/\lambda}} - \frac{2\lambda}{P} - 1. \qquad (30)$$

Using (29) and (30) the amplitude-suppression ratios were computed for several different values of P/λ and compared with the corresponding suppression ratios for the case of the sine wave as plotted in Figure 19. The resulting values are shown in Table 1.

Table 1

Amplitude-Suppression Ratios for Three Periodic $T_a(t)$ Waveforms

Waveform	$P/\lambda = 0.1$	$P/\lambda = 1$	$P/\lambda = 10$	$P/\lambda = 100$
Sine wave	0.02	0.16	0.85	0.99
Square wave	0.03	0.25	0.99	0.99
Sawtooth wave	0.05	0.18	0.80	0.98

Table 1 shows that differences in suppression effects do exist for the three waveforms; but they are not so great that one would be seriously in error to use the values for the sine wave to describe the general response characteristics as a function of period of the driving function $T_a(t)$ for either of the others. It seems, as a rule of thumb, that one must employ a sensing element whose lag-time is not greater than one-tenth of the smallest period regarded as present in the ambient temperature fluctuations, if one hopes to record that period with any degree of fidelity at all. Or, conversely, for any given sensing element, one must not expect to be able to find in the record obtained with that element appreciable evidence for the presence of component periods lower than about 10λ. If it is indeed true that the thermal turbulence near the ground has an appreciable content of eddies with Eulerian periods near 0.1 second (to ascertain this is one of the objectives of the present study), then it would be desirable to employ a sensing element whose lag-time was of the order of 0.01 second. Electrical compensation offers the only hope in an attempt to use bead thermistors at this lower end of the probable range of fluctuation periods.

b. Apparent mean for an arbitrary $T_a(t)$. For the special case of a purely sinusoidal waveform of $T_a(t)$, comparison of the solution (26) and (25) reveals that the apparent mean temperature is identical with the true mean

after the transient effects have died out. It is important to know whether this equality exists for an arbitrary $T_a(t)$, since actually observed waveforms are never pure sine waves. Averaging the inverted lag equation (22) over the period of time from t_o to t_1 yields

$$\overline{T}_a = \overline{T} + \frac{\lambda}{t_1 - t_o}\int_{t_o}^{t_1} \dot{T}dt \equiv \overline{T} + \frac{\lambda}{t_1 - t_o}\int_{T(t_o)}^{T(t_1)} dT. \qquad (31)$$

But

$$\frac{\lambda}{t_1 - t_o}\int_{T(t_o)}^{T(t_1)} dT \leq \lambda \frac{T_u - T_l}{t_1 - t_o}, \qquad (32)$$

where T_u and T_l are the upper and lower limits on $T(t)$ in the interval $t_o \leq t \leq t_1$. Since $T(t)$ is, for physical reasons, bounded in any interval of time, the right member of (32) may always be made arbitrarily small by taking the averaging interval $t_1 - t_o$, sufficiently large. Hence in this limit of sufficiently large averaging interval the last term of the last member of (31) goes to zero and

$$\overline{T}_a \doteq \overline{T}, \qquad (33)$$

to within an error which for any given case is equal to or less than the value of the right side of (32). Even on a day with well developed thermal turbulence, $T_u - T_l$ may safely be assumed to remain below 10 C^o over periods short compared to the full diurnal period, and the expected length of any one run during field observations is planned to be at least five minutes. Hence if a lag-time of 0.5

seconds is assigned to the bead thermistor the discrepancy between the apparent five-minute mean derived from the record of the thermistor and the corresponding true mean will, according to (32), be equal to or less than 0.5(10/300) C^{o} or 1/60 C^{o}, a negligibly small error in the mean.

Thus, it may be concluded that for the case of the time average, the apparent statistic approaches equality with the true statistic in the large-sample limit, and the requirement of "largeness" here is quite readily fulfilled in practice.

This result is seen to be qualitatively implicit in (20) itself, since it is the very nature of the response law that the element will continuously hunt for the condition of zero error, thereby causing the apparent cumulative mean to regress towards the true cumulative mean after each successive thermal disturbance passes by (insofar as the true cumulative mean neither increases nor decreases monotonically with time). The proof given above, however, not only establishes this point, but also yields an estimate of the upper limit on the error of the apparent mean.

c. Apparent variance for an arbitrary $T_a(t)$. The obvious choice of a statistic expressing the degree of variability of $T_a(t)$ is the standard deviation, σ_a, or its square, σ_a^2, the variance. It is thus indispensable, in fluctuation studies, to have some measure of how biased an estimate of σ_a^2 is given by σ^2, the apparent variance

derived from the record of a lagging sensor exposed to the T_a-fluctuations. From the definition of the variance and from the inverted lag equation (22) it follows that

$$N\,\sigma_a^2 = \Sigma\left[(T_i + \lambda \dot{T}_i - \overline{T}_a)^2\right], \qquad (34)$$

where, for convenience here, the recorded T(t) will be regarded as represented by a set of N instantaneous values T_i read off at equal small time increments on the interval $t_o \leq t \leq t_1$ under consideration. The summation indicated in (34) and elsewhere below is thus to be understood to be taken over these N values. On expanding the right side of (34), noting that

$$N\,\sigma^2 = \Sigma T_i^2 - N\overline{T}^2,$$

and making use of (33) to replace $\overline{T}_a$ by $\overline{T}$, one finds that

$$\sigma_a^2 = \sigma^2 + \overline{\lambda^2(\dot{T})^2} + 2\,\overline{\lambda T\dot{T}}. \qquad (35)$$

But

$$\lambda\,\overline{T\dot{T}} = \frac{\lambda}{t_1 - t_o}\int_{t_o}^{t_1} T\dot{T}dt = \frac{\lambda}{t_1 - t_o}\int_{T(t_o)}^{T(t_1)} T\,dT$$

$$\leq \frac{\lambda}{2}\,\frac{T_u^2 - T_l^2}{t_1 - t_o}, \qquad (36)$$

where T_u and T_l are the upper and lower limits of T(t) on the interval $t_o \leq t \leq t_1$. By taking the interval large enough to make the last member of (36) negligibly small, one makes the last term on the right in (35) go to zero, and (33),

which has already been used here, will be satisfied *a fortiori*; so the desired relation between the true variance and the apparent variance of the response of a lagging element becomes

$$\sigma^2 \doteq \sigma_a^2 - \lambda^2\overline{(\dot{T})^2} . \qquad (37)$$

It is seen from (37) that the degree to which the apparent variance approximates the true variance depends on the magnitude of the lag-time and on the mean-square slope of the response waveform. By tabulating the slopes at equal small intervals of time over a representative period of a given record, averaging, and inserting the result into (37), one can estimate the magnitude of the discrepancy between the computed σ^2 and the desired σ_a^2. Such an operation would be quite tedious if performed manually, but can be carried out quite rapidly by use of the electromechanical tabulator described by Kassander and Stebbins (1951), an enlarged and improved model of which is being built for the present study.

For waveforms of $T_a(t)$ that are geometrically simple, such as a sine wave or a square wave, one can actually calculate directly the correction term on the right in (37). For the case where $T_a(t)$ is the sinusoidal fluctuation defined earlier in (25), the ratio σ^2/σ_a^2 is found to be simply $(A'/A)^2$, the square of amplitude-suppression ratio plotted in Figure 19. For the case where $T_a(t)$ is a square wave with equally long plateaus and valleys the same ratio is

found to have somewhat smaller values for the intermediate range of P/λ than was the case for the sinusoidal case. Thus for P/λ equal to 1 the ratio is found from Figure 19 to be 0.026 for the sinusoidal case, but is only 0.021 for the square wave.

If, as is really preferable, the comparison of true and apparent variability is made with the standard deviation rather than the variance, it may be concluded (as before) that to estimate the true value to within an error of less than about 10% requires that the sensing element employed have a lag-time which is not more than one-tenth as large as the shortest periods to be measured. And it must be noted that the possibility of a sort of circular deception as to the degree of reliability of a given estimate of σ_a^2 exists here. If one forms his notion as to what are the shortest important periods solely from visual inspection of the record of a lagging instrument, the attenuation of the shorter-period fluctuations that suppresses the apparent role of these components will mislead one into thinking that the variance estimate is better than it really is. The cycle of deception might then be completed by using this faulty estimate of reliability of the computed σ^2 value to congratulate oneself on the apparent faithfulness with which the response reproduces the forcing function.

d. Effects on the correlation coefficient. Growing interest in the spectrum of atmospheric turbulence has led

recently to attempts to gain information concerning the frequency spectrum by means of observations of the variation of the coefficient of correlation between simultaneous temperature values observed with two sensing elements. The two elements are located at points whose separation is varied (in successive runs) from some very small distance, where the correlation coefficient is nearly 1.0, to very large distances, where the correlation coefficient approaches zero. The basis for the deduction of the frequency spectral characteristics from a correlation function so obtained was given by Taylor (1938), who showed that the spectral intensity function is, under certain conditions, the Fourier transform of the correlation function (and vice versa). (The required conditions for the existence of this relation are satisfied much less exactly in the natural wind than in wind tunnel airflows.) In addition to such an application, correlation studies may also be used to determine quite directly the average dimensions of thermal eddies; so it was felt desirable to examine the effects that lag may have on the correlation coefficient.

If the two sensing elements used for correlation observations have appreciably different lag-times, the associated differences in amplitude-suppression and phase-lag imposed by each may lead to bias in the correlation coefficients computed from their recorded outputs. An examination of the

sensitivity of the correlation coefficient to such attenuation and phase-shift effects was carried out and will be summarized below. The results may be interpreted as a measure of the sensitivity of the correlation coefficient to lag differences occurring due to manufacturing variations among a group of elements, due to errors in laboratory determinations of the lag-times, or due to differences in lag-time imposed by systematic variations of wind speed with height above the ground.

For the purpose of the analysis, perfect correlation was assumed to exist between the two waveforms of $T_a(t)$ occurring at the two points of observation, and the extent to which the apparent correlation could drop due just to differences in the lag-times of the two sensors was determined. In the simplest case of purely sinusoidal $T_a(t)$ fluctuations (single period present) it can be seen that amplitude-suppression effects cannot by themselves produce any reduction in the apparent correlation since the correlation coefficient for a pair of variables is unchanged if one of them is multiplied by a constant k, and the other is multiplied by a constant q ($k, q > 0$). Only unequal phase-shifts produced by the assumed unequal lag-times of the two sensors is capable of decreasing the apparent correlation between the temperature fluctuations recorded at the two points when these fluctuations are simple sine waves. Analysis of the effects of phase-shift for this simple case revealed that even for very improbable differences in

the two lag-times the reduction in the apparent correlation was quite negligible. Thus, even for a ten-fold ratio in the lag-times of the two sensors ($P/\lambda = 1$ versus $P/\lambda = 10$), the apparent correlation was found to be 0.990 for an assumed perfect value of 1.000.

For the more general case in which the $T_a(t)$ waveform is composed of a number of harmonic components, amplitude-suppression as well as phase-shift affects the reduction (and possibly also the increase) of the apparent correlation. If the two $T_a(t)$ waveforms contain widely different frequency components and if the two sensors' lag-times are appreciably different it becomes possible that the unequal attenuation and phase-shift of the various frequency components by the two sensors will yield response waveforms which have quite a different degree of correlation from that existing between the two driving functions.[1]

The nature and magnitude of this sort of lag bias in the apparent correlation can be examined analytically for driving functions containing any finite number of distinct frequency components, but the arithmetic complexity of numerical evaluation increases rapidly with the number of components, so only the simple case of the two sinusoidal components was examined using the general result derived here. The approach again

---

[1]The author is indebted to Dr. J. M. Keller for having pointed out this possibility which, for meteorological reasons, is a case that undoubtedly occurs frequently.

involved the assumption that the two $T_a(t)$ waveforms were identical at the two sensors, so the problem consisted in determining how much reduction could occur in the apparent correlation coefficient due to lag effects.

The two perfectly correlated waveforms were regarded as actually identical and defined by the relation

$$T_a(t) = \sum_i A_i \sin \frac{2\pi t}{P_i}, \qquad (38)$$

where the summation is taken over all of the harmonic components of amplitude A_i and period P_i. So long as one limits the discussion to cases in which there exist no simple integral relations between the several P_i and so long as all averages are taken over periods of time long compared to even the greatest of the P_i, little generality is lost in omitting parametric phase angles in (38) since phase effects will be randomized out under the restrictions mentioned. If a sensing element of lag-time λ_j is exposed to the fluctuations defined by (38) its steady-state response waveform will, in view of the linearity of the lag equation, be given by a sum of phase-shifted harmonic components of the same periods as those contained in $T_a(t)$ but with amplitudes suppressed. From (26) the response function is seen to be

$$T_j(t) = \sum_i A'_{ij} \sin\left(\frac{2\pi t}{P_i} - \epsilon_{ij}\right) \qquad (39)$$

where A'_{ij} and ϵ_{ij} are given by (27) and (28) respectively, with λ taken here as λ_j and P taken here as P_i.

The correlation coefficient r_{12} between $T_1(t)$ and $T_2(t)$ is given formally by

$$r_{12} = \frac{\int_0^{t_1} T_1(t)\, T_2(t)\ dt}{\int_0^{t_1} dt\ \ \sigma_1\ \ \sigma_2} \qquad (39a)$$

where the sampling time t_1 is large compared to the greatest P_i and where σ_j is the standard deviation of $T_j(t)$. The evaluation of the numerator integral and the determination of the σ_j is straightforward but tedious, so only the results will be given here. Under the restriction cited earlier that no simple integral relations shall exist among any pairs of the P_i, all cross-product terms that arise go to zero in the large-sample limit and one finds that

$$r_{12} = \frac{\Sigma_i \left[A'_{i1}A'_{i2}(\cos \epsilon_{i1}\cos \epsilon_{i2} + \sin \epsilon_{i1}\sin \epsilon_{i2})\right]}{(\Sigma_i A'^2_{i1}) \cdot (\Sigma_i A'^2_{i2})} \qquad (39b)$$

where the indicated summation is to be taken over all frequency components present in $T_a(t)$, their number being assumed finite.

By way of illustration of the lag bias effects implicit in (39b), a few different cases may be considered for which $T_a(t)$ contains just two harmonic components of appreciably different periods. First, suppose $\lambda_1 = \lambda_2$, about as large a discrepancy between the lag-times of the two sensors as is likely for the case of thermistors, at least. Also, let $P_1/\lambda_1 = 10$ while $P_2/\lambda_1 = 1$, and $P_1/\lambda_2 = 20$ while $P_2/\lambda_2 = 2$.

Furthermore, take $A_1 = A_2$, i.e., let the high-and low-frequency components be of equal importance in controlling $T_a(t)$. Under these conditions, both sensors reproduce the first harmonic component with fair fidelity, as can be seen from Figure 19, but neither sensor reproduces the higher-frequency second component very well. Evaluation of (39b) for this case shows, however, that only very slight reduction occurs in the apparent correlation coefficient, a value of 0.98 appearing in place of the true value of 1.00. In view of the fairly strong attentuation of the second component by each sensor, this result was somewhat surprising. The explanation was found on inspection of the four ϵ_{ij} values pertaining to this situation: $\epsilon_{11} = 32^o$, $\epsilon_{12} = 20^o$, $\epsilon_{21} = 81^o$, and $\epsilon_{22} = 70^o$. It will be seen that the first component is shifted in phase by 32^o by the first sensor and 20^o by the second sensor, a difference of only 12^o in the shifts. Two simple sine waves which differ in phase by only 12^o would exhibit very high correlation, though less than perfect. At the same time, the second component of shorter period is shifted in phase by 81^o by the first sensor and by 70^o by the second sensor, a difference of only 11^o -- again a small enough difference in shift that these two components must correlate well between the two records. Since the difference in phase shift of corresponding components in each of the two response waveforms is small, but above all, because these two differences are nearly the same (12^o versus 11^o), the two response waveforms must tend to be similar in their general form,

though each is quite unlike the driving function, $T_a(t)$. This picture, to be sure, is complicated somewhat by the unequal amplitude-suppression imposed by the two sensors on corresponding components, but this effect is unable, in the case under consideration, to suppress the apparent correlation coefficient very much.

As a next case, all conditions were taken the same as in the first case, but the high-frequency component was assumed to be of predominant importance in $T_a(t)$. Specifically, take $A_2 = 10A_1$. This case is one for which the component of major importance is the one which suffers the most serious attenuation and phase shift. From (39b), however, one finds that the apparent correlation coefficient falls only to 0.96, still a negligible drop by meteorological standards. One may conclude that for cases in which the lag-times of the two sensors employed in correlation studies differ by no more than a factor of two, lag bias in the correlation coefficient will not be very serious. This conclusion is strengthened by the fact that the numerical evaluations were carried out for P/λ values for which Figure 19 reveals there exist marked dependence on P/λ ; but it is weakened by the fact that only two, instead of a large number of components was considered, so their periods could not be spread over all of the important middle section of the P/λ range portrayed by Figure 19.

To see how the lag bias would behave for very extreme differences in lag-time, the case $\lambda_1 = 10\ \lambda_2$ was examined

for $A_1 = A_2$, $P_1/\lambda_1 = 10$, and $P_2/\lambda_1 = 1$. From (39b) the apparent correlation coefficient was found, for these conditions, to be reduced to 0.70, an appreciable drop, but still not one that wholly obscures the existing relationship. On the basis of this and the previous results, lag bias seems not too serious in correlation studies.

2. Fluctuation distortions due to variable lag-time

The preceding discussions of the effects of lag on fluctuation statistics have assumed that the lag-time remains constant. There remain for examination the effects produced by variations in the ambient wind speed. These effects may be due to spatial variations of wind speed, as in the case of the increase of the mean wind speed with height above the ground surface, or to temporal variations resulting from gustiness or longer-period changes in the mean wind speed.

a. Vertical variation of lag bias in apparent fluctuations. The systematic increase of wind speed with height, being most pronounced very near the ground, leads to increases in the mean dissipation rate and hence decreases in the mean lag-time of identical sensing elements located at a series of levels close to the ground. These lag variations introduce systematic bias into the apparent fluctuation statistics derived from these elements' records. To obtain a notion of the seriousness of this effect a power law wind profile

$$u(z) = u_1 z^p \qquad (14)$$

was assumed and two different reference velocities u_1 employed:

u_1 = 1 meters per second and u_1 = 5 meters per second, where u_1 is the mean wind speed at a height of 1 meter. To gain some additional information as to possible diurnal variations, two different exponents p were considered: p = 0.1, representative of daytime conditions, and p = 0.3, representative of nighttime conditions. Finally, to assess the relative attenuation of different periods in $T_a(t)$, three different periods of a sinusoidal waveform were examined: P = 0.1 second, P = 1 second, and P = 10 seconds. This yielded twelve cases, and for each the profile of the sinusoidal amplitude suppression ratio A'/A of (27) was computed for the layer of air extending from the surface up to a height of 10 meters. The results are presented in Figure 20.

Figure 20 shows that for both rather large (10 second) and rather small (0.1 second) periods a bead thermistor does not impose very serious vertical variation of distortion; but in the former case this is because there exists uniformly faithful reproduction of the true fluctuations, whereas in the latter it is because there exists uniformly poor reproduction of the true fluctuations at all heights.

The most marked vertical variation of A'/A occurs for the middle pair of curves in both Figure 20-a and 20-b, corresponding to P = 1 second. That the strongest variation of bias with height develops for this one of the three periods considered is a reflection of the steepness of the slope of the curve of A'/A vs. P/λ in the middle range of

Figure 20-a. Vertical variation of the amplitude-suppression ratio, A'/A for a bead thermistor in light winds (u_1 = 1 meter per second).

Each curve is labeled with the period P of the assumed temperature fluctuations and with the exponent p in the power law wind profile used in its computation.

Figure 20-b. Vertical variation of the amplitude-suppression ratio, A'/A for moderate winds (u_1 = 5 meters per second)

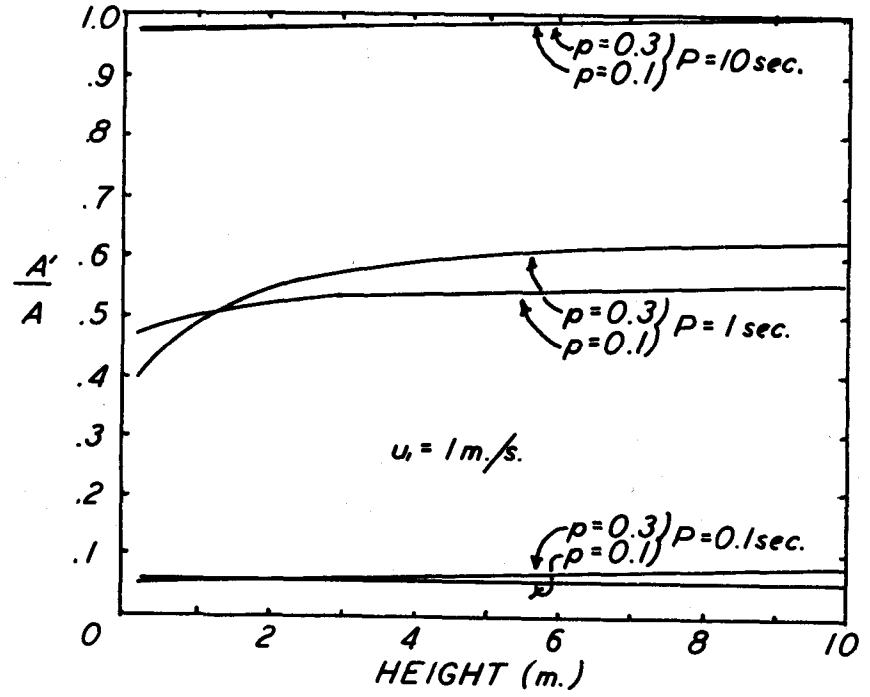
1.0
.9
.8
.7
.6
.5
.4
.3
.2
.1
0
A'/A
p=0.3
p=0.1
P=10 sec.
P=1 sec.
P=0.1 sec.
u₁ = 1 m./s.
2
4
6
8
10
HEIGHT (m.)

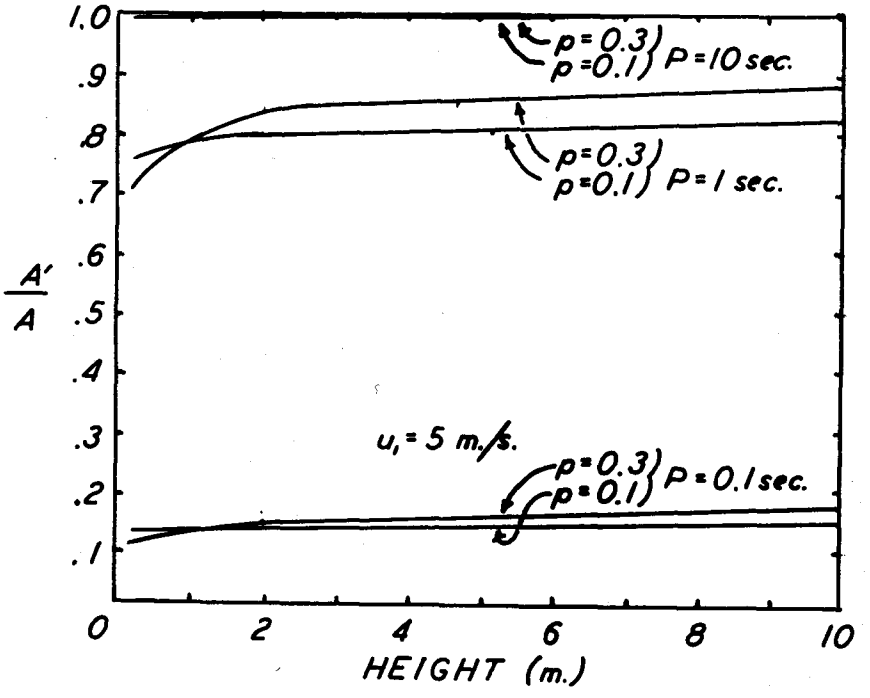
1.0
.9
.8
.7
.6
.5
.4
.3
.2
.1
0
A'/A
p=0.3
p=0.1
P=10 sec.
P=1 sec.
P=0.1 sec.
u₁ = 5 m./s.
2
4
6
8
10
HEIGHT (m.)

the P/λ values, as shown in Figure 19. (For the thermistor lag-time of several tenths of a second, the case P = 1 second corresponds to a P/λ of about two or three.)

Of all twelve curves in Figure 20, the greatest vertical variation of distortion is for u_1 = 1 meter per second, P = 1 second, and p = 0.3, and it occurs within the layer of air from about 0.2 meters to about 2 meters above the ground. At the top of this layer there is about 50% better reproduction of the 1-second periods in $T_a(t)$ than there is at the bottom of this layer. Mere visual comparison, or uncorrected quantitative comparison, of the records of thermistors mounted at the top and bottom of this layer would yield an appreciably distorted impression of the relative importance, at the two levels, of thermal fluctuations with periods of the order of 1 second. It is to be noted, however, that the most intense thermal fluctuations are a daytime phenomenon, hence represented more closely in Figure 20 by the curves for p = 0.1 and u_1 = 5 meters per second. The latter curves do not exhibit extremely marked vertical variation of amplitude suppression for any of the fluctuation periods represented in the figure, a fortunate circumstance.

b. Variation of lag distortion with varying scale of turbulence. As has been pointed out earlier, the "periods" under discussion here are Eulerian periods which really measure the times of transit of thermal inhomogeneities past the fixed sensor. This means that, for a thermal in-

homogeneity of a given size, its period varies inversely with the speed of the wind in which it is embedded. This circumstance, coupled with the inverse dependence of lag-time upon ventilation rate, leads one to speculate optimistically that perhaps the disadvantageous effect of a wind speed increase on the period may be canceled by the concurrent advantageous effect of the wind speed increase on the lag-time of the element. The issue is determined entirely by the functional form of $\lambda(u)$ for the sensing element employed.

Figure 21 shows the results of a check on this point. Six different wavelengths, L, were considered, where L represents the downwind distance between successive temperature maxima (or minima). The sinusoidal amplitude-suppression ratio, A'/A, was used as the criterion of distortion, and is seen to decrease (grow worse) with increasing wind speed for all of the scales of thermal turbulence represented in the figure. (A particularly well-marked variation of the degree of suppression appears to accompany wind speed increases when the air stream contains eddies of wavelength near 1 meter.) Hence the initial hypothesis that cancellation of opposing effects might leave lag distortion independent of mean wind speed was found to be incorrect. Instead, the extent to which the Eulerian fluctuation effects due to an eddy of given size are represented in the thermistor output fluctuations becomes steadily less with

Figure 21. Variation of thermistor lag distortion with varying scale of turbulence.

Each curve represents the variation of amplitude-suppression ratio, A'/A with varying mean wind speed $\bar{U}$ for the wavelength L entered above the curve.

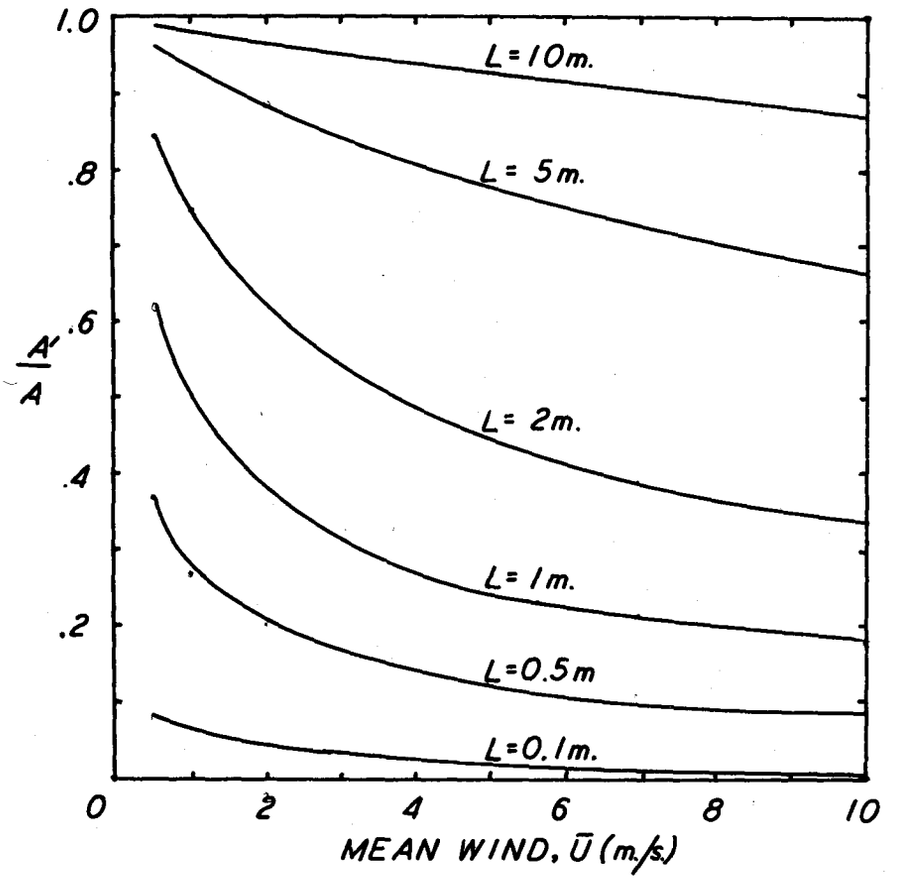
1.0
.8
.6
.4
.2
A'/A
L = 10m.
L = 5m.
L = 2m.
L = 1m.
L = 0.5m
L = 0.1m.
0
2
4
6
8
10
MEAN WIND, Ū (m/s)

increasing transit speed, ventilational advantages notwithstanding.

Although the curves of Figure 21 are extended only down to a mean wind of 0.5 meter per second (because the $u^{\frac{1}{2}}$ dependence of lag-time on air speed fails to hold below there) one can see that all of the curves must converge to the point $A'/A = 0$, $\overline{u} = 0$, since this point corresponds to infinite periods for all scales of turbulence, but is associated with a finite lag-time (of about 0.7 seconds). Hence Figure 21 fails to reveal directly that the strongest variation of distortion really occurs with the very smallest of eddies for almost calm conditions.

c. Response to simultaneous wind-and temperature-fluctuations. If a bead thermistor with lag function of the form given by (23) is exposed not only to sinusoidal temperature fluctuations of the form (25), but simultaneously to wind speed fluctuations of the form

$$u(t) = U + u_o \sin\left(\frac{2\pi t}{P} - \alpha\right), \qquad (40)$$

where U is the mean wind speed, u_o the amplitude of the speed fluctuations, P the same period as that characterizing the thermal fluctuations, and α the phase separation between epochs of highest temperature and epochs of highest wind speeds, then the problem of deducing the possible distortions of the fluctuation statistics becomes the problem of solving the response equation

$$\frac{dT}{dt} + \frac{u^{\frac{1}{2}}}{\lambda_1} T = \frac{u^{\frac{1}{2}}}{\lambda_1}(\overline{T}_a + A \sin\frac{2\pi t}{P}) \qquad (41)$$

where $u = u(t)$ is the periodic function given by (40) and λ_1 is the constant introduced in (23).

Equation (41), unlike (20), has variable coefficients, the presence of which make (41) much less readily soluble than was (20). Since the coefficient $u^{\frac{1}{2}}$ is periodic in time, (41) is an equation of the Floquet type (Ince, 1926, p. 381) for which a solution cannot be obtained in closed form. Since, as has been elaborated in the discussions of confounding errors, the mean amplitude of fluctuation of the wind is only about one-fourth of the mean wind speed under most meteorological conditions, it was thought possible to reduce the complexity of (41), without introducing serious error, by expanding $u^{\frac{1}{2}}$ in a binomial series and using only a small number of the initial terms. For the above-mentioned case where u_o/U is one-fourth, one can, in fact, retain only the first two terms of the binomial expansion of $u^{\frac{1}{2}}$ at the expense of an error of less than 1% (determinate here since the expansion yields an alternating series). Upon making this simplification, it was found possible to reduce (41) to quadrature by the method of variation of parameters, but the then required integrations could only be carried out numerically. Hence it seemed more expedient to integrate (41) by numerical methods from the beginning,

so this was done.

Any distortion in the apparent temperature waveform due to fluctuations in effective lag-time would be expected to be a function of the phase difference α between the temperature and the wind-fluctuations. Since the wind speed tends to rise in the surface layer during periods when a mass of air descends from the faster-moving overlying layers which are also generally cooler than the surface layers at midday, values of α which correspond to this situation should be the one on which to base the integration of (41). If the wind were highest just when the temperature was dropping most rapidly, the lowering of the lag-time due to increased ventilation rate might be expected to cause the element to follow the ambient temperature more closely than it would during the lulls when the ambient temperature was rising. This combination of effects would lower the apparent mean and might also distort the waveform. It was the objective of the integration of (41) to determine how important these effects due to simultaneous fluctuations of wind and temperature might be.

The integrations were carried out for $P/\lambda = 10$ in order to examine a case for which the lag suppression of amplitudes is not already so great as to be the limiting factor. The wind speed employed in the calculations was 1 meter per second, a case for which fairly large variations of lag-time with wind speed occur, tending to give an upper

estimate of distortion effects due to wind speed fluctuations. Since the lag-time of the thermistor at 1 meter per second is about 0.3 second (Figure 18), the period considered became about 3 seconds in view of the selection of $P/\lambda = 10$.

The integration was performed in 0.1-second increments over the approximately 3.0-second range of integration (one full period of the fluctuation). In each case, three sucessive complete integrations were carried out, using results of the first to improve the selection of the initial conditions on $T(t_o)$ in the second, etc., in order to obtain a final response waveform which was as nearly periodic as possible. One set of integrations was carried out for the case $\alpha = 180^o$ (wind-and temperature-fluctuations exactly out of phase) and one set for $\alpha = 90^o$. The results, in each case, showed clearly that there is only a very slight displacement of the apparent mean from the true mean, and completely negligible distortion of the waveform occurs. For an α-value of 180^o, the final integration (of the set of three) yielded a mean which was lower than the true mean by only 2% of the amplitude of the temperature fluctuations. Even for this third integration, $T(t_o + P)$ was still not quite identical with $T(t_o)$; but further iterations seemed unjustifiable in view of the fact that any improved approximation to a truly periodic solution to (41) was only going to decrease the already negligibly small error in the appar-

ent mean. For the other case, $\alpha = 90^{o}$, the discrepancy was slightly greater than for $\alpha = 180^{o}$, the apparent mean being lower than the true mean by about 5% of the true amplitude, the waveform itself being distorted in a negligible fashion again.

After plotting the results of each final integration, another response curve was plotted on the same axes under the assumption of constant lag-time equal to that associated with the mean wind speed of 1 meter per second employed in the numerical integrations. Comparison of these two response curves with a third plotted curve representing the true ambient temperature fluctuations revealed the useful fact that the discrepancies between the true curve and the curve resulting from the integration for the case of fluctuating wind speed were, for all practical purposes of the present study, essentially the same as the discrepancies between the true curve and the curve computed for the case of the constant lag-time. This implies that it will be sufficient to make any corrections for lag distortion solely on the basis of the mean lag-time that is effective during any given observation in the field.

Since the amplitude of the true temperature fluctuations is expected to be of the order of 1 C^{o}, a suppression of the apparent mean by, at most, 5% of the amplitude, implies an error of only about 0.05 C^{o} in the apparent mean. This is nearly identical with the confounding error magnitudes as

predicted in Part III above; but it is distinct in its nature from the confounding error, which represented the superposition of spurious fluctuations of that magnitude and not a lowering of the apparent mean, as is the case here.

V. SUMMARY AND CONCLUSIONS

The radiative heating of a Western Electric D-176980 bead-type thermistor was determined by calculations of the contributions of direct solar radiation, diffuse sky radiation, ground-reflected radiation, and infrared radiation. The effects of radiative heating of the lead wires and heavier support wires which are in thermal communication with the bead were examined and the tentative conclusion reached that these may serve to exaggerate the radiation errors under field conditions. Unfortunately, no firm conclusions in this important matter could be drawn because of lack of reliable experimental data concerning the dissipation rates of small wires operated at temperatures only slightly higher than ambient temperatures. Some estimates of radiation errors and of confounding errors due to wind speed fluctuations were made solely on the basis of bead absorption rates and experimentally determined overall dissipation rates and these indicated that the errors will not be prohibitively large.

An analysis of radiation errors of a thermocouple of 0.0025 cm. diam. was carried out in a similar manner. Because of marked disagreement among previously published studies of the dissipation rates of small wires, it was emphasized that no firm conclusions could be drawn, but on the basis of the dissipation rates determined from an equation given by King

(1914), tentative error values were computed. These suggest that thermocouples of the size considered may suffer appreciably lower radiation errors than the bead thermistor, possibly only about 10% as large. The advantage of much greater signal voltages from the thermistor than from the thermocouple and the fact that even the thermistor errors are not intolerably large, make the thermistor the more desirable sensing element for use in fluctuation studies. An examination of the benefit derivable from applying a high-albedo coating to the thermistor bead suggests that thermistor radiation errors might be reduced by 90% if a silver or aluminum film could be deposited successfully on the bead.

The effects of instrument lag were analysed on the basis of the differential equation of response of a lagging element. Several general relationships between the true and the apparent fluctuation statistics (mean, variance, correlation coefficient) were derived and quantitative determinations of certain lag errors of the bead thermistor carried out. It was concluded that the bead thermistor will respond in a biased manner to the range of turbulent fluctuation periods predicted to be present in the natural wind (0.1 second to 100 seconds, approximately). This bias takes the form of marked attenuation of the shorter-period fluctuations in the range of interest. Electrical lag compensation of the thermistor output seems essential if this element is to serve in the

exploration of the full spectrum of atmospheric turbulence.

The lag times of a thermocouple of 0.0025 centimeter diameter, as computed from the King equation, were found to be less than one-tenth as great as those experimentally determined for the thermistor. The uncertainty of the validity of using the King equation to predict the dissipation rates of thermocouples carries over into the lag-time calculations, so it is not felt that any final conclusions as to the relative merits of thermistor and thermocouple should be drawn. Further experimental study of the dissipation rates of wires at room temperatures is essential to any further analyses of thermocouple radiation - and lag-errors. The anomalous results of Ayrton and Kilgour (1892) raise questions which particularly need attention.

VI. LITERATURE CITED

Albrecht, F. 1927. Thermometer zur Messung der Wahren Lufttemperatur. Meteorologische Zeitschrift. 44: 420-424.

Anderson, L. J. and Heibeck, H. L. 1951. A tau-meter for rapid-response temperature recording systems. Bulletin of the American Meteorological Society. 32: 67-71.

Ayrton, W. E. and Kilgour, H. 1892. The thermal emissivity of thin wires in air. Philosophical Transactions of the Royal Society of London. Series A, 183: 371-406.

Barrows, W. E. 1912. Light, photometry, and illumination. N. Y., McGraw-Hill Book Co., Inc.

Becker, J. A., Green, C. B., and Pearson, G. L. 1946. Properties and uses of thermistors--thermally sensitive resistors. Electrical Engineering. Transactions Section. 65: 711-725.

Best, A. C. 1931. Horizontal temperature differences over small distances. Quarterly Journal of the Royal Meteorological Society. 57: 169-175.

Bilham, E. G. 1935. On the interpretation of some measurements by A. C. Best of horizontal temperature differences over small distances. Quarterly Journal of the Royal Meteorological Society. 61: 159-164.

Brunt, D. 1944. Physical and dynamical meteorology. Cambridge, Cambridge University Press.

Cramer, H. E. 1951. Preliminary results of a program for measuring the structure of turbulent flow near the ground. Paper presented at the Symposium on Atmospheric Turbulence, Massachusetts Institute of Technology, Cambridge, Massachusetts, June 4-8, 1951. (To be published in Proceedings of the Symposium.)

Dryden, H. L. and Kuethe, A. M. 1929. The measurement of fluctuations of air speed by the hot-wire anemometer. Fifteenth annual report of the National Advisory Committee for Aeronautics. Technical Report No. 320: 359-382.

Geiger, R. 1950. The climate near the ground. Cambridge, Massachusetts, Harvard University Press.

Geiss, W. 1950. Versuche über den Strahlungseinfluss auf kleine Platindrahtthermometer mit Cellonglasrahmen. Zeitschrift für Meteorologie. 2: 356-358.

Giblett, M. A. 1932. The structure of wind over level country. Meteorological Office, London. Geophysical Memoirs No. 54.

Hall, F. 1949. A method for improving the response of recording instruments. Journal of Meteorology. 6: 160-161.

Hand, I. F. 1946. Pyrheliometers and pyrheliometric measurements. Washington, D. C., U. S. Department of Commerce.

Harper, D. R. 1913. Thermometric lag. Bulletin of the U. S. Bureau of Standards. 8: 659-714.

Haude, W. 1934. Temperatur und Austausch der bodennahen Luft über eine Wüste. Beiträge zur Physik der freien Atmosphäre. 21: 129-142.

Heywood, G. S. P. 1931. Wind structure near the ground and its relation to temperature gradient. Quarterly Journal of the Royal Meteorological Society. 57: 433-452.

Humphreys, W. J. 1940. Physics of the air. 3d ed. N. Y., McGraw-Hill Book Co., Inc.

Huss, P. O. and Portman, D. J. 1949. Study of natural wind and computation of the Austausch turbulence constant. Daniel Guggenheim Airship Institute, the University of Akron, Akron, Ohio. Report No. 156.

Ince, E. L. 1926. Ordinary differential equations. London, Longmans, Green and Co.

Jenkins, F. A. and White, H. E. 1937. Fundamentals of physical optics. N. Y., McGraw-Hill Book Co., Inc.

Kassander, A. R. 1951. Investigations of turbulent temperature fluctuations in the lower atmosphere. Iowa State College, Department of Physics, Ames, Iowa. Report No. 1.

Kassander, A. R. and Stebbins, D. W. 1951. The application of electrical counting to the compilation of frequency distributions and correlation tables. Transactions of the American Geophysical Union. 32: 341-346.

Kimball, H. H. 1927. Measurement of solar radiation intensity and determinations of its depletion by the atmosphere with bibliography of pyrheliometric measurements. Monthly Weather Review. 55: 155-169.

Kimball, H. H. and Hand, I. F. 1921. Sky-brightness and daylight-illumination measurements. Monthly Weather Review. 49: 481-488.

King, L. V. 1914. On the convection of heat from small cylinders in a stream of fluid: Determination of the convection constants of small platinum wires with applications to hot-wire anemometry. Philosophical Transactions of the Royal Society of London. Series A, 214: 373-432.

Langmuir, I. 1912. Convection and conduction of heat in gases. Physical Review. 34: 401-422.

Lettau, H. 1949. Isotropic and non-isotropic turbulence in the atmospheric surface layer. Base Directorate for Geophysical Research, Air Force Cambridge Research Laboratories, Cambridge, Massachusetts. Geophysical Research Papers, No. 1.

Linke, F. 1931. Die nächtliche effektive Ausstrahlung unter verschiedenen Zenitdistanzen. Meteorologische Zeitschrift. 48: 25-31.

McAdams, W. H. 1942. Heat transmission. N. Y., McGraw-Hill Book Co., Inc.

Middleton, W. E. K. 1947. Meteorological instruments. 2d ed. Toronto, University of Toronto Press.

Monthly Weather Review. 1949. Washington, D. C., U. S. Department of Commerce. 77: 28, 131, 216, 300.

Moon, P. 1936. The scientific basis of illumination engineering. N. Y., McGraw-Hill Book Co., Inc.

Richardson, E. G. 1950. The fine structure of atmospheric turbulence in relation to the propagation of sound over the ground. Proceedings of the Royal Society of London. Series A, 203: 149-164.

Sanford, E. R. 1951. A wind-tunnel investigation of the limitations of thermistor anemometry. Journal of Meteorology. 8: 182-190.

Schilling, H. K., Drumheller, C. E., Nyborg, W. L., and Thorpe, H. A. 1946. On micrometeorology. American Journal of Physics. 14: 343-353.

Sherlock, R. H. and Stout, M. B. 1936. Atmospheric turbulence during winter storms. Review and analysis of airship design and construction past and present. Report No. 2. Palo Alto, California, Stanford University Press.

Slater, A. E. 1948. Discussion. Quarterly Journal of the Royal Meteorological Society. 74: 189-190.

Sutton, O. G. 1948. Convection in the atmosphere near the ground. Quarterly Journal of the Royal Meteorological Society. 74: 13-30.

Swinbank, W. C. 1951. The measurement of vertical transfer of heat and water vapor by eddies in the lower atmosphere. Journal of Meteorology. 8: 134-145.

Taylor, G. I. 1938. The spectrum of turbulence. Proceedings of the Royal Society of London. Series A, 164: 476-490.

Thornthwaite, C. W. 1949. Micrometeorology of the surface layer of the atmosphere. The Johns Hopkins University Laboratory of Climatology, Seabrook, New Jersey. Interim Report No. 5.

Thornthwaite, C. W. 1950. Micrometeorology of the surface layer of the atmosphere. The Johns Hopkins University Laboratory of Climatology, Seabrook, New Jersey. Interim Report No. 11.

Vehrencamp, J. E. 1951. An experimental investigation of heat and momentum transfer at a smooth air-earth interface. University of California, Department of Engineering, Los Angeles, California.

VII. ACKNOWLEDGMENTS

This research was sponsored by the Atmospheric Analysis Laboratory of the Base Directorate for Geophysical Research, Air Force Cambridge Research Laboratories, under contract No. AF19(122)-440.

The author is indebted to Dr. A. R. Kassander for providing the experimental data on bead thermistors and to Mr. R. W. Green for his part in the experimental work. The author is grateful to Dr. J. M. Keller and to Dr. L. T. Earls for reading various parts of the manuscript and for their recommendations for its improvement. Appreciation is also expressed for Mrs. E. O. Hansen's assistance in the preparation of the manuscript.

Above all, the author thanks his wife, whose single-handed care of numerous offspring made possible an early completion of this work.